KINETICS AND CORRELATION OF CAVEOLIN-1 AND MCL-1 PROTEINS WITH LUNG CANCER CELL ANOIKIS

Mr. Preedakorn Chunhacha

A Dissertation Submitted in Partial Fulfillment of the Requirements
for the Degree of Doctor of Philosophy Program in Pharmaceutical Technology
Department of Pharmaceutics and Industrial Pharmacy
Faculty of Pharmaceutical Sciences
Chulalongkorn University
Academic Year 2011

จลนศาสตร์และความสัมพันธ์ของโปรตีนคาวีโอลิน-1 และโปรตีนเอ็มซีแอล-1 ต่ออนอยคิสของเซลล์มะเร็งปอด

นายปรีดากร ชุณหะชา

วิทยานิพนธ์นี้เป็นส่วนหนึ่งของการศึกษาตามหลักสูตรปริญญาวิทยาศาสตรดุษฎีบัณฑิต
สาขาวิชาเทคโนโลยีเภสัชกรรม ภาควิชาวิทยาการเภสัชกรรมและเภสัชอุตสาหกรรม
คณะเภสัชศาสตร์ จุฬาลงกรณ์มหาวิทยาลัย
ปีการศึกษา 2554

Thesis Title	KINETICS AND CORRELATION OF CAVEOLIN-1 AND MCL-1 PROTEINS WITH LUNG CANCER CELL ANOIKIS
By	Mr. Preedakorn Chunhacha
Field of Study	Pharmaceutical Technology
Thesis Advisor	Assistant Professor Pithi Chanvorachote, Ph.D.

Accepted by the Faculty of Pharmaceutical Sciences, Chulalongkorn University in Partial Fulfillment of the Requirements for the Doctoral Degree

Pintip Pongpech .....Dean of the Faculty of Pharmaceutical Sciences

(Associate Professor Pintip Pongpetch, Ph.D)

THESIS COMMITTEE

Parkpoom Tengamnuay ..... Chairman

(Associate Professor Parkpoom Tengamnuay, Ph.D.)

Pithi Chanvorachote ..... Thesis Advisor

(Assistant Professor Pithi Chanvorachote, Ph.D.)

..... Examiner

(Professor Apiwat Mutirangura, M.D., Ph.D.)

Nontima V. ..... Examiner

(Assistant Professor Nontima Vardhanabhuti, Ph.D.)

Angkana Tantituvanont ..... Examiner

(Assistant Professor Angkana Tantituvanont, Ph.D.)

..... External Examiner

(Kriengsak Lirdprapamongkol, Ph.D.)

ปรีดากร ชุณหะชา : จลนศาสตร์และความสัมพันธ์ของโปรตีนคาวีโอลิน-1 และโปรตีนเอ็มซีแอล-1 ต่ออนอยคิสของเซลล์มะเร็งปอด. (KINETICS AND CORRELATION OF CAVEOLIN-1 AND MCL-1 PROTEINS WITH LUNG CANCER CELL ANOIKIS) อ.ที่ปรึกษาวิทยานิพนธ์หลัก:ผศ.ดร.ปิติ จันทร์วรโชติ, 160 หน้า.

โปรตีนคาวีโอลิน-1 และโปรตีนเอ็มซีแอล-1 ต่างมีบทบาทในการควบคุมการตายแบบอนอยคิสในเซลล์มะเร็งหลายชนิด แต่ความสัมพันธ์และกลไกของโปรตีนทั้งสองชนิดต่อการควบคุมการตายแบบอนอยคิสยังไม่เป็นที่แน่ชัด งานวิจัยนี้ได้ใช้การศึกษาทางจลนศาสตร์เพื่อแสดงให้เห็นว่าโปรตีนทั้งสองชนิดดังกล่าวต่างควบคุมการตายในเซลล์มะเร็งปอดชนิดเซลล์ใหญ่ซึ่งได้ใช้เซลล์มะเร็งปอดชนิดเอช-460 เป็นตัวแทนในการศึกษา การเปลี่ยนแปลงระดับของโปรตีนคาวีโอลิน-1 และเอ็มซีแอล-1 โดยใช้การเหนี่ยวนำด้วยพลาสมิดให้มีการแสดงออกของโปรตีนในระดับที่สูงขึ้นหรือลดลงต่างก็มีผลต่อการมีชีวิตรอดของเซลล์ รวมถึงอัตราการเกิดการตายแบบอะพอพโทซิสหลังจากที่เซลล์หลุดออกจากที่ยึดเกาะ ซึ่งแสดงให้เห็นถึงบทบาทที่สำคัญของโปรตีนทั้งสองชนิดนี้ต่อการควบคุมการตายแบบอนอยคิสในมะเร็งชนิดดังกล่าว นอกจากนี้ หลังจากที่เซลล์หลุดออกจากที่ยึดเกาะ ระดับของโปรตีนคาวีโอลิน-1 และเอ็มซีแอล-1 ต่างลดลงอย่างต่อเนื่องแปรผันตามเวลาที่เซลล์หลุดออก การศึกษาสหสัมพันธ์ได้แสดงให้เห็นว่าการลดลงของโปรตีนทั้งสองชนิดมีความใกล้ชิดกันมากซึ่งแสดงด้วยค่าเพียร์สัน = 0.986 (p-value< 0.0001) ทำให้เกิดสมมติฐานเกี่ยวกับการที่โปรตีนจะมีปฏิสัมพันธ์กันโดยตรง การทดสอบ Immunoprecipitation และการทดสอบ immunofluorescence ทำให้ทราบว่าโปรตีนคาวีโอลิน-1 มีปฏิสัมพันธ์กับโปรตีนเอ็มซีแอล-1 และช่วยป้องกันการสลายของโปรตีนเอ็มซีแอล-1 ผ่านทางการยับยั้ง ubiquitin-proteasome ในระหว่างที่เซลล์หลุดออกจากที่ยึดเกาะ งานวิจัยนี้พบว่าระดับโปรตีนเอ็มซีแอล-1 และ Cav-1-Mcl-1 complex มีระดับสูงขึ้นในเซลล์ที่มีการแสดงออกของคาวีโอลิน-1 มาก แต่พบว่ามีระดับที่ลดลงในเซลล์ที่มีแสดงออกของคาวีโอลิน-1 น้อย ผลการศึกษายังแสดงให้เห็นว่าการเกิด Mcl-1 ubiquitination ยังลดลงหากมีระดับของโปรตีนคาวีโอลิน-1 มาก และให้ผลตรงกันข้ามหากในเซลล์มีระดับของโปรตีนคาวีโอลิน-1 น้อยลง งานวิจัยนี้ได้แสดงให้เห็นบทบาทใหม่ของโปรตีนคาวีโอลิน-1 ในการควบคุมกันตายแบบอนอยคิสผ่านทางการมีปฏิสัมพันธ์กับโปรตีนเอ็มซีแอล-1 ซึ่งส่งผลให้โปรตีนเอ็มซีแอล-1 มีการสลายตัวน้อยลง ซึ่งทำให้เกิดความเข้าใจเกี่ยวกับกลไกการเกิดการแพร่กระจายของเซลล์มะเร็งปอดและอาจนำไปสู่การเป็นเป้าหมายสำคัญในการพัฒนายาเพื่อยับยั้งโปรตีนดังกล่าว

ภาควิชาวิทยาการเภสัชกรรมและเภสัชอุตสาหกรรม ลายมือชื่อนิสิต.....

สาขาวิชา.....เทคโนโลยีเภสัชกรรม..... ลายมือชื่อ อ.ที่ปรึกษาวิทยานิพนธ์หลัก.....

ปีการศึกษา.....2554…….....

 # 5177105533 : MAJOR PHARMACEUTICAL TECHNOLOGY

KEYWORDS : CAVEOLIN-1 / MCL-1 / ANOIKIS / LUNG CANCER CELLS

PREEDAKORN CHUNHACHA: KINETICS AND CORRELATION OF CAVEOLIN-1 AND MCL-1 PROTEINS WITH LUNG CANCER CELL ANOIKIS. ADVISOR: ASST PROF. PITHI CHANVORACHOTE, Ph.D., 160 pp.

Both Caveolin-1 (Cav-1) and Mcl-1 have been implicated in the regulation of cancer cell anoikis but their relationship and underlying mechanisms of regulation are not known. By using the kinetics, the present study demonstrated that Cav-1 and Mcl-1 both regulate anoikis in non small cell lung cancer cells (NSCLCs). Modulation of Cav-1 and Mcl-1 levels by overexpressing or short hairpin containing plasmids was shown to influence the cell viability and apoptosis after detachment in H460 cells which indicates the pivotal role of Cav-1 and Mcl-1 in regulating anoikis in this cancer cell model. The western blot results have been shown that the levels of Cav-1 and Mcl-1 were gradually reduced over time of detachment. Correlation analysis shows that the reduction of these two proteins has closely correlated with Pearson correlation $(r) = 0.986$ (p-value< 0.0001) leading to the hypothesis of the interaction between Cav-1 and Mcl-1 proteins. Immunoprecipitation and immunofluorescence studies suggested that Cav-1 interacted with Mcl-1 and prevented it from degradation via the ubiquitin-proteasome pathway during cell anoikis. Mcl-1 and Mcl-1-Cav-1 complex were highly elevated in Cav-1 overexpressing cells, but were greatly reduced in Cav-1 knockdown cells. Consistent with this finding, it was found that Mcl-1 ubiquitination was significantly attenuated by Cav-1 overexpression but increased by Cav-1 knockdown. Together, our results indicate a novel role of Cav-1 in anoikis regulation through Mcl-1 interaction and stabilization, which provides a new insight to the pathogenesis of metastatic lung cancer and its potential treatment.

Department: Pharmaceutics and Industrial Pharmacy. Student's Signature Preedakorn Chunhacha.
Field of Study: Pharmaceutical Technology..... Advisor's Signature Pithi Chanvorachote
Academic Year:.....2011.....

ACKNOWLEDGEMENTS

Though only my name appears on the cover of this dissertation, a great many people have contributed to its production. I owe my gratitude to all those people who have made this dissertation possible and because of whom my graduate experience has been one that I will cherish forever.

My deepest gratitude is to my advisor, Asst. Prof. Dr. Pithi Chanvorachote. I have been amazingly fortunate to have an advisor who gave me the freedom to explore my own idea, and at the same time the guidance to recover when my steps faltered. He taught me how to question thoughts and adequately express ideas. His patience and support helped me overcome many crisis situations and finish this dissertation. I hope that one day, if I have an opportunity to be like him, I would become as good an advisor to my students as Dr. Pithi has been to me.

I am grateful to Prof. Dr. Yon Rojanasakul for his encouragement and practical advice. I am also thankful to him for reading my manuscript, commenting on my views and helping me understand and enrich my ideas.

I am also indebted to the members of the molecular biology laboratory, Faculty of Pharmaceutical Sciences, Chiba University, Japan, with whom I have interacted during the course of my Chula-Chiba student exchange program. Particularly, I would like to acknowledge Prof. Dr. Naoto Yamaguchi, Assoc. Prof. Dr. Yuji Nakayama and Asst. Prof. Dr. Yasunori Fukumoto for the many valuable discussions that helped me understand my research area better. I am indebted to all

my Japanese friends who gave me the warmest welcome and their unforgettable treatment throughout my living in Japan.

Many friends have helped me stay sane through these difficult years. Their support and care helped me overcome all difficulties and stay focused on my graduate study. I greatly value their friendship and I deeply appreciate their belief in me. I would like to express my sincere thanks to Dr. Varisa Pongrakananon, Mr. Chatchai Chaotham, Dr. Suidjit Luanpitpong, Mr. Hasseri Halim, Dr. Pimuma Rungtabnapa and last but not least, Miss Kanuengnit Choochuay who always stay beside me during the day with long experiments which sometimes ended up with nothing. I also extend my deepest gratitude to all my younger friends that gave me tons of laughing during this endeavor.

Most importantly, none of this would have been possible without the love and patience of my family. My family to which this dissertation is dedicated, has been a constant source of love, concern, support and strength all these years. I would like to express my heart-felt gratitude to my father Mr. Boonchoo Chunhacha and my mother Mrs. Vadjana Chunhacha who always believe in me and encourage me even in the hard time of my life since my undergrad until Doctoral degree.

CONTENTS

Page

LIST OF TABLES

Table **Page**

Page

Page

Page

LIST OF FIGURES

Figure **Page**

Page

Page

Page

LIST OF ABBREVIATIONS

%	= percentage
°C	= degree Celsius
µM	= micromolar
ANOVA	= analysis of variance
Cav-1	= caveolin-1
Mcl-1	= myeloid cell leukemia sequence 1
CO_2	= carbon dioxide
DMSO	= dimethyl sulfoxide
et al.	= et alibi, and others
g	= gram
h	= hour, hours
min	= minute (s)
ml	= milliliter
mM	= millimolar
PI	= propidium iodide
LAC	= lactacystin
NSCLC	= non-small cell lung cancer
SCLC	= small cell lung cancer
HCav-1	= H460 cell clone that overexpressed Cav-1
shCav-1	= H460 cell clone that down-regulated Cav-1

HMcl-1	= H460 cell clone that overexpressed Mcl-1
shMcl-1	= H460 cell clone that down-regulated Mcl-1
PAGE	= polyacrylamide gel electrophoresis
Poly-HEMA	= poly(2-hydroxyethylmethacrylate)
FBS	= fetal bovine serum
SDS-PAGE	= sodium dodecyl sulfate-polyacrylamide gel electrophoresis
TBST	= Tris-buffered saline, 0.1% Tween 20
Ub	= ubiquitin
XTT	= 2,3-Bis(2-methoxy-4-nitro-5-sulfophenyl)-2H-tetrazolium-5-carboxanilide inner salt
CSD	= Caveolin-1 scaffolding domain
Phe	= Phenylalanine
Tyr	= Tyrosine
Trp	= Tryptophan
PI3K/Akt	= phosphatidyl inositol-3-kinase and protein kinase B pathway
GSK-3β	= glycogen synthase kinase 3 beta
shRNA	= short hairpin RNA
kDa	= kilodaltons
RPMI	= Roswell Park Memorial Institute's medium
S.D.	= standard deviation
U	= unit

CHAPTER I

INTRODUCTION

Resistance to anoikis, a form of apoptotic cell death induced by loss of cell anchorage to extracellular matrixes, has been accepted as a key determinant of cancer cell metastasis [Boisvert et al., 2009; Chiarugi and Giannoni, 2008]. Recently, a number of proteins have been identified to facilitate anoikis resistance in various cancer types. Among these, Caveolin-1 (Cav-1) has perhaps received the most attention since its expression has been linked to cancer progression and aggressiveness [Thompson et al., 2010]. Although, some evidence have suggested the tumor suppressing role of Cav-1 [Engelman et al., 1998; Hurlstone et al., 1999; Racine et al., 1999], in lung cancer Cav-1 potentiates cancer progression and aggressiveness. Cav-1 expression has been shown to relate to poor prognosis and reduced tumor-free periods in lung cancer patients [Ho et al., 2007]. Moreover, Cav-1 was shown to facilitate metastasis and induce anoikis resistance in lung carcinoma cell lines [Chanvorachote et al., 2009; Rungtabnapa et al., 2011; Yeh et al., 2009]. Not only does Cav-1 play a role in cell death and survival, but also in cell migration [Luanpitpong et al., 2010], invasion [Tang et al., 2011], and lipid transportation [Quest et al., 2004]. Cav-1 was reported to exhibit scaffold function and to be essential in regulating several proteins such as endothelial nitric oxide synthase (eNOS), G protein subunit, and non receptor tyrosine kinases [Lajoie and Nabi 2010], supporting the wide range of activities of this protein in various cellular processes.

The pro-survival member of Bcl-2 family protein named myeloid cell leukemia sequence 1 (Mcl-1) has recently been implicated as a key regulator of cell anoikis [Simpson et al., 2008]. In melanoma, the depletion of Mcl-1 renders mutant B-RAF melanoma cells sensitive to anoikis [Boisvert et al., 2009]. Likewise, Mcl-1 degradation and Bim up-regulation are a critical determinant of anoikis initiation in wild-type and c-Src-transformed NIH3T3 fibroblast cells. Increasing evidence also indicates the role of Mcl-1 in progressive prostate cancer [Zhang et al., 2010], supporting its clinical significance in cancer metastasis.

Not only Cav-1 and Mcl-1 share the similar function in negatively regulating cancer cell anoikis, but also the dramatic decrease of these protein levels after cell detachment has been reported [Chanvorachote et al., 2009; Woods et al., 2007]. It is widely accepted that the down-regulation of Cav-1 and Mcl-1 after cell detachment is mainly through ubiquitin-proteasomal degradation, and such protein down-regulations may responsible for the anoikis of the cells [Woods et al., 2007; Chanvorachote et al., 2009; Rungtabnapa et al., 2011].

Both of Cav-1 and Mcl-1 have been identified as the key survival proteins in non small cell lung cancer (NSCLC) [Sunaga et al., 2004; Borner et al., 1999]. In order to clarify the influence of Cav-1 and Mcl-1 reductions on NSCLCs anoikis, kinetic of this cellular response over times is introduced. Not only the kinetic requires the detection of several time points which strongly ensures the relevance of factor in regulation of cell process, but also provides the regression coefficients which are a constant value that allow suitable comparison.

Since the intervention data in between Cav-1 and Mcl-1 proteins are still far from clear, and there is no solid evidence indicating anoikis resisting influence of these proteins, the present study thus aims to investigate the following perspectives;

1. The kinetic of cell anoikis after detachment influencing by an alteration of Cav-1 and Mcl-1 protein levels
2. The correlation of Cav-1 and Mcl-1 reduction after cancer cell detachment
3. The intervention in between Cav-1 and Mcl-1 that involve anoikis regulation and underlying mechanism

By comparing the regression coefficient, this study will precisely elucidate the critical proteins that regulate anoikis in NSCLC. The study also provide the information of the key proteins in regulating anoikis in NSCLC that is an initial step in the development of cancer marker which then might be a drug target for the treatment of NSCLC. All experiment of the present study used non-small cell lung carcinoma H460 cells as a model to determine the effect of the proteins that regulate anoikis.

CHAPTER II

Literature Review

1. Lung cancer and metastasis

Lung cancer is the leading cause of cancer death in the United States and throughout the world. Non-small-cell lung cancer (NSCLC), one category of lung cancer, is accounted for 80% of overall lung cancer that had been diagnosed. From 1995 to 1999, cigarette smoking and exposure to secondhand smoke accounted for approximately 440,000 annual deaths in the United States. Worldwide, approximately 4 million people die annually from tobacco-attributable diseases, and this number is predicted to rise to 8.4 million by 2020 [Rosell et al., 2004].

1.1 Classification of lung cancer

Base on histological type, lung cancer can be classified into different subgroup which is necessary for clinical management and prognosis of the disease. The majority of lung cancers are carcinomas, malignancies that arise from epithelial cells. The two most prevalent histological types of lung carcinoma, categorized by the size and appearance of the malignant cells scored by a histopathologist under a microscope: non-small cell and small-cell lung carcinoma [Travis et al., 1995]. The non-small cell type is the most prevalent type among various lung cancer cells (Table 1).

Histological type	Frequency (%)
Non-small cell lung carcinoma	80.4
Small cell lung carcinoma	16.8
Carcinoid	0.8
Sarcoma	0.1
Unspecified lung cancer	1.9

Table 1: Frequency of histological types of lung cancer

Non-small cell lung cancer (NSCLC) frequently presents as advanced, metastatic disease that is primarily treated with systemic chemotherapy. In addition, many patients with earlier stage, potentially curable, NSCLC relapse at distant metastatic sites, resulting in the dismal 5-year survival rate of only 15% for all patients with this disease [**Rachel et al., 2009].** Primary NSCLC themselves most commonly metastasize to the adrenal glands, pancreas, liver, brain, and bone [**Rachel et al., 2009;** Vaporciyan 2000]. These highlight the metastatic potential of NSCLC which turns from curable to the difficult to treat disease.

1.2 Cancer metastasis

During the development of most cancers, rapid cell growth generated some malignant strain that have their abilities to dissociate from their primary tumor, invade adjacent tissue and survive in the blood circulation or lymphatic system that allow them to travel to distant site and settle at new location and then form new colonies. This phenomenon can be termed as metastasis, which is the cause of 90% of human cancer deaths. [Hanahan and Weinberg 2000].

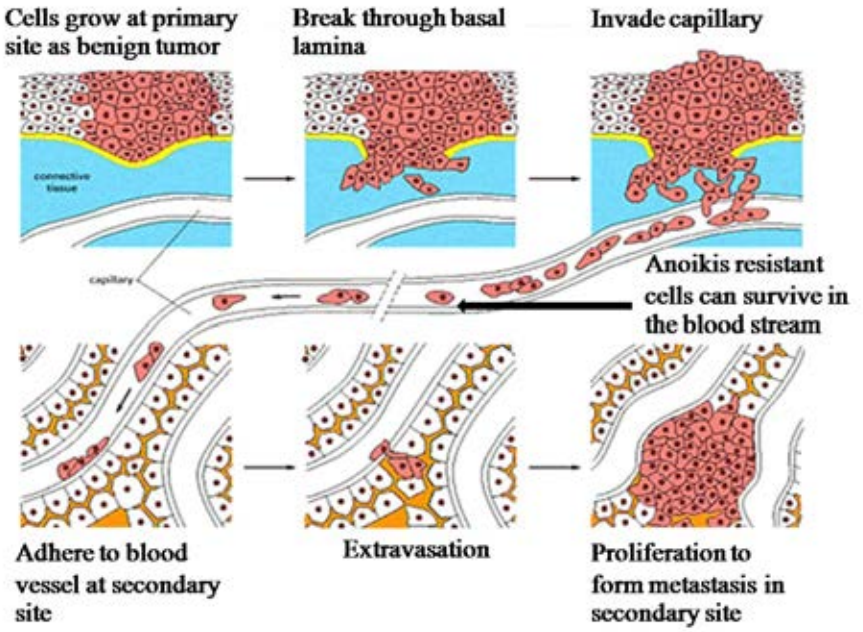

Figure 1 Multistep of metastasis [Alberts et al., 2008]

Metastasis is exceedingly complex processes, and their genetic and biochemical determinants remain incompletely understood. As a barrier to developing metastases, cells normally undergo apoptosis after they lose contact from neighbouring cells or from their extra cellular matrix (ECM). This cell death process has been termed ‘‘anoikis” [Fig. 1] which is necessary to maintain normal cell growth. Tumor cells that acquire malignant potential have developed mechanisms to resist anoikis and thereby survive after detachment from their primary site and while travelling through the lymphatic and circulatory systems [Craig et al., 2008].

2. Anoikis and mechanisms of anoikis resistance

2.1 Integrin is the key regulator that initiates anoikis

As anoikis resistant capability is the key determinant that enable cancer cells to succeed their colonization at the secondary site, intensive investigate to explore the mechanisms of anoikis resistance have been took place but still remain elusive and may dependent on particular context. The change in protein expression especially the marker of epithelial to mesenchymal transition (EMT) is one mechanism to explain how the cancer cells become anoikis resistance [Nieman et al., 1999]. Another explanation dealing with the integrins which sense the mechanical forces between cells and ECM, however, when the cell detached from their ECM, the unligated integrins will act as a cell death promoters through the integrin-mediated death (IMD) process [Stupack et al., 2001]. However, integrin signaling can be ignored and the cells can bypass the survival signal that obtained from constitutively activate downstream pro-survival signals, such as PI3K, Ras-Erk, NF-kB and Rho GTPase [Tsuji et al., 2009]. These resulted from autocrine secretion of growth factors, such as basic fibroblast (bFGF), hepatocyte growth factor (HGF) [Li et al., 2003].

In clinical study of NSCLC, two main types of protein that frequently found overexpressed in this type of tumor were Caveolin-1 (Cav-1) and Myeloid cell leukemia -1 (Mcl-1) protein [Ho et al., 2007; Song and Coppola, 2005]. However, the anoikis resistance mechanism regarding with Cav-1 and Mcl-1 in NSCLC is still far from clear. In general, the mechanism (s) involved in making cancer cells anoikis-resistant may comprise the stimulation of alternative (i.e. non-ECM) survival signals and/or the inhibition of apoptotic pathways.

3. **Caveolin-1**

3.1 **Definition and function**

Caveolin-1, a 22-kDa scaffold protein, is the essential constituent of caveolae, flask-shaped (50–100 nm) invaginations that can occupy up to 20% of the plasma membrane (Fig. 2). Caveolin-1 belongs to a highly conserved gene family and is co-expressed with caveolin-2 in cells and tissues of various origins including mesenchymal, endo/epithelial, neuronal/glial. The caveolin-1 gene is composed of three exons and alternatively translated into the endoplasmatic reticulum (ER) as a full-length 178 amino acids α-isoform and a β-isoform lacking the first 32 aa [Fig. 2]. Structural topology of caveolin-1 is membrane spanning, where both N-termini and C-termini are exposed to the cytoplasm. A central membrane spanning domain (TMD), C- and N-terminal membrane attachment domains (MAD) and three palmitoyl groups at the C-terminus enable its insertion into the inner leaflet of the membrane. Caveolin-1 binds to cholesterol and sphingolipids within ‘‘lipid rafts” which are considered as specialized ‘‘detergent-insoluble cholesterol- and glycolipid-rich” (DIG) membrane microdomains.

When cav-1 completely translated and moved out from endoplasmic reticulum as an monomers, they assemble into higher molecular weight to become homo or hetero oligomers by using their oligomerization domain (amino acid 61-101), resulting in the forming of striated caveolar coat structure named caveolae. This particular structure plays an important role in regulating versatile cellular transport

processes such as cholesterol efflux, clathrin-independent endocytosis, lipid and protein sorting [Sanna et al., 2007]. Moreover, Cav-1 was found in various vesicle-like compartment inside the cell including caveosome, exocytic vesicle, cytoplasmic/lipid-droplet associated form. Cav-1 also reported to localize at nuclear localization by chromatin-immunoprecipitations assay, however, this finding still needs further validation [Williams and Lisanti, 2005].

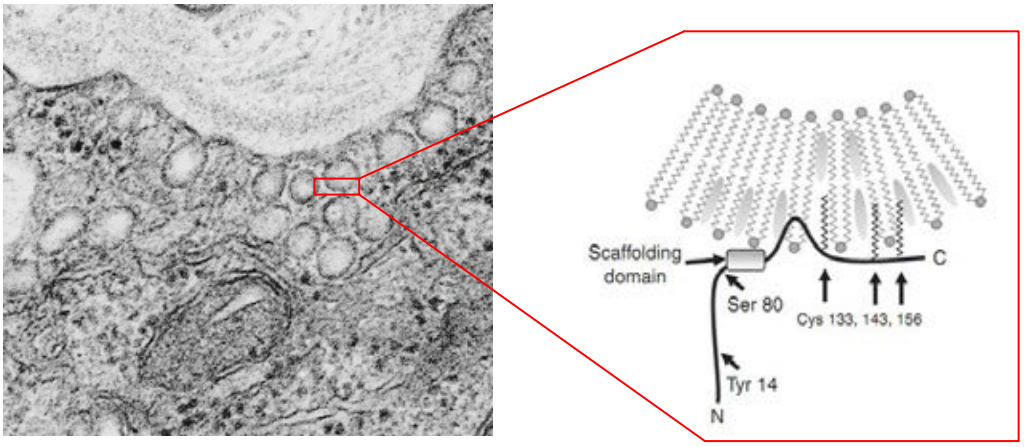

Figure 2 Caveolae structure and caveolin-1 protein. [Parat, M.D., 2009]

3.2 Caveolin-1 is an interacting molecule

Domain that exerts the interaction between cav-1 and another partner molecules is caveolin-1 scaffolding domain (CSD) (residues 82-101). Interestingly, only a select group of peptides showed high affinity binding to the CSD; several lines of studies showed that the prefer sequences matched the following motifs: ΦXΦXXXXΦ, ΦXXXXΦXXΦ, ΦXΦXXXXΦXXΦ, where Φ is an aromatic residue (Phe, Tyr or Trp). Furthermore, a study of known cav-1 interacting molecules

demonstrated that at least one such motif could be found in their sequence, indicating that these regions are particularly important for direct interaction with the cav-1 [Couet et al., 1997]. Such interactions are mostly inhibit the interacting protein function if that interaction occurs at the active catalytic domain, the example of this inhibition effect from direct interaction of cav-1 is practical significance in the case of tyrosine and serine kinases.

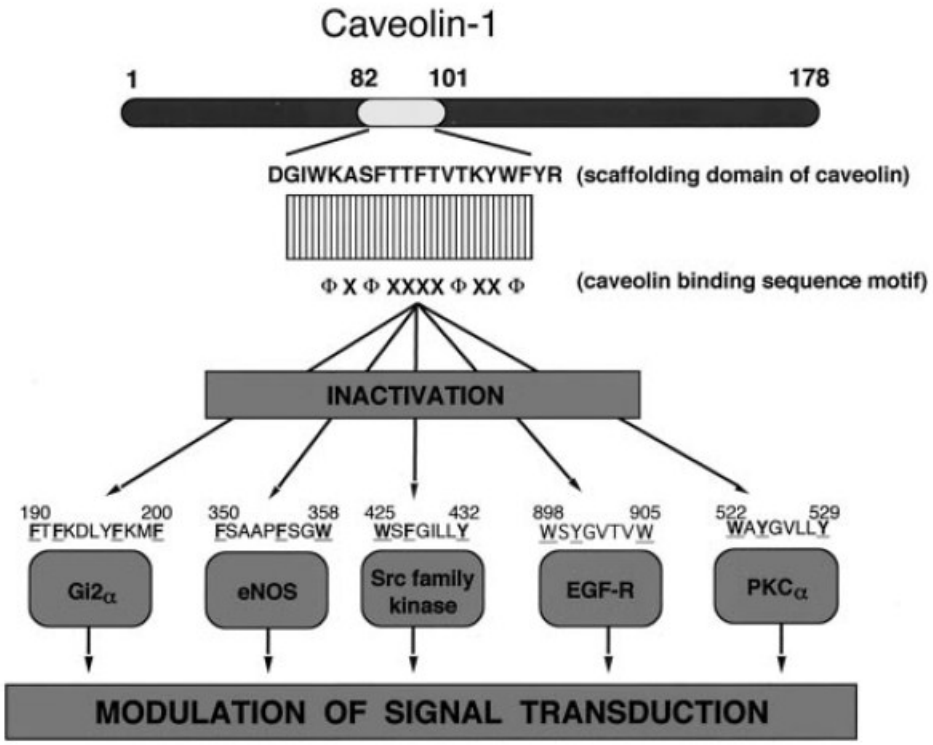

Figure 3 Scaffolding domain of Cav-1 indicates the caveolin binding motif that cause the modulation of various down-stream signaling [Razani, 2002].

3.3 Caveolin-1 and tumorigenesis

Several lines of evidence including the *in vivo* studies have shown that Cav-1 expression may attribute to the aggressiveness of cancer. Evidences regarding the role of Cav-1 in promoting drug resistance were demonstrated in human lung carcinoma, ovarian caricinoma, colon adenocarcinoma and breast adenocarcinoma cell lines, all of these drug resistant variants were found overexpression of Cav-1 [Lavie et al., 1998]. Morover, highly invasive phenotype of lung adenocarcinoma had elevated Cav-1 levels [Ho et al., 2002]. Strikingly, secreting Cav-1 from prostate cancer cells were taken up by tumor cells and endothelial cells may promote tumor angiogenesis [Tahir et al., 2001]. Studies in lung metastases of mice with prostate cancer were found to have increased Cav-1 expression compared with the primary tumor. In human, the lymph node metastases of human prostate and breast cancers were shown to have higher Cav-1 level than those of normal epithelial tissues from prostate and breast [Yang et al., 1998]. These in vivo studies highlighted the role of Cav-1 as an oncogenic, premetastatic potential. Indeed, several types of cancer in human patients having increased in Cav-1 level were found decreasing in survival rate. However, contradictory results have also been obtained from mice with breast cancer, genetic deletion of Cav-1 in this animal model induces the increasing in tumorigenesis and lung metastasis. To reconcile some of these contradictory finding, some of the model also propose the Cav-1 levels vary during the course of tumor progression. In early stage, the down regulation of Cav-1 is necessary for facilitating oncogenic transformation, however, in some tumor, the reexpression of Cav-1 at later stage possibly confer to its potential to become drug resistance and metastatic cancer.

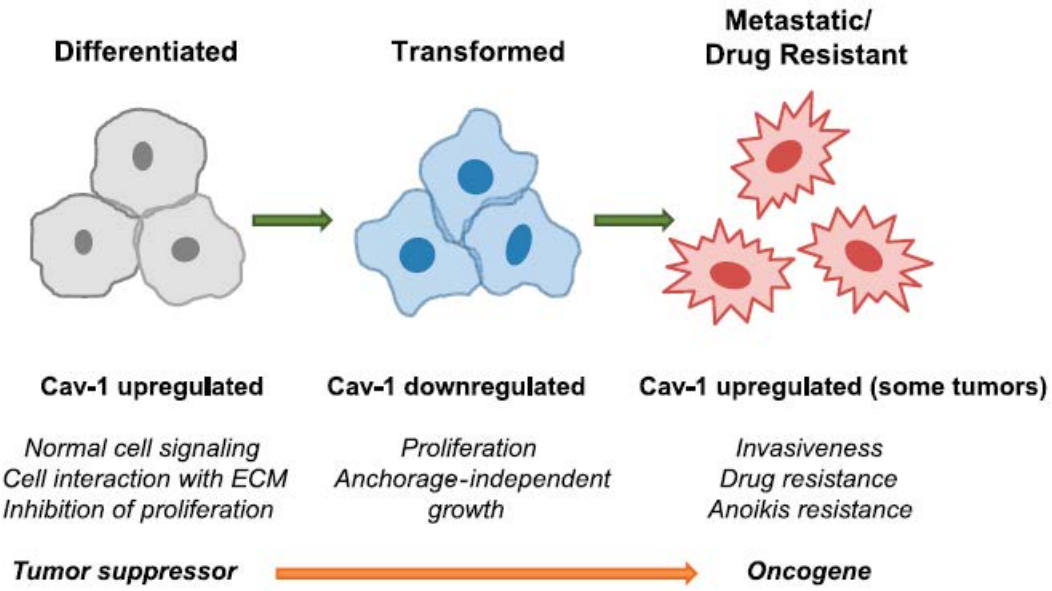

Figure 4 Different role of Cav-1 depending on the stage of oncogenic transformation and extent of tumor progression [Lloyd and Hardin, 2011]

3.4 Caveolin-1 in non small cell lung cancer

Even though cav-1 is abundantly expressed in normal human epithelial lung culture, but its role in regulating cell survival and metastatic potential may different between SCLC and NSCLC. In SCLC, cav-1 expression was found reduce or absent in 95% of small cell lung cancer. On the other hands, Cav-1 expression in NSCLC was retained in this cancer subtype exceed to 76% of overall NSCLC studied. In addition, Cav-1 expression in NSCLC was found tightly correlate with the cell proliferation and metastatic potential assessed by liquid colony formation assay [Sunaga, 2004]. Clinicopathologic profiles of pulmonary squamous cell carcinomas,

which are NSCLC subtypes, were shown that Cav-1 expression is associated with poorer prognosis than those in Cav-1 negative group [Yooa et al., 2003]. Additional studies on the role of Cav-1 had also extended to the drug resistance capacity in NSCLC, in advanced NSCLC patients treated with gemcitabine-based chemotherapy were found the correlation of Cav-1 expression with drug resistance and poor prognosis.

3.5 Caveolin-1 and anoikis resistance

In the metastatic potential point of view, the ability of cancer cells to become metastasized may depend on an extent of anoikis resistance. Current evidences demonstrated that Cav-1 seems to regulate anoikis resistance in various *in vitro* studies. The studies performed in breast cancer MCF-7, the overexpression of Cav-1 induces the cells to become fully resistant to anoikis by inhibiting the activation of p53 which then further suppressed $p21^{WAF1/Cip1}$ [Ravid et al., 2006].

In attached condition, Integrin engagement normally provide survival signal through phosphatidyl inositol-3-kinase (PI3K)/Akt signaling by sensing the mechanical forces arising from the extracellular matrix (ECM). Integrins are a family of αβ-heterodimeric cell-surface receptors that mediate attachment to the extracellular matrix. Integrins associate with signaling molecules in the focal adhesion complex, which serves as a signaling device and provides a direct link to the cytoskeleton [Rungtabnapa et al., 2011]. As a consequence, when the cells undergo detachment

from primary site, the loss of integrin engagement will further reduce survival signal through PI3K/Akt and culminate in apoptosis.

It is well documented that cav-1 can activate PI3K/Akt pathway which promote the cell survival. Cav-1 has been shown to interact with and inhibit serine/threonine protein phosphatases PP1 and PP2A, leading to sustained Akt activation and inhibition of apoptosis by thapsigargin in prostate cancer cells [Kozopas et al., 1993]. In addition, a transient increase in the activity of the tyrosine kinases c-Src and c-Fyn after the detachment of intestinal epithelial cells was shown to be mediated by PI3K pathway and Cav-1. This transient activation of Src-family kinases (SFK) plays crucial role in the transient protection against anoikis in these cell [Loza-Coll et al., 2005]. Taken together, cav-1 promotes anoikis resistant in cancer cells by providing survival signal through PI3K/Akt pathway when the cells lose their integrin engagement upon detachment.

4. Myeloid cell leukemia-1

4.1 Definition and function

Mcl-1 (myeloid cell leukemia 1) is a pro-survival member of the Bcl-2 family that was initially identified as an immediate-early gene expressed during PMA-induced differentiation of ML-1 myeloid leukemia cells [Vaux et al., 1988]. Mcl-1 was identified sequence similarity to the previously known pro-survival protein Bcl-2. Bcl-2 family protein promoted oncogenesis regarding its abilities of maintaining cell

viability through inhibition of apoptosis [Lutz, 2000]. According to the characteristic of Bcl-2 family proteins that can regulate apoptosis, virtually all malignancies were found to be dysregulated of Bcl-2 family expression.

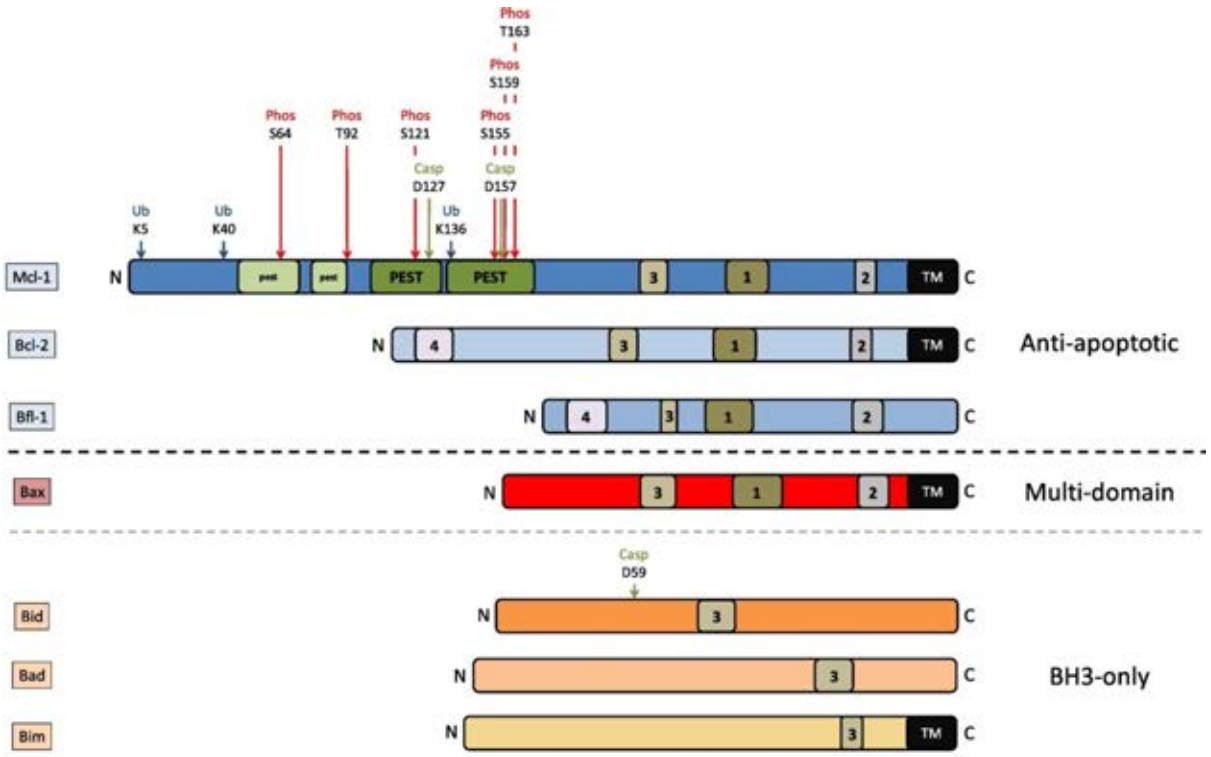

Figure 5 Structure of Mcl-1 protein, to scale, showing the relative positions of the functional regions and sites of post-translational modification including ubiquitination (Ub),caspase cleavage (Casp), and phosphorylation (Phos). These include the Bcl-2 homology domains (number 1-4), two weak (lower case) and two strong (upper case) PEST sequences. A schematic of a representative selection of other members of the Bcl-2 family are shown below, to scale, to compare the relative sizes and molecular organization of the proteins [Thomas et al., 2010].

Unlike others anti-apoptotic Bcl-2 family members, Mcl-1 contained 3 putative BH domains resembles to proapoptotic protein Bax. However, its large N-terminal region contained regulatory motif that could participated in its anti-apoptotic function (Fig. 5). Mcl-1 differs from its pro-survival relatives in its larger size of 350 residues, as compared to Bcl-2 at 239 residues (Fig. 4) and Bcl-2 like protein X (Bcl-X_L) at 233 residues. Residues 170–300 of Mcl-1 share a great deal of structural and functional homology to both Bcl-2 and Bcl-X_L, containing its three BH domains (Bcl-2 and Bcl-X possess 4), which confer the ability to heterodimerize with other family members [Lutz, 2000]. The ability of Mcl-1 that can inhibit apoptosis involved its ability to sequester proapoptotic proteins Bcl-1 homologous antagonist killer (Bak) and Bcl-2-associated protein X (Bax) which localized at the mitochondrial membrane and in the cytoplasm, respectively. Both Bak and Bax trigger the release of cytochrome c into the cytoplasm by their abilities to form pores in the mitochondrial membrane. The released cytochrome c induces the activation of a family of cysteine proteases named caspase which are responsible for the degradation of many macromolecules that were observed during the apoptotic processes. The interaction of Mcl-1 with the subset of BH3-only Bcl-2 family protein can result in different apoptotic outcome, if Mcl-1 interacts with BH3-only pro-apoptotic protein, it will inhibit Bak and Bax polymerization and prevent apoptosis. On the other hands, the Mcl-1 repressing effects on the polymerization of Bak and Bak can be reduced by the degradation of Mcl-1 or the interaction with another subset of BH-3 only protein, which further allow the release of Bak and Bax from Mcl-1 and promotes apoptosis. Because Mcl-1 sometimes found to be localized at mitochondrial membrane, the ability of Mcl-1 to be localized at the membrane could be due to its transmembrane

domain at the C-terminal portion of Mcl-1, the deletion of this region inhibits membrane insertion and localization of the protein [Akgul et al., 2000].

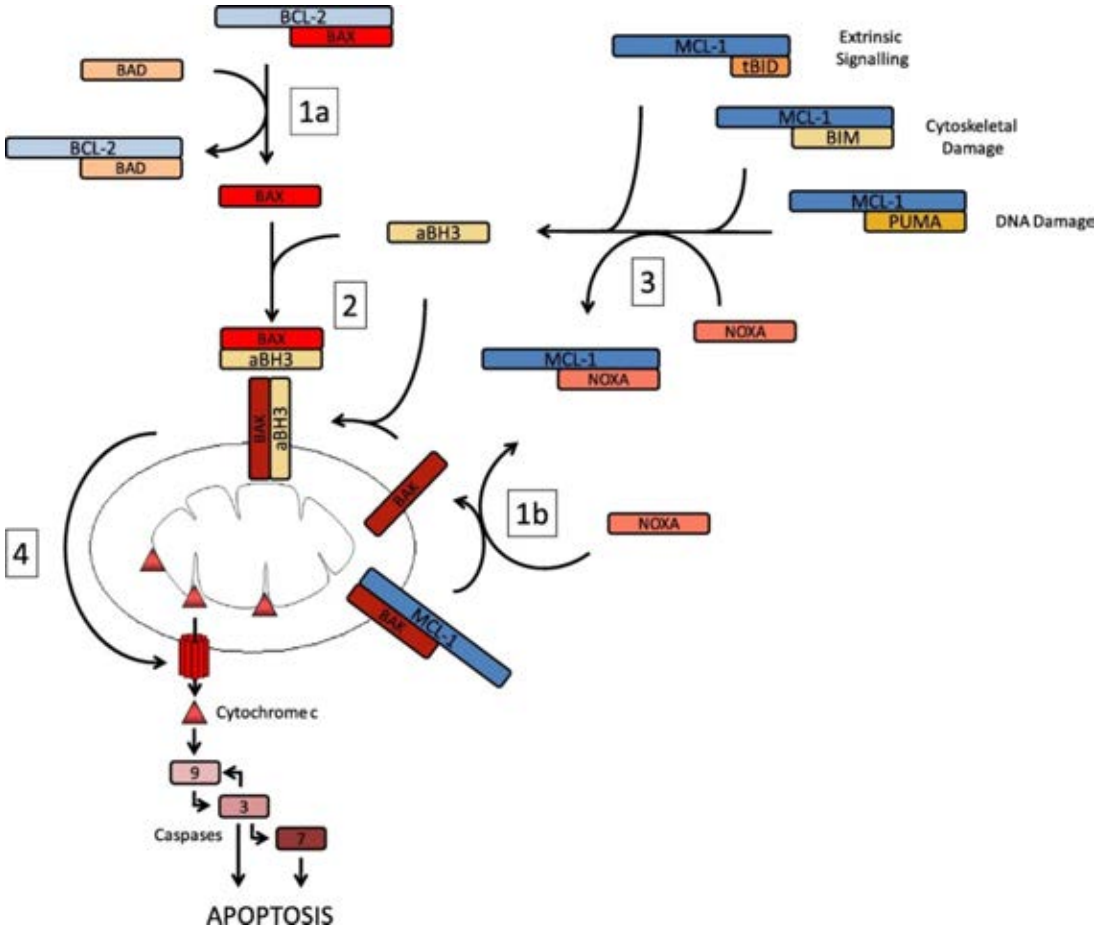

Figure 6 Mcl-1 function as anti-apoptotic. Proapoptotic Bax and Bak can be prevented to form homo-oligomerization by interact with various anti-apoptotic Bcl-2 family members such as Mcl-1. In the presence of BH3 inactivator, the competitive inhibition allow the free cytosolic Bax or free mitochondrial membrane bound Bak. In the case of Bax, the association with BH3 activator proteins may be required for their conformational changes and targeting to the mitochondria. After successfully formed the homo-oligomerization of Bax and Bak this will generate outer mitochondrial membrane spanning pore which then permit the release of cytochrome c into

the cytoplasm, which triggers activation of the caspase cascade, and culminate in apoptosis [Thomas et al., 2010].

4.2 Mcl-1 is an interacting molecule

Several reports rely on the study of the interaction between Mcl-1 and various Bcl-2 family protein partners. As mentioned earlier, Mcl-1 was found to interact with Bak and prevent its oligomerization. Moreover, Mcl-1 was found to selectively interacts with the BH3-only proteins, Bim, tBid, Bik, PUMA and NOXA (Shimazu et al., 2007; Han et al., 2007; Clohessy et al., 2006; Chen et al., 2005; Willis et al., 2005]. These interaction between BH-3 only proteins and Mcl-1 will displaced Bak from Mcl-1 leading to Bak oligimerization and cytochrome c release. Apart from interactions among Bcl-2 family proteins, the interaction between Mcl-1 and mitochondrial import receptor Tom70 targets Mcl-1 to mitochondria and such interaction requires EELD motif which is the internal domain of Mcl-1 [Chou et al., 2006].

4.3 Mcl-1 and tumorigenesis

Since Mcl-1 was identified as an early response gene induced during the differentiation of ML-1 human myeloblastic leukaemia cells, it draws first attention on its role in haematological malignancies. In the *in vivo* model, transgenic mice expressing Mcl-1 under the control of the endogenous Mcl-1 promotor show enhanced survival of B and T cells which finally developed myeloid malignancy

[Zhou et al., 2001]. Antisense experiments have demonstrated that the expression of Mcl-1 is required for the multiple myeloma cells survival [Zhang et al., 2002]. Likewise, in the clinical treatment of plasma cell malignancy, a *mcl-1* antisense therapeutic strategy has been more advocacy than the *bcl-2* antisense [Derenne et al., 2002]. However, the role of Mcl-1 in cancer tumorigenesis is not specific to only haematological malignancies, in various kind of solid tumors were found the elevated level of Mcl-1 and its expression also impact on the cancer cell aggressiveness. In hepatocellular carcinoma (HCC), the ectopic expression of miR-101 significantly inhibited the ability of hepatoma cells to form colonies *in vitro* and to develop tumors in nude mice. This miR-101 was found that it may exert its proapoptotic function in HCC by targeting Mcl-1 which was shown by the reduction of Mcl-1 endogenous protein level and repressed the expression of luciferase carrying the 3'-untranslated region of Mcl-1 [Su et al., 2009]. In another cancer type, Mcl-1 was strikingly linked with poor prognosis of human breast cancer, in which the high level of Mcl-1 was related to high tumor grade and poor survival of breast cancer patients. Moreover, in various kinds of cancer cell line including breast cancer, Mcl-1 stabilization by GSK-3β inactivation that is involved with the phosphorylation at Ser^{9} allows Mcl-1 to be more pronounce effects in tumorigenesis in that such cancer [Ding et al., 2007].

4.4 Mcl-1 and non small cell lung cancer

Evidence in the role of Mcl-1 on NSCLC tumorigenesis stem from the study of NSCLC resected from the patients. In the group of specimens that were evaluated, Mcl-1 seems to be overexpressed in larger proportion compared to Bcl-2

overexpressed subgroup [Borner et al., 1999]. NSCLC cell lines including A549, H460 and H1299 that are abundant in Mcl-1 protein were found dramatically increase in apoptotic rate when using antisense targeting Mcl-1 oligonucleotide. Reduced Mcl-1 level can sensitize NSCLC to apoptosis induced by cytotoxic agents. Moreover, NSCLC taken from clinical specimens were found to have elevated level of Mcl-1 protein when compared to normal adjacent lung tissue [Song et al., 2005]. All of these evidences emphasize the role of Mcl-1 protein that is contributing to the tumorigenesis of NSCLC. However, some studies have suggested that Mcl-1 does not correlate with prognosis in NSCLC [Borner et al., 1999; Wesarg et al., 2007]. Recently, Allen *et al*. has reevaluated the prognostic value of Mcl-1 expression in NSCLC and found that Mcl-1 overexpression does correlate with poor patient's survival, but this impact was limited to the accompanying by the overexpression of MYC protein. Then, further study on the Mcl-1 in partner with Myc may be necessary to identify the detail mechanisms regulating each other and to assess their role in another form of such tumors.

4.5 Mcl-1 and anoikis resistance

Because Mcl-1 is the member of the Bcl-2 family protein, the role of Mcl-1 in anoikis regulation is relied heavily on the mitochondrial pathway. Upon cell detachment, the loss of signal from PI3K/Akt enable Bim releasing from dynein complex and then translocate to the mitochondria to support Bax, Bak oligomerization which then culminate in triggering cytochrome c release and caspase activation

[Akiyama et al., 2009]. However, in the present of sufficient amount of Mcl-1, it will sequester Bim at the mitochondrial membrane, thereby preventing activation of related BH3-only factors that function to induce apoptosis [Opferman et al., 2003]. Researchers found a tightly controlled balance between Mcl-1 and Bim, as Mcl-1 reduction was insufficient to stimulate Bax in the absence of Bim expression [Woods et al., 2007). Additionally, inhibition of Mcl-1 reduction and over-expression of Bim had opposite effects on cell survival; the first resulted in anoikis resistance, while the second induced a dose-dependent cell death response.

5. Cav-1 and Mcl-1 reduction allows anoikis initiation

As mentioned above on the involvement of Cav-1 and Mcl-1 on anoikis resistance capability, reducing level of these two proteins in detachment state might enable cancer cells to undergo anoikis. Evidences demonstrated that the reduction of Cav-1 or Mcl-1 can initiates anoikis [Rungtabnapa et al., 2010; Woods et al., 2007]. However, the reduction of these two proteins might due to the reduction in protein transcription or increase in the degradation.

5.1 Ubiquitin-proteasomal degradation

The ubiquitin-proteasomal degradation is the pathway that the cells use for protein destruction. For instance, when the protein subject to be destroyed, tagging of the particular protein by ubiquitin results in their destruction by proteasome.

Ubiquitin, is a small protein that able to form covalent attachment to target protein, is prepared for conjugation to other proteins by the ATP-dependent ubiquitin-activating enzyme (E1), which creates an activated, E1-bound ubiquitin that is subsequently transferred to one of a set of ubiquitin-conjugating (E2) enzymes. The E2 enzymes act in conjunction with accessory (E3) proteins. In the E3-E3 complex, called ubiquitin ligase, the E3 component binds to specific degradation signals, called degrons, in protein substrates, helping E2 to form a polyubiquitin chain linked to a lysine of the substrate protein. In this chain, the C-terminal residue of each ubiquitin is link to a specific lysine of the proceding ubiquitin molecule, producing a linear series of ubiquitin-ubiquitin conjugates. It is this polyubiquitin chain on a target protein that is recognized by a specific receptor in the proteasome.

There are roughly 30 structurally similar but distinct E2 enzymes in mammals, and hundreds of different E3 proteins that form complexs with specific E2 enzymes. The ubiquitin-proteasome system thus consists of many distinct but similarly organized proteolytic pathways, which have in common both the E1 enzyme at the "top" and the proteasome at the "bottom," and differ by the compositions of their E2-E3 ubiquitin ligases and accessory factors. Distinct ubiquitin ligases recognize different degradation signals, and therefore target distinct subsets of intracellular proteins for destruction [Alberts et al., 2008].

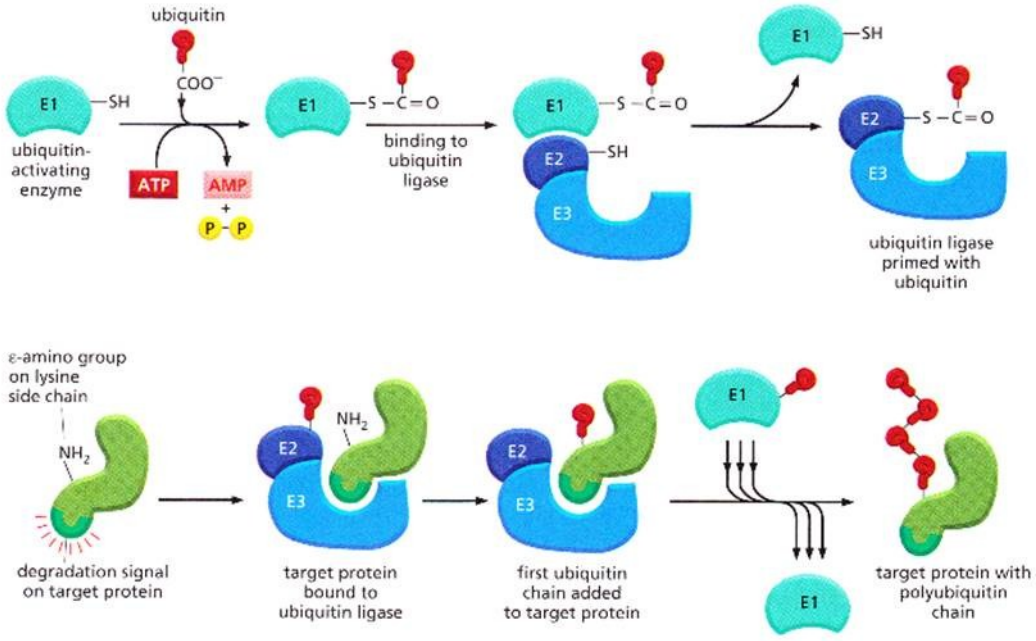

Figure 7 Ubiquitin and the marking of proteins with polyubiquitin chains.

[Alberts et al., 2008]

The proteasome cap recognizes a substrate protein that marked by a polyubiquitin chain and subsequently translocates it into the proteasome core, where it is digested. At an early stage, the ubiquitin is cleaved from the substrate protein and is recycled. Translocation into the core of the proteasome is mediated by a ring of ATP-dependent proteins that unfold the substrate protein as it is threaded through the ring and into the proteasome core [Prakash and Matouschek, 2004].

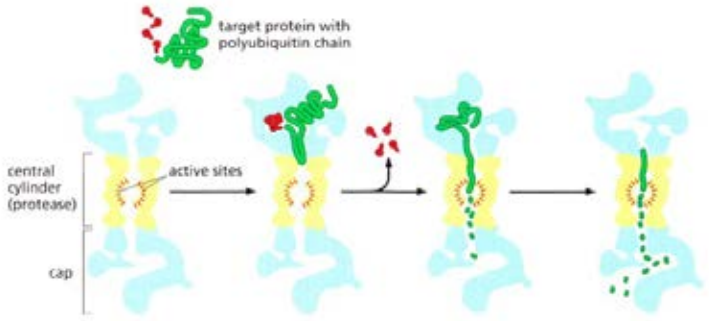

Figure 8 Processive protein digestion by the proteasome. [Prakash and Matouschek, 2004]

6. Mode of Cav-1 reduction during anoikis

When properly formed, caveolin-1 resides in the caveolae with slow turnover rate, however, cav-1 can participate in the fusion or fission process of the plasma membrane indicating the cav-1 dynamic. Some evidences showed that cav-1 may be targeted to endosomes, ubiquitinated, sequestered in intralumenal vesicles by the endosomal sorting complex and degraded in lysosome [Hayer et al., 2010]. Recently, the evidences show that targeting cav-1 to the lysosome is not necessary to alter the degradation rate of cav-1 but may participate for intracellular cholesterol trafficking [Mundy et al., 2012].

Once the cells detach from their extra cellular matrix, the mode of cav-1 degradation still not well documented, however, cav-1 degradation seems to be involved with the ubiquitin proteasomal system. After detachment, cav-1 reduction by non-transcriptional mechanism involving ubiquitin proteasomal degradation and nitric

oxide (NO) can promote cav-1 stability by interfering with cav-1 ubiquitination through the process regarding with protein S-nitrosylation [Chanvorachote et al., 2009]. Recently, evidences also highlight the role of hydrogen peroxide (H_2O_2) in reducing cav-1 ubiquitination after cell detachment which finally sustains cav-1 level during detachment [Rungtabnapa et al., 2011]. Considering the transcriptional regulation should also take into account in the anoikis context, however, cav-1 mRNA level was shown to be unchanged during cell detachment [Ravid et al., 2005; Chanvorachote et al., 2009]. Taken together, the mode of cav-1 reduction during cell detachment involve, at least in part, with ubiquitin proteasomal degradation pathway.

7. Mode of mcl-1 reduction during anoikis

Mcl-1 can be regulated through various post translational modifications which then abrogate its anti-apoptotic activities and promote subsequent degradation. Mcl-1 can be eliminated by caspase-mediated cleavage generating a potent proapoptotic protein that can enhance the cell death response [Michels et al., 2004]. The degradation of Mcl-1 has been reported to involve with E3 ubiquitin ligase (MULE) which poly ubiquitinates Mcl-1 to promote its degradation by the proteasome [Zhong et al., 2005]. This ubiquitination can also be directed by phosphorylation events involving the kinase GSK-3β at serine159 of Mcl-1 [Maurer et al., 2006]. Detachment rapidly degraded Mcl-1 via GSK-3β-dependent proteasomal pathway concomitant with transcriptionally up-regulate Bim expression in NIH3T3 cells [Woods et. al., 2007]. Moreover, phosphorylation of Mcl-1 by GSK-3β at consensus motif (Serine

155, Serine 159 and Threonine 163) which will lead to the association of Mcl-1 with the E3 ligase β-TrCP, this association facilitates the ubiquitination and degradation of phosphorylated Mcl-1 [Ding et al., 2007].

In contrary, the Mcl-1 degradation seems not only limited for ubiquitination processes. By generating the Mcl-1 mutant lacking of lysine residue required for ubiquitination, the mutate protein is still eliminated at a rate similar to that of wild type Mcl-1 under basal and stress conditions and these may be due to its direct targeting to the 20S proteasome without tagging with the ubiquitin [Stewart et al., 2010]. Taken together, the mode of Mcl-1 degradation process appears to depend on the stimuli and may be cell type specific.

CHAPTER III

MATERIALS AND METHODS

1. Cells and reagents

Non small cell lung cancer (NSCLC)-H460 cells and melanoma G361 cells were obtained from American Type Culture Collection (Manassas, VA). H460 cells were cultured in RPMI 1640 medium, while G361 cells were cultured in DMEM medium. RPMI 1640 was supplemented with 5% fetal bovine serum (FBS), 2 mM L-glutamine, and 100 units/ml penicillin/ streptomycin. DMEM was supplemented with 10% FBS, 2 mM L-glutamine, and 100 units/ml penicillin/streptomycin. All cell cultures were incubated in a 5% CO_2 environment at 37°C. Lactacystin (LAC), MG 132, dimethysulfoxide (DMSO) were obtained from Sigma Chemical, Inc. (St. Louis, MO); propidium iodide (PI) and Hoechst 33342 from Molecular Probes, Inc. (Eugene, OR); rabbit Cav-1 antibody, rabbit Mcl-1 antibody, mouse monoclonal ubiquitin antibody, mouse monoclonal Cav-1 antibody and peroxidase-conjugated secondary antibody from Abcam (Cambridge, MA); MitoTracker Red CMXRos, Alexa Fluor 350 goat anti-mouse IgG (H+L), Alexa Fluor 488 goat anti-rabbit IgG (H+L) and Lipofectamine 2000 were from Invitrogen (Carlsbad, CA). Antibody for ubiquitin, protein G-agarose bead, and β-actin antibody were from Santa Cruz Biotechnology (Santa Cruz, CA).

2. Plasmid and transfection

The Cav-1 expression plasmid (pEX_Cav-1-YFP) and control plasmid (pDS_XB-YFP) were obtained from American Type Culture Collection (Manassas, VA), the Mcl-1 expression plasmid 25375:pCDNA3.1-hMcl-1 was obtained from Addgene (Cambridge, MA), Cav-1 knockdown plasmid (cav-1 shRNA plasmid) and control plasmid (control shRNA plasmid A) was obtained from Santa Cruz Biotechnology (Santa Cruz, CA). Stable transfection of cells with Cav-1 expression plasmid or Cav-1 knockdown plasmid was performed by culturing H460 cells in a 6-well plate until they reached approximately 60% confluence. 15 μl of Lipofectamine reagent and 2 μg of Cav-1, shRNA-Cav-1, Mcl-1, shRNA-Mcl-1 or control plasmids were used to transfect the cells in the absence of serum. After 12 h, the medium was replaced with culture medium containing 5% FBS. Approximately 36 h after the beginning of transfection, the cells were digested with 0.03% trypsin, and the cell suspensions were plated onto 75-ml culture flasks and cultured for 24 to 28 days with G418 selection (600 μg/ml). The stable transfectants were pooled and the expression of Cav-1 and Mcl-1 protein in the transfectants was determined by Western blotting. The cells were cultured in antibiotic-free RPMI 1640 medium for at least two passages before being used in each experiment.

3. Anoikis assay

For anoikis evaluation, 6-well tissue culture plates were coated with 200 μl (6 mg/ml in 95% ethanol) of poly 2-hydroxyethylmethacrylate (poly-HEMA; Sigma) and left for 10 h in a laminar flow hood. Cells in a single cell suspension were seeded in poly-HEMA-coated plates at the density of 1×10^5 cells/ml and incubated for

various times up to 24 h at 37°C. Cells were harvested, washed, and incubated with 20 μM of 2,3-bis(2-methoxy-4-nitro-5-sulfophenyl)-2H-tetrazolium-5-carboxanilide (XTT) for 4 h at 37°C. Optical density was then determined using V-max photometer (Molecular Devices, Menlo Park, CA) at the wavelength of 450 nm. Absorbance ratio of treated to non-treated cells was calculated and presented as relative cell viability. For Hoechst 33342 and PI assays, cells were incubated with 10 μM of Hoechst 33342 or 15 μM of PI for 30 min at 37°C. Apoptotic cells having condensed chromatin and/or fragmented nuclei and PI-positive necrotic cells were scored under a fluorescence microscope (Olympus IX51 with DP70).

4. Western blotting

After specific treatments, cells were incubated in lysis buffer containing 20 mM Tris-HCl (pH 7.5), 1% Triton X-100, 150 mM sodium chloride, 10% glycerol, 1 mM sodium orthovanadate, 50 mM sodium fluoride, 100 mM phenylmethylsulfonyl fluoride, and a commercial protease inhibitor cocktail (Roche Molecular Biochemicals, Basel, Switzerland) for 30 min on ice. Cell lysates were collected and determined for protein content using the Bradford method (Bio-Rad Laboratories, Hercules, CA). Equal amount of proteins of each sample (40 μg) were denatured by heating at 95°C for 5 min with Laemmli loading buffer, and subsequently loaded on 10% SDS-polyacrylamide gel electrophoresis. After separation, proteins were transferred onto 0.45 μm nitrocellulose membranes (Bio-Rad). The transferred membranes were blocked for 1 hour in 5% nonfat dry milk in TBST (25 mM Tris-HCl (pH 7.5), 125 mM NaCl, 0.05% Tween-20) and incubated with the appropriate primary antibodies at 4°C overnight. Membranes were washed twice with TBST for

10 min and incubated with horseradish peroxidase–coupled isotype-specific secondary antibodies for 1 h at room temperature. The immune complexes were detected by enhanced with chemiluminescence substrate (Supersignal West Pico; Pierce, Rockford, IL) and quantified using analyst/PC densitometry software (Bio-Rad).

5. Immunoprecipitation

Cells were washed after treatment and lysed in lysis buffer at 4°C for 20 min. After centrifugation at 14,000 g for 15 min at 4°C, the supernatants were collected and determined for protein content. Cell lysates were normalized and equal amount of protein per sample (60 μg) were incubated with anti-Cav-1 antibody conjugated to protein G plus-agarose beads (Santa Cruz) for 6 h at 4°C. The immune complexes were washed five times with ice-cold lysis buffer, resuspended in 2x Laemmli sample buffer, and boiled at 95°C for 5 min. Immune complexes were separated by 10% SDS-PAGE and detected for Cav-1 and Mcl-1 complexes by Mcl-1 antibody. For detecting ubiquitin-Mcl-1 complex, the anti-Mcl-1 antibody was incubated with the cell lysate in the immunoprecipitation step followed by Western blot analysis using anti-ubiquitin antibody.

6. Quantitative real time RT-PCR

One microgram of Trizol-extracted RNA was reverse-transcribed in a 100 μl reaction mixture containing 500 μM dNTP, 125 units of MultiScribe Reverse Transcriptase (Applied Biosystems, Foster City, CA), 40 units of RNase inhibitor, 2.5 μM oligo (dT), 1x TaqMan reverse transcriptase buffer, and 5 mM $MgCl_2$ at 48°C for 40 min. The primer for *Mcl-1* (Hs03043899_m1*) and 18s rRNA (Hs99999901_s1)

were obtained from Applied Biosystems. Amplification was performed at the following cycling conditions: 95°C for 10 min, followed by 40 cycles at 95°C for 15 sec and 60°C for 1 min. A SYBR Green PCRMasterMix (Applied Biosystems) was used with 1 ng of cDNA and with 100-400 nM primers. A negative control without any cDNA template was run with every assay. All PCR reactions were performed by using ABI PRISM7900 Sequence Detection System (Applied Biosystems). Relative mRNA levels were determined by using the comparative C_T (threshold cycle) method [Livak and Schmittgen, 2001], where the Mcl-1 target is normalized to the control and compared with a reference sample (assigned a relative value of 1) by the equation: $2^{-\Delta\Delta CT}$.

7. Immunofluorescence

Cells (0.5×10^6/well) were seeded in 6-well plates for 24 h to allow the cell to completely adhere to the surface. Then, the cells were fixed in 3.7% formaldehyde for 10 min at room temperature, and then permeabilized and blocked in a solution containing 0.5% saponin, 1% FBS, and 1.5% goat serum for 30 min. After primary antibody incubation with both Cav-1 mouse monoclonal antibody (Abcam) at 1:100 dilution and Mcl-1 rabbit polyclonal antibody (Abcam) at 1:100 dilution for 1 h, cells were washed and incubated together with Alexa Fluor 350 goat anti-mouse IgG (H+L) conjugated secondary antibody (Invitrogen) and Alexa Fluor 488 goat anti-rabbit IgG (H+L) conjugated secondary antibody (Invitrogen) for 30 min. Mitochondria were stained with MitoTracker Red CMXRos (Invitrogen). Cells were cytospun onto a glass slide and mounted using the anti-fade reagent Fluoromont-G

(Southern Biotech, Birmingham, AL). Images were acquired by confocal laser scanning microscopy (Zeiss LSM 510).

8. Statistical analysis

Mean data from independent experiments were normalized with control treatment groups. All the experiments were repeated at least three times. Statistical analysis between various treatments versus control was performed using One-way ANOVA with post hoc test. A statistical analysis between treatments versus control was verified by Student's *t* test. The strength of relationships, correlation coefficient (*r*), between each protein level after detachment was determined with SPSS version 16 (SPSS Inc., Chicago, IL, USA). A P-value of less than 0.05 would be considered as statistically significant.

9. Experimental design

9.1 Generation of Cav-1 or Mcl-1 overexpressed and down-regulated clones.

9.1.1 Cav-1 and Mcl-1 plasmid transfections.

In order to investigate the involvement of Cav-1 and Mcl-1 on anoikis, exogenous expression by the transfection of plasmids carrying gene for Cav-1 and Mcl-1 have been employed. In this experiment, pEX_Cav-1-YFP (ATCC, Manassas, VA) plasmid and 25375: pCDNA3.1-hMcl-1 plasmid (Addgene, Cambridge, MA)

were used as a plasmid for generation of Cav-1 and Mcl-1 overexpression cells, respectively. The control transfectants also transfect with pcDNA3.1D V5-His-TOPO and pDS_XB-YFP plasmid and named as Mock and pDS_XB-YFP, respectively. For the generation of down-regulated Cav-1 and Mcl-1, the study use Cav-1 shRNA and Mcl-1 shRNA to knock down target proteins while the control transfection was performed by using scrabled shRNA which then named as control shRNA plasmid A.

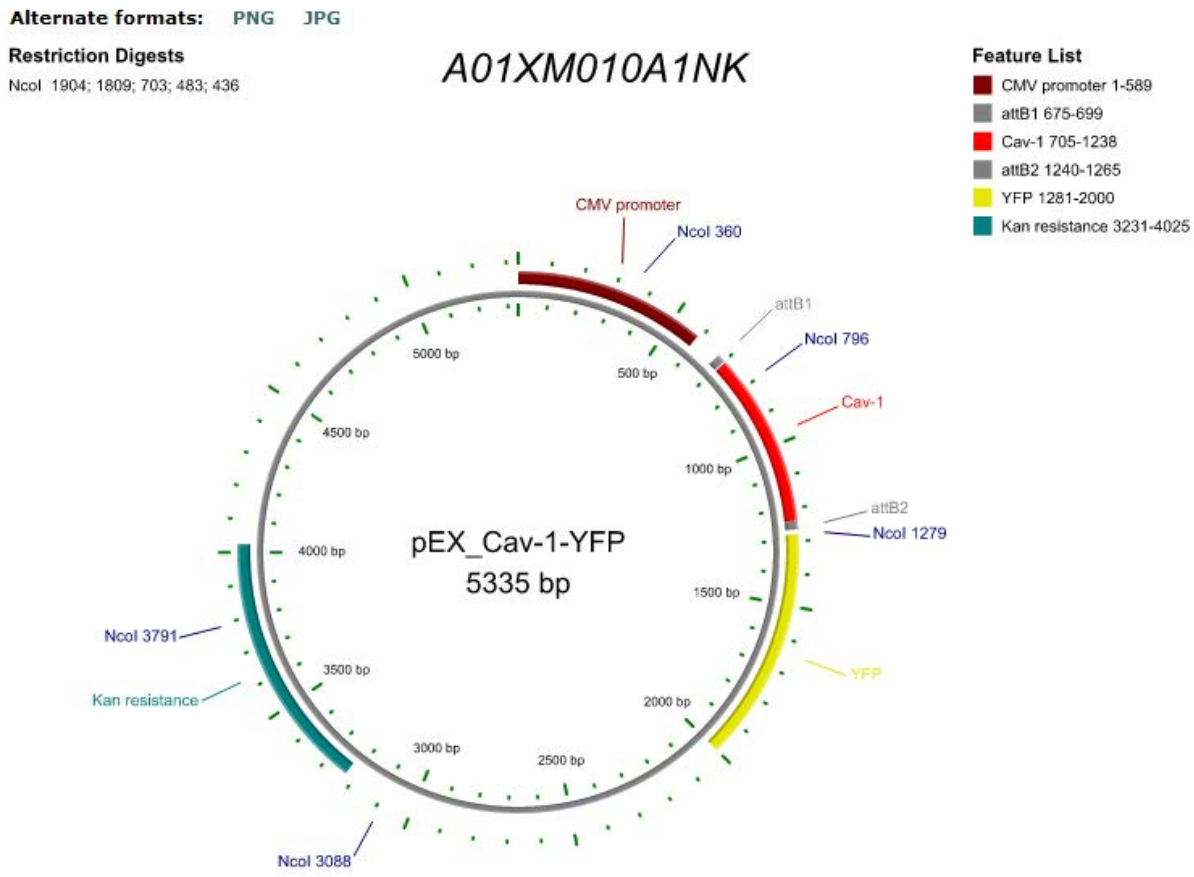

Figure 9 pEX_Cav-1-YFP plasmid

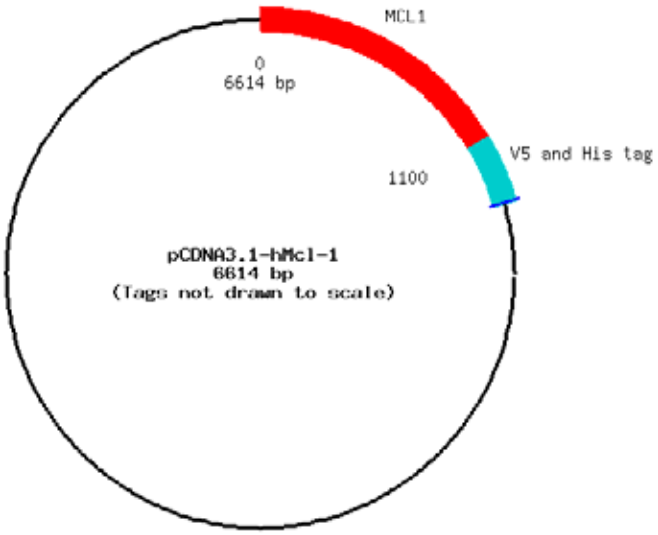

Figure 10 pCDNA3.1-hMcl-1 Plasmid

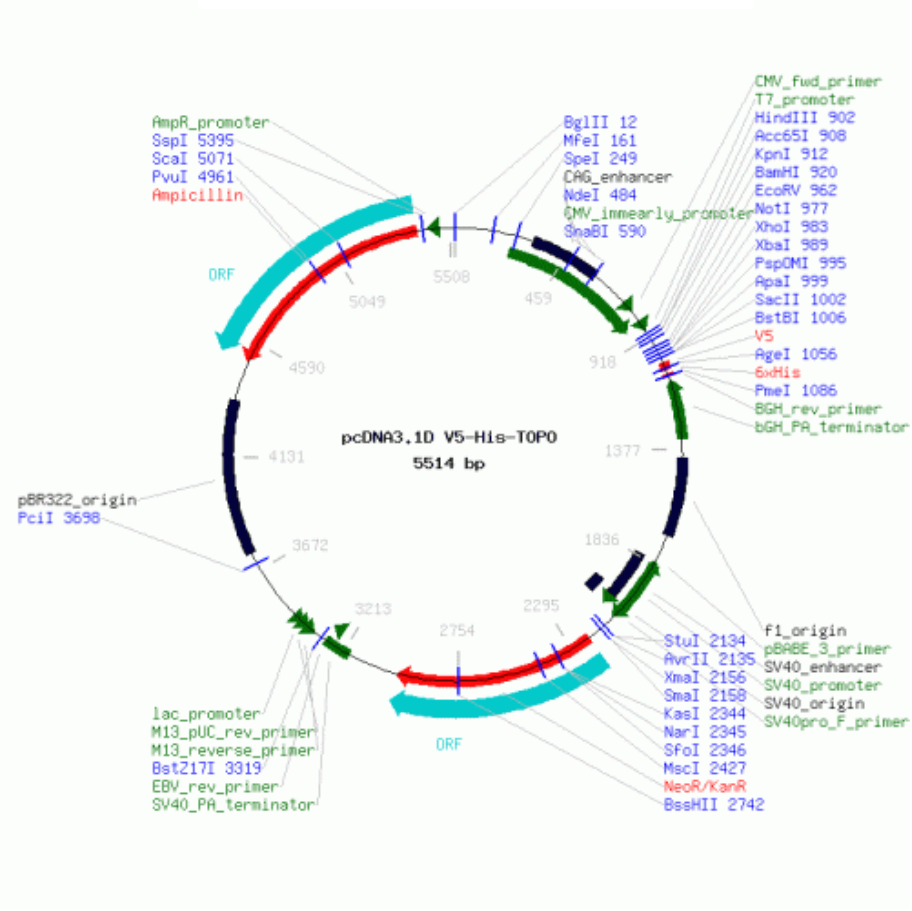

Figure 11 pcDNA3.1D V5-His-TOPO Plasmid

Stable transfectants of Cav-1 and Mcl-1expression plasmid were generated by culturing H460 cells in a 6-well plate until they reached 60% confluence. 15 µl of Lipofectamine reagent and 2 µg of Cav-1, Mcl-1 and control plasmid were used to transfect the cells in the absence of serum. After 12 h the medium was replaced with culture medium containing 5% fetal bovine serum. Approximately 36 h after the beginning of transfection, the cells were digested with 0.03% trypsin, and the cell suspensions are plated onto 75-ml culture flasks and cultured for 30 days with G418 selection (600 µg/ml) for both overexpressed plasmid and puromycin (3 µg/ml) for both shRNA transfection.

9.1.2 Selection of clones of Cav-1 and Mcl-1 overexpressed and down-regulated H460 cells

Because of the level of the expression after transfection procedure vary among the cells population, the selection of clone cells was essential in order to control the consistency for further experiments. Stably transfected cells obtained from previous step will then further selection for single cells and then grow to generate the clone cells in 6-wells plate. The level of expression for each protein was confirmed by western blotting. The three clones that exhibit a significantly higher or lower than control transfected cells were then used for the further experiments. The clones were named as pEX_cav-1-YFP, Cav-1 shRNA plasmid, pDS_XB-YFP and control shRNA plasmid for Cav-1 overexpressed, down-regulated and two difference control transfected cells respectively. For Mcl-1, the clones were named as HMcl-1, shMcl-1,

Mock and control shRNA plasmid for Mcl-1 overexpressed, down-regulated and two difference control transfected cells respectively

9.2 Investigation of the kinetics of anoikis in Cav-1 and Mcl-1 transfectants

All selected cloned were used for anoikis assay by culturing the cells in the adhesion resistance plates (polyHEMA coated plate) for 0, 3, 6, 12 and 24 h in an absent of serum. After indicated time, the cells were further tested for cell viability by XTT and apoptosis assay by Hoechst 33342.The apoptotic cells having condensed chromatin and/or fragmented nuclei were visualized and scored under a fluorescence microscope. The %viability and %apoptosis at each time point will be plotted against time after detachment at time 0, 1, 2, 3, 4, 5 and 6 h. The strength of relationships between apoptosis or cell viability versus time after detachment is determined with linear regression analysis via SPSS version 16 (SPSS Inc., Chicago, IL, USA). The regression equations were validated by F-test by using this following hypothesis:

$$H_0 : \beta = 0$$

$$H_1 : \beta \neq 0 \text{ (Where } \beta \text{ is the slope of the graph)}$$

The study will reject H_0 when the p-value less than significance level at <0.05. The regression coefficient (β) were used for comparison between each transfectant clones.

9.3 Investigation of anchorage independent growth in Cav-1 and Mcl-1 transfectants

In order to support the anoikis assay and test the ability of cells in growing in detached condition, the investigation of anchorage independent growth in soft agar is employed. All transfectant clones were detached and single cell suspensions are subjected into soft agar containing RPMI, 10% FBS and 0.33% agarose for colony formation assay. After two weeks, the colonies are photographed and evaluated for number and size.

9.4 Investigation of kinetics of Cav-1 and Mcl-1 reduction after detachment of H460

H460 cells were detached and culture in the adhesion resistance plate (polyHEMA coated plate) for 0, 3, 6, 12 and 24 h in an absent of serum. After indicated time, the cells were centrifuged at 6,000 rpm for 5 minutes to obtain the cells pellet and subjected to evaluate the expression of Cav-1 and Mcl-1 by western blotting. The relative expression of each protein will be obtained by using densitometry. The relative level of each protein will be plotted against time after detachment.

9.4.1 Correlation of Cav-1 and Mcl-1 reduction

The relative expression of the Cav-1 and Mcl-1 were correlated against each other by using Pearson correlation via SPSS version 16 (SPSS Inc., Chicago, IL, USA). The Pearson's correlation coefficient (r) was used to evaluate the strength of relationship of the two proteins.

9.5 Interactions of Cav-1 and Mcl-1

9.5.1 Immunoprecipitation study of Cav-1 and Mcl-1

To investigate the possibility of direct interaction between Cav-1 and Mcl-1 protein, cell lysate of Hcav-1, H460 and shCav-1 were used to perform immunoprecipitation study. The cell lysate were precipitate for Cav-1 protein as described and detected by Mcl-1 antibody and vice versa. The resulting band were quantified by densitometry and normalized to control H460 cells.

9.5.2 Localization of Cav-1 and Mcl-1

In order to assess the localization of Cav-1 and Mcl-1 protein, the immunofluorescence technique was used to investigate their localization. The Hcav-1, H460 and shCav-1 Cells were stained with Mitotracker (Mitochondrial marker) for 30 min prior to fixation and permeabilization following with the same method as described in *Materials and Methods*.

9.6 Cav-1 stabilizes Mcl-1 in H460 cells

9.6.1 Mcl-1 basal level is dependent on Cav-1 level

To study the role of Cav-1 in regulating Mcl-1 level, the H460 cells with different level of cav-1 were used to investigate the basal Mcl-1 level by using western blot technique as described in *Materials and Methods.* Relative Mcl-1 levels were normalized with the band intensity obtained from H460 cells.

9.6.2 Cav-1 stabilized Mcl-1 in detached state

To further study the Mcl-1 stabilization effect by Cav-1, after the cell detachment, HCav-1, shCav-1, and H460 cells were detached and incubated in adhesion-resistant plates for 0-12 h. Western blot analysis of Mcl-1 was then performed at 0, 6, and 12 h post-detachment as described in *Materials and Methods*. Relative Mcl-1 levels were normalized with the band intensity obtained from those of time = 0.

9.7 Mcl-1 reduction after cell detachment is mediated through ubiquitin-proteasomal degradation

9.7.1 Mcl-1 mRNA level during detachment

To verify the level of Mcl-1 transcriptions while detachment, H460 cells were detached and cultured in the adhesion resistance plate (polyHEMA coated plate) for 0, 3, 6, 12 and 24 h in an absent of serum. After indicated time, the cells were extracted for total RNA and quantified the target mRNA by quantitative real-time PCR as described in *Materials and Methods*.

9.7.2 Mcl-1 down regulation after cell detachment is mediated by ubiquitin-proteasome system

By using the data from experiment **9.4**, the time that protein density is reduced begins significantly at 6 h after detachment onward. H460 cells were treated with proteasome inhibitors; lactacystin (LAC; 20 μM) or MG132 (10 μM) for 30 min prior to detached for 6 h. The relative Mcl-1 protein levels were quantified by western blot.

9.8 Mcl-1 ubiquitination after cell detachment

To identify the ubiquitination of Mcl-1 after detachment, H460 cells were treated with proteasome inhibitors; lactacystin (LAC; 20 μM) for 30 min prior to detached for 0, 1, 3, 6. Cell lysates were prepared and immunoprecipitated (IP) with anti-Mcl-1 antibody. The resulting immune complexes were analyzed for ubiquitin by Western blotting (WB) using anti-ubiquitin antibody. The immunoblot signals were quantified by densitometry.

9.9 Cav-1 stabilizes Mcl-1 by attenuating Mcl-1 ubiquitination

To test the potential involvement of Cav-1 in regulating Mcl-1 ubiquitination, Mcl-1 immunoprecipitation and ubiquitination studies were performed in various Cav-1 expressing cells. HCav-1, H460 and shCav-1 were treated with proteasome

inhibitors; lactacystin (LAC; 20 μM) for 30 min prior to detached for 1 and 6 h. The resulting immune complexes were analyzed for ubiquitin by Western blotting (WB) using anti-ubiquitin antibody. The immunoblot signals were quantified by densitometry.

9.10 Generation of Cav-1 overexpressed and down-regulated G361 cells

9.10.1 Cav-1 plasmid transfections.

The generation of Cav-1 plasmid transfection in G361 is similar to the method described in **9.1.1** in *Materials and methods* for H460 cells.

9.10.2 Selection of clones of Cav-1 overexpressed and down-regulated G361 cells

The selection of transfectant clones of G361 is similar to the method described in **9.1.2** in *Materials and methods* for H460 cells.

9.11 Investigation of the kinetics of anoikis in Cav-1 transfectants G361 cells

All selected cloned were used for anoikis assay by culturing the cells in the adhesion resistance plates (polyHEMA coated plate) for 0, 3, 6, 12 and 24 h in an absent of serum. After indicated time, the cells were further tested for cell viability by

XTT and apoptosis assay by Hoechst 33342.The apoptotic cells having condensed chromatin and/or fragmented nuclei were visualized and scored under a fluorescence microscope. The %viability and %apoptosis at each time point will be plotted against time after detachment.

9.11 Cav-1 stabilizes Mcl-1 in G361 cells

To further the study the effect of Cav-1 stabilization after the cell detachment, G361-Cav-1, G361-shCav-1, and G361 cells were detached and incubated in adhesion-resistant plates for 0 and 6 h. Western blot analysis of Mcl-1 was then performed at 0 and 6 h post-detachment as described in *Materials and Methods*. Relative Mcl-1 levels were normalized with the band intensity obtained from those of time = 0.

CHAPTER IV

RESULTS

1. Generation of Cav-1 overexpressed and downregulated H460 cells

The stably transfected cells for Cav-1 overexpressed and downregulated cells were obtained by transfections method as describe in CHAPTER III MATERIALS AND METHODS. After successfully selected the mutant clones by antibiotic treatment, the cells were subjected to western blotting for the assessment of Cav-1 level.

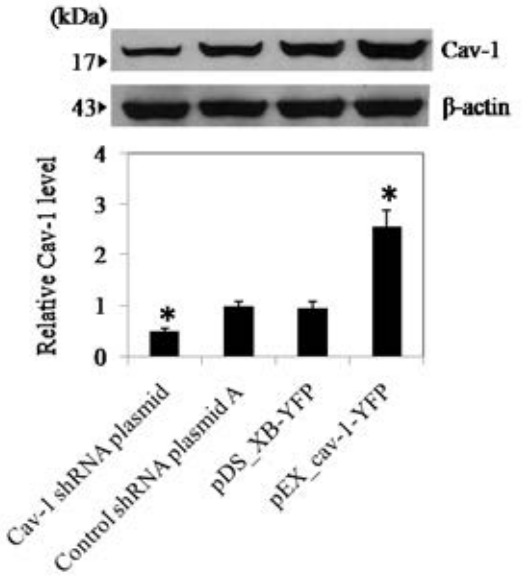

Figure 12 Different levels of Cav-1 expression in transfectants. Control, overexpression and down-regulation of Cav-1 in H460 cells were constructed and grown in culture which then analyzed for Cav-1 expression by western blotting. Blots were reprobed with β-actin antibody to confirm equal loading of samples. Columns are the mean ± S.D. (n = 3). *, $P < 0.05$ versus control transfected cells.

2. Caveolin-1 inhibits anoikis of H460 cells

2.1 Caveolin-1 increase cell viability after detachment in H460 cells

2.1.1 Overexpression of Caveolin-1 increase cell viability after detachment in H460

To study anoikis, cav-1 overexpressed and vector control cells were detached and incubated in adhesion-resistant poly-HEMA coated plates. Analysis of cell viability after detachment was determined by XTT assay. The detachment caused the cell gradually decrease in cell viability, after 6 h detachment, the cell viability were approximately 80% (85.36±3.35%), and 50% (47.10±2.62%) of the overexpressed and vector control cells respectively. Moreover, at 24 h after cell detachment, Cav-1 overexpressing cells (HCav-1) exhibited ~60% (62.27±5.23%) viability, whereas control cells showed a survival rate of less than 40% (32.04±2.87%).

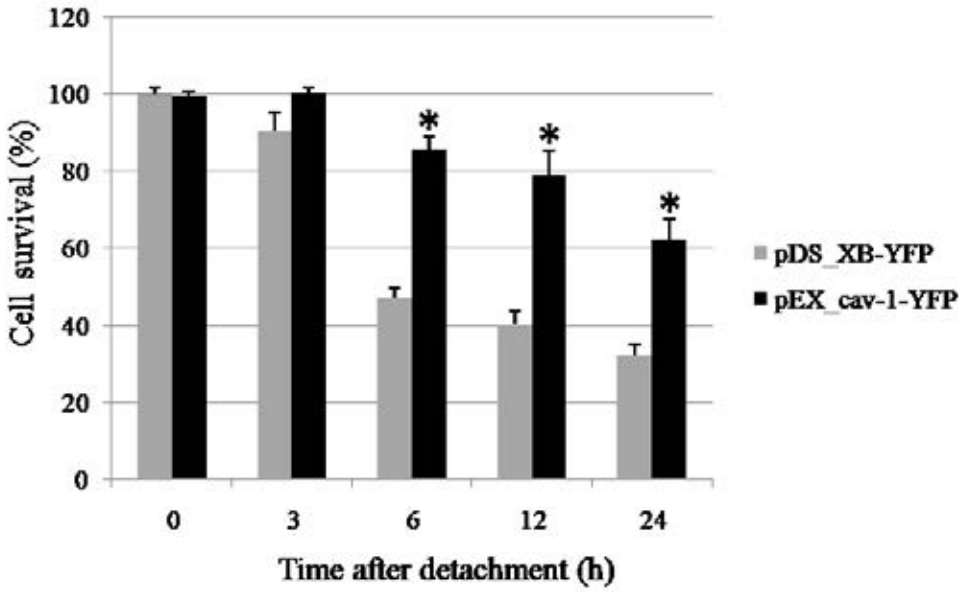

Figure 13 Overexpression of Caveolin-1 increase cell viability after detachment in H460. Subconfluent (90%) monolayer of control transfected and cav-1 overexpressing H460 cells were detached and suspended in poly-HEMA coated plates for various times (0-24 h). At the indicated times after detachment, the cells were collected and the survival was determined by XTT assay. Viability of detached cells at time 0 h was considered as 100%. Columns are the mean ± S.D. (n = 3). *, $P < 0.05$ versus control transfected cells.

2.1.2 Downregulation of Caveolin-1 decrease cell viability after detachment in H460

To verify the role of knockdown Cav-1 on cell anoikis, cav-1 shRNA transfected cells and vector control cells were detached and incubated in adhesion-resistant poly-HEMA coated plates. Analysis of cell viability after detachment was determined by XTT assay. The detachment caused the cell gradually decrease in cell viability, after 6 h detachment, the cell viability were approximately 50% (51.34±7.43%), and 30% (32.67±7.21%) of the vector control cells and cav-1 shRNA transfected cells respectively. Moreover, at 24 h after cell detachment, knockdown Cav-1 cells exhibited less than 20% (17.85±4.53%) viability, whereas control cells showed a survival rate around 30% (30.22±3.5%).

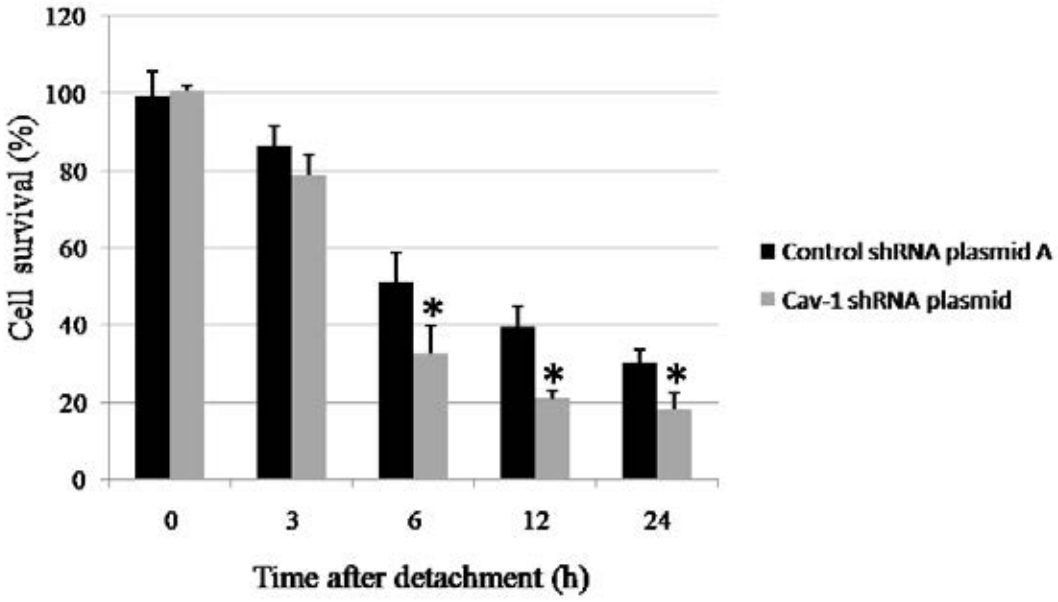

Figure 14 Downregulation of Caveolin-1 decrease cell viability after detachment in H460. Subconfluent (90%) monolayer of control transfected and Cav-1 knockdown H460 cells were detached and suspended in poly-HEMA coated plates for various times (0-24 h). At the indicated times after detachment, the cells were collected and the survival was determined by XTT assay. Viability of detached cells at time 0 h was considered as 100%. Columns are the mean ± S.D. (n = 3). *, $P < 0.05$ versus control transfected cells.

2.1.3 Cav-1 alter the kinetic of cell viability after detachment in H460

To assess the role of cav-1 in regulating cell death after detachment, generation of the plot between cell viability versus time after detachment was constructed. The resulting graph demonstrated that, cav-1 has a profound effect on cell death after cell detachment at the first six hour while the remaining seems to be parallel. These indicate that any alteration effects on cav-1 protein level will be the consequences in only the first six hours after cell detachment.

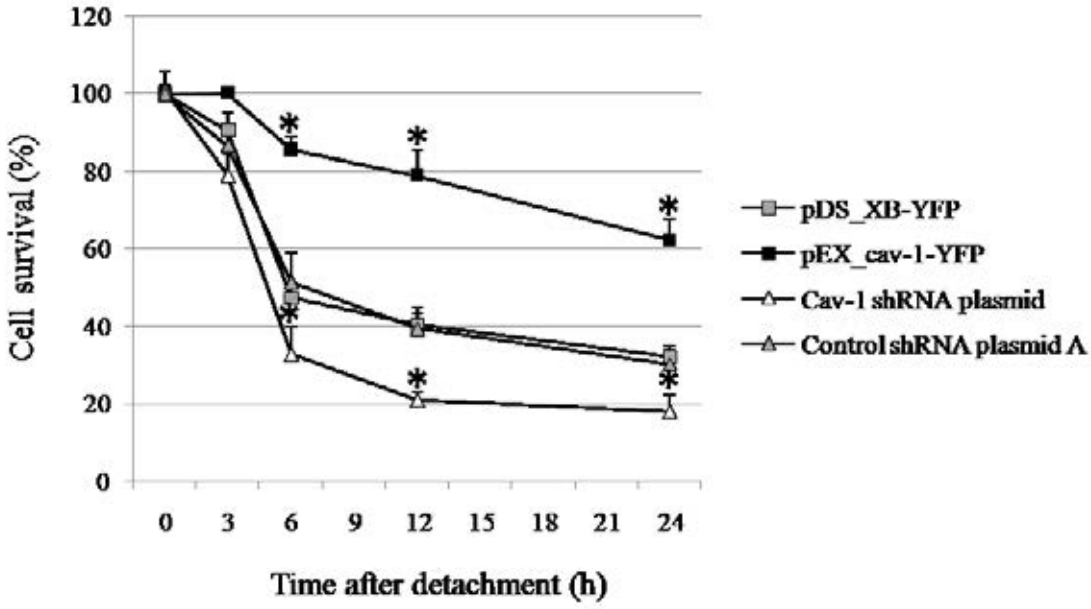

Figure 15 Plots between cell viability versus time after detachment in Cav-1 variants H460 cells. Data point represents the mean ± S.D. (n = 3) *, $P < 0.05$ versus control transfected cells.

2.1.3.1 Cav-1 alter the regression coefficient of cell viability after detachment

To accurately elucidate the role of cav-1 in regulating cell viability after detachment for the first six hours, monitoring of cell viability at every hour after detachment had to be performed, and the results were shown in appendix table 9. The obtained data were used for generating the equation and the resulting regression coefficient (β) were used to compare between each different set of various cav-1 levels in H460 cells. Table 2 and Fig. 16 shows the change of regression coefficient (β) in regard to the cav-1 level, in the pEX_Cav-1-YFP which increased in cav-1, the regression coefficient changed from -9.15 to -2.50 suggesting the slow rate of cell death after cell detachment. As expected, the reducing level of cav-1 as in cav-1 shRNA plasmid had increased the magnitude of cell death, the regression coefficient changed from -8.56 to -11.95, after the detachment for the first six hours. This result suggests the involvement of cav-1 in regulating cell death after the detachment in H460 cells.

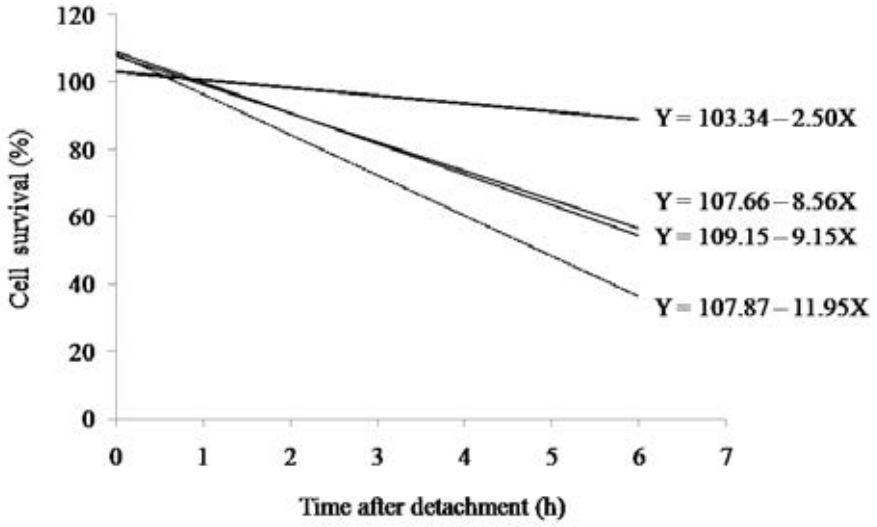

Figure 16 Regression plots of cell viability versus time after detachment in each different set of Cav-1 variants H460 cells

Transfectants	Equation	R^2	β	P-value
pDS_XB-YFP	Y = 109.15 – 9.15X (P-value = 0.002)	0.887	-9.15	-
pEX_Cav-1-YFP	Y = 103.34 – 2.50X (P-value = 0.01)	0.765	-2.50	<0.0001
Control shRNA plasmid A	Y = 107.66 – 8.56X (P-value = 0.001)	0.909	-8.56	-
Cav-1 shRNA plasmid	Y = 107.87 – 11.95X (P-value < 0.0001)	0.964	-11.95	<0.0001

Table 2 Regression analysis of cell viability in cav-1 variants H460 cells after detachment for 6 h.

2.2 Caveolin-1 reduce apoptosis after detachment in H460 cells

2.2.1 Overexpression of caveolin-1 reduce apoptosis after detachment in H460

Because anoikis is the terms that define the apoptotic cell death, the experiments that monitor that specific form of cell death had to be performed in conjunction with cell viability assay. Analysis of cell apoptosis by Hoechst 33342 assay showed that cav-1 overexpressing cells had less apoptotic rate than control transfected cells (Fig. 17). At 6 h after detachment, the cav-1 overexpressed H460 cells exhibit less than 10% (6.34±5.21%) apoptotic rate, whereas control transfectants showed approximately 20% (19.35±4.32%) apoptotic rate. Maximum apoptotic rate were found at 24h post-detachment, control cells exceed their apoptotic rate to approximately 60% (55.39±6.5%) while the cav-1 overexpressed cells remain lower than 15% (11.99±3.04%) apoptotic rate.

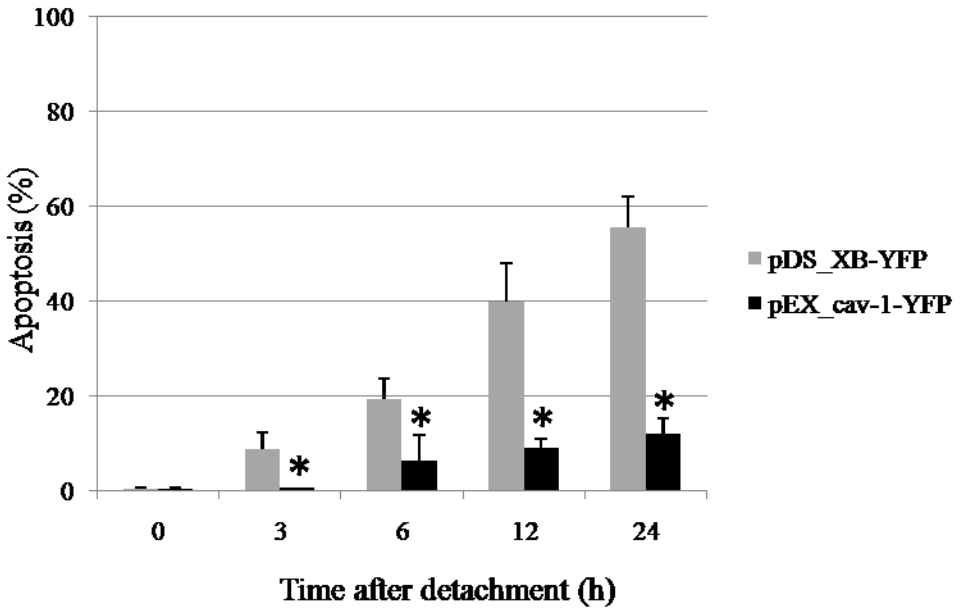

Figure 17 Overexpression of caveolin-1 reduce apoptosis after detachment in H460. Subconfluent (90%) monolayer of control transfected, cav-1 overexpressing were detached and suspended in poly-HEMA coated plates for various times (0-24 h). At the indicated times after detachment, percentage of cell detachment-induced apoptosis was analyzed by Hoechst 33342 nuclear fluorescence. Columns are the mean ± S.D. (n = 3). *, $P < 0.05$ versus control transfected cells.

2.2.2 Down-regulation of caveolin-1 increase apoptosis after detachment in H460

Analysis of cell apoptosis by Hoechst 33342 assay showed that cav-1 knock down cells had higher apoptotic rate than control transfected cells (Fig. 18). At 6 h after detachment, the cav-1 knockdown cells exceed their apoptotic rate to over 40% (39.98±10.54%), whereas control transfectants showed approximately 20% (17.32±5.98%) apoptotic rate. Maximum apoptotic rate was found at 24h post-detachment, control cells exceed their apoptotic rate to approximately 50% (52.55±6.5%) while the cav-1 down-regulated cells exceed their apoptotic rate to almost 80% (77.85±3.21%)

.

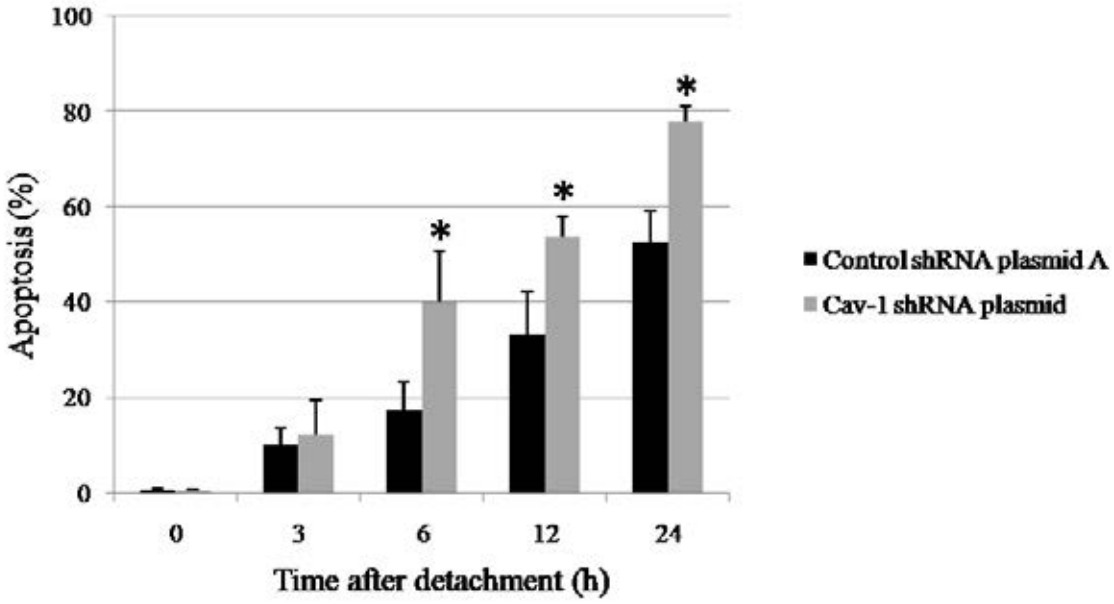

Figure 18 Down-regulation of caveolin-1 increase apoptosis after detachment in H460**.** Subconfluent (90%) monolayer of control transfected and cav-1 knockdown cells were detached and suspended in poly-HEMA coated plates for various times (0-24 h). At the indicated times after detachment, percentage of cell detachment-induced apoptosis was analyzed by Hoechst 33342 nuclear fluorescence. Columns are the mean ± S.D. (n = 3). *, $P < 0.05$ versus control transfected cells.

2.2.3 Cav-1 alters the kinetic of apoptosis after detachment in H460

By obtaining the data from apoptotic studies, the resulting graph demonstrated that, cav-1 has a profound effect on apoptosis after cell detachment at the first six hour while the remaining seems to be paralleled. These results are concordant with the cell viability assay after cell detachment that indicates the role of Cav-1 in preventing cell death after detachment.

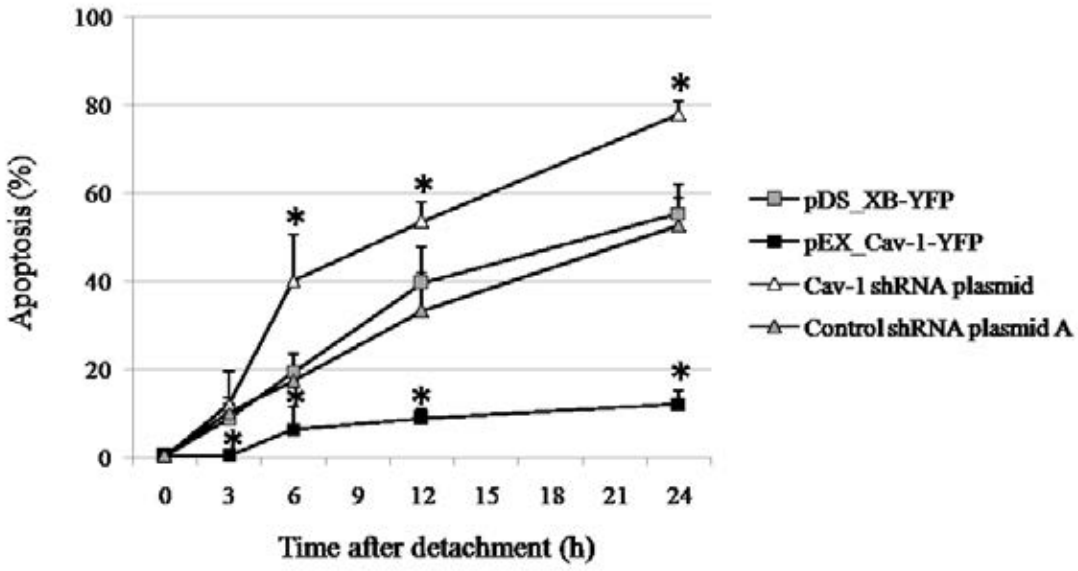

Figure 19 Plots between percent apoptosis versus time after detachment in Cav-1 variants H460 cells. Data point represents the mean ± S.D. (n = 3) *, $P < 0.05$ versus control transfected cells.

To visualize the primary mode of cell death after the detachment, morphological analyses of apoptotic and necrotic cell death by Hoechst 33342 and propidium iodide assays has been performed and the results showed that apoptosis was the primary mode of cell death induced by cell detachment in H460 cells (Fig. 20).

A.

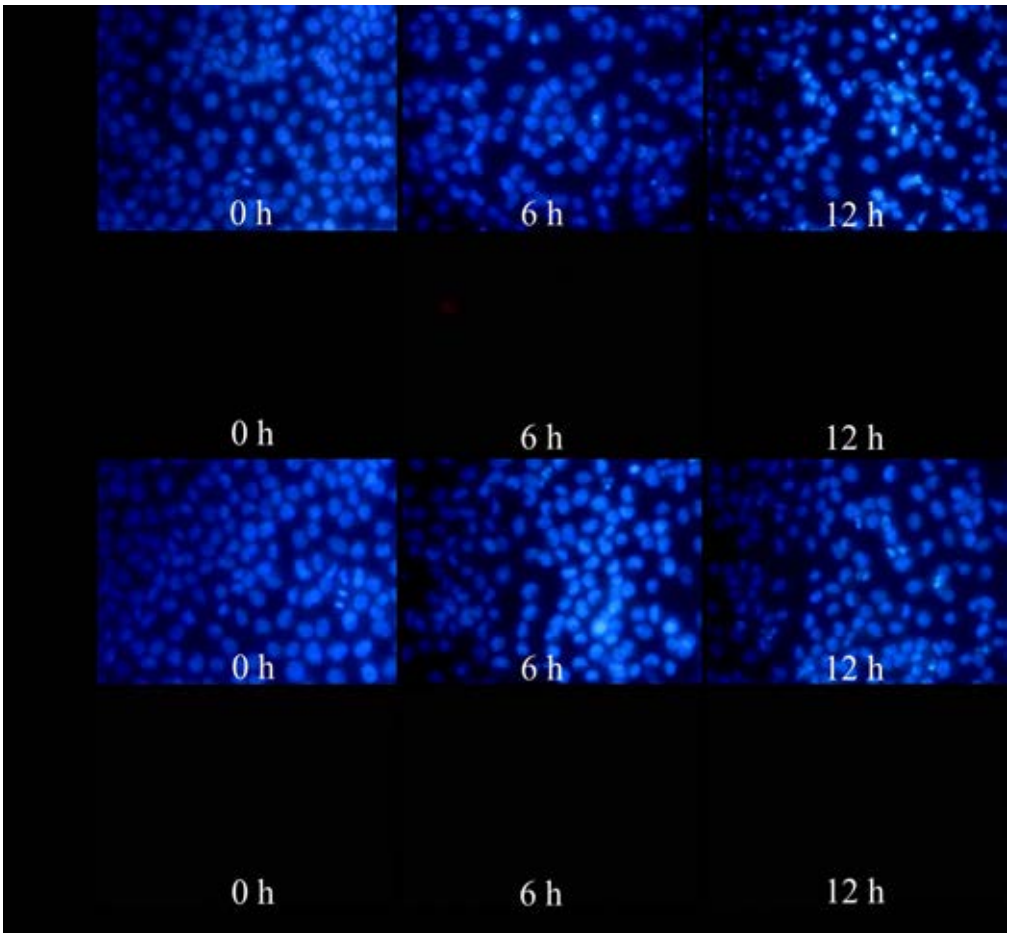

B.

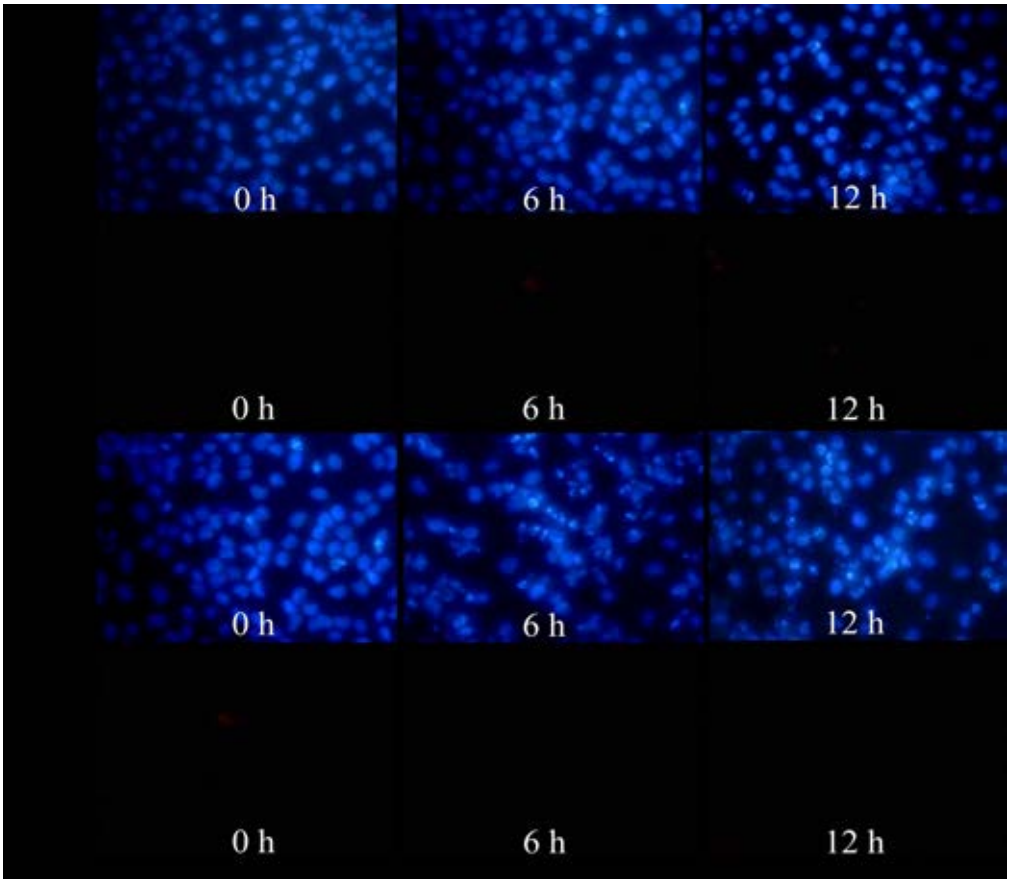

Figure 20 Morphology of detachment-induced apoptosis and necrosis in control transfected cells, cav-1 overexpressing (**A**) and cav-1 knockdown cells (**B**). Detached cells were suspended in poly-HEMA coated plates for 0-12 h and cell apoptosis and necrosis were determined by Hoechst 33342 and PI fluorescence measurements, respectively.

2.2.3.1 Cav-1 alter the regression coefficient of apoptosis after detachment

Table 3 and Fig. 21 shows the change of regression coefficient (β) in regard to the cav-1 level, in the pEX_Cav-1-YFP which increased in cav-1, the regression coefficient changed from 3.12 to 1.01 suggesting the slower rate of apoptosis after cell detachment. As expected, the reducing level of cav-1 as in Cav-1 shRNA plasmid had increased the magnitude of apoptosis after detachment for the first six hours in which the regression coefficient was shifted from 2.94 to 6.72. This result suggests the involvement of cav-1 in regulating apoptosis after the detachment in H460 cells. Taken together, both cell viability studies and apoptosis studies highlighted the role of cav-1 in regulation of anoikis in H460 cells.

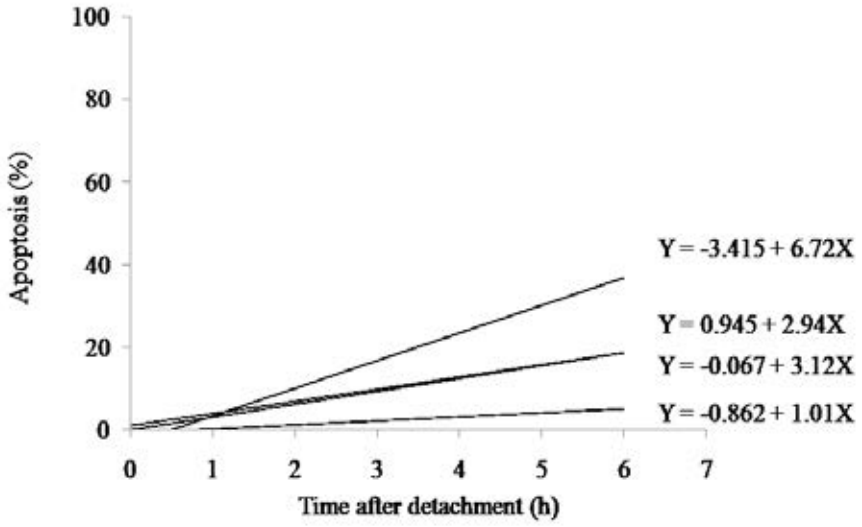

Figure 21 Regression plots of apoptosis versus time after detachment in each different set of Cav-1 variants H460 cells.

Transfectants	Equation	R^2	β	P-value
pDS_XB-YFP	Y = -0.067 + 3.12X (P-value < 0.0001)	0.992	3.12	-
pEX_Cav-1-YFP	Y = -0.862 + 1.01X (P-value = 0.008)	0.785	1.01	< 0.0001
Control shRNA plasmid A	Y = 0.945 + 2.94X (P-value < 0.0001)	0.994	2.94	-
Cav-1 shRNA plasmid	Y = -3.415 + 6.72X (P-value < 0.0001)	0.956	6.72	< 0.0001

Table 3 Regression analysis of apoptosis in cav-1 variants H460 cells after detachment for 6 h.

3. Cav-1 promotes anchorage-independent growth of H460 cells

Anchorage-independent growth is the key characteristic of metastatic cancer cells. To assess whether cav-1 could promote anchorage-independent growth, cav-1 variants H460 cells were grown in soft agar for two weeks and the colony was determined by microscopy. Figure 22 shows that differential cav-1 expression could significantly affect the ability of H460 cells to grow under anchorage-independent conditions. The formation of large cell colonies were found in the cav-1 overexpression H460 cells, whereas in the moderate cav-1 level H460 cells have much smaller colonies. Moreover, cav-1 shRNA H460 cells have the smallest colonies containing most dead cells as determined by trypan blue exclusion assay. These results indicated that cav-1 is a key determinant for anchorage-independent growth of H460 cells.

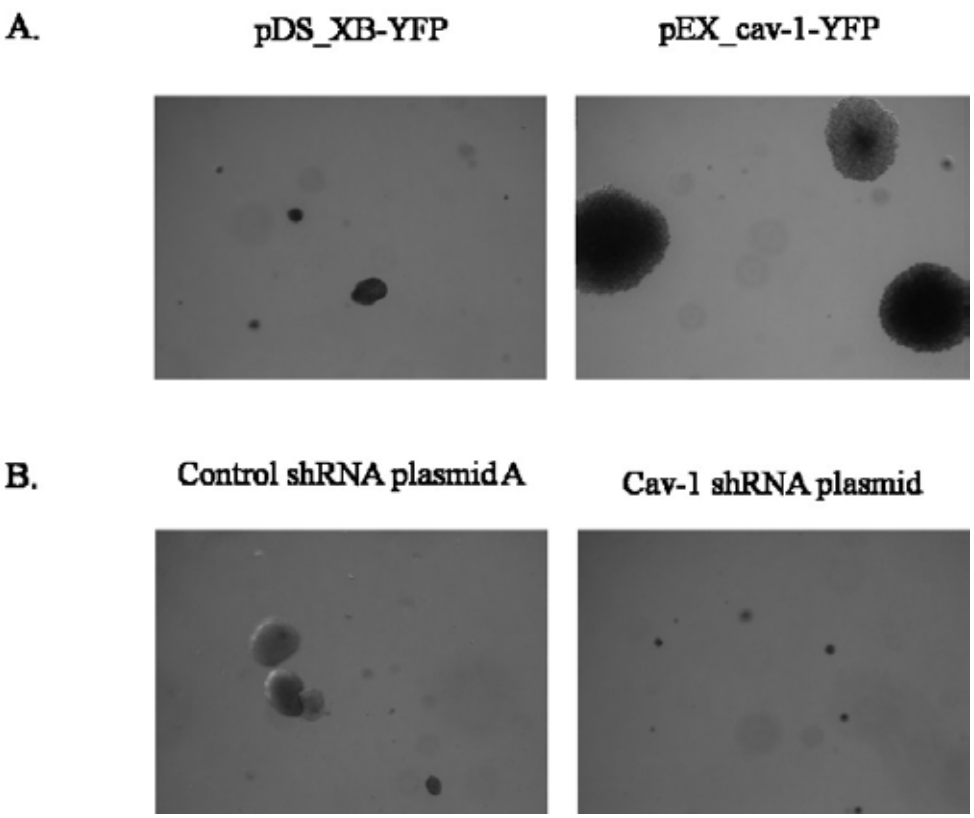

Figure 22 Effect of Cav-1 expression on anchorage-independent growth of H460 cells in soft agar. A: pDS_XB-YFP and pEX_cav-1-YFP transfectants H460 cells were detached and cultured under suspending conditions in soft agar containing growth medium (RPMI), 10% FBS, and 0.33% agarose as described in MATERIALS AND METHODS. B: Control shRNA plasmid A and cav-1 shRNA plasmid transfectants H460 cells were detached and suspended in soft agar using the same conditions as in A. Cells were fed twice a week and photographed after 2 wk for their ability to proliferate and form colonies. The representative fields were photographed at ×10 magnification. The results are representative of three independent experiments.

4. Generation of Mcl-1 overexpressed and downregulated H460 cells

In order to assess Mcl-1 role in regulating H460 anoikis, like cav-1, the stably transfected cells for Mcl-1 overexpressed and down-regulated cells were obtained by transfections method. After successfully selected the mutants clone by antibiotic treatment, the cells were subjected to western blotting for the assessment of Mcl-1 expression level.

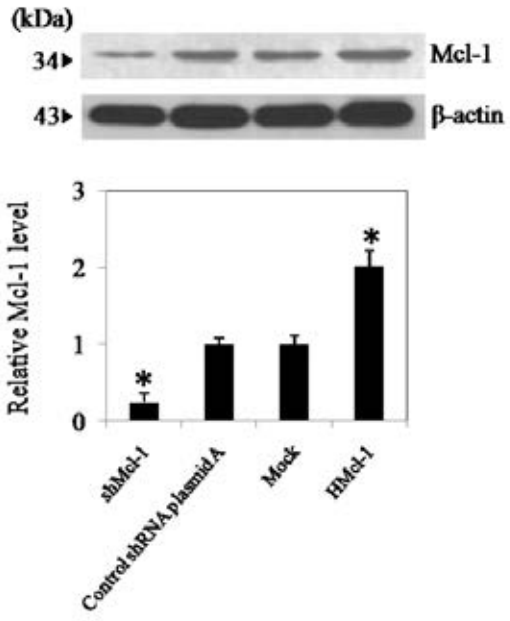

Figure 23 Different levels of Mcl-1 expression in transfectants. Control transfectant, shMcl-1 and HMcl-1 cells were grown in culture and analyzed for Mcl-1 expression by Western blotting. Blots were reprobed with β-actin antibody to confirm equal loading of samples. The immunoblot signals were quantified by densitometry, and mean data from independent experiments were normalized to the results. Columns are the mean ± S.D. (n = 3). *, $P < 0.05$ versus control transfected cells.

5. Mcl-1 inhibits anoikis of H460 cells

5.1 Mcl-1 increase cell viability after detachment in NSCLC

5.1.1 Overexpression of Mcl-1 increase cell viability after detachment in H460

Mcl-1 has been shown to regulate anoikis in some cancer types [Woods N T., et al., 2007], to confirm the Mcl-1 role on anokis in H460 cells. The Mcl-1 overexpressing H460 cells (HMcl-1) were used for anoikis studied. Like Cav-1, the HMcl-1 cells also showed resistance to anoikis as indicated by their increased viability after cell detachment over control cells. As shown in Fig. 24, the overexpression of Mcl-1 allows the cell to have anoikis resistance capability by significantly increase their survival after detachment in every time point compared to control transfectants. Even at 24 h post-detachment, the HMcl-1 exhibit their viability more than 70% (72.31±2.82%) whereas approximately 40% (36.82±1.24) in control transfectants.

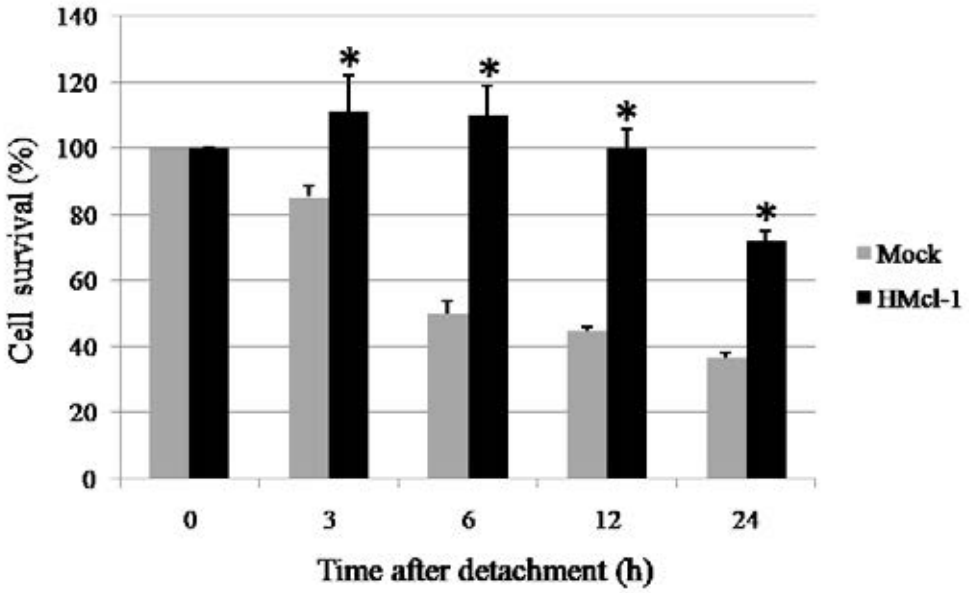

Figure 24 Overexpression of Mcl-1 increase cell viability after detachment in H460. Subconfluent (90%) monolayers of Mock and HMcl-1 cells were detached and suspended in poly-HEMA coated plates for various times (0-24 h). At the indicated times, the cells were collected and their survival was determined by XTT assay. Viability of detached cells at time 0 was considered as 100%. Columns are the mean ± S.D. (n = 3). *, $P < 0.05$ versus control transfected cells.

5.1.2 Downregulation of Mcl-1 decrease cell viability after detachment in H460

To verify the role of knockdown Mcl-1 on cell anoikis, Mcl-1 shRNA and vector control transfected cells were detached and incubated in adhesion-resistant poly-HEMA coated plates. The detachment caused the cell gradually decrease in cell viability, after 6 h detachment, the cell viability were approximately 50% (55.09±7.32), and 40% (41.26±7.43) of the vector control cells and Mcl-1 shRNA transfected cells respectively. Moreover, at 24 h after cell detachment, knockdown Mcl-1 cells have approximately 10% (10.77±5.32) in cell viability, whereas control cells showed a survival rate around 40% (37.98±3.32) as shown in Fig. 25.

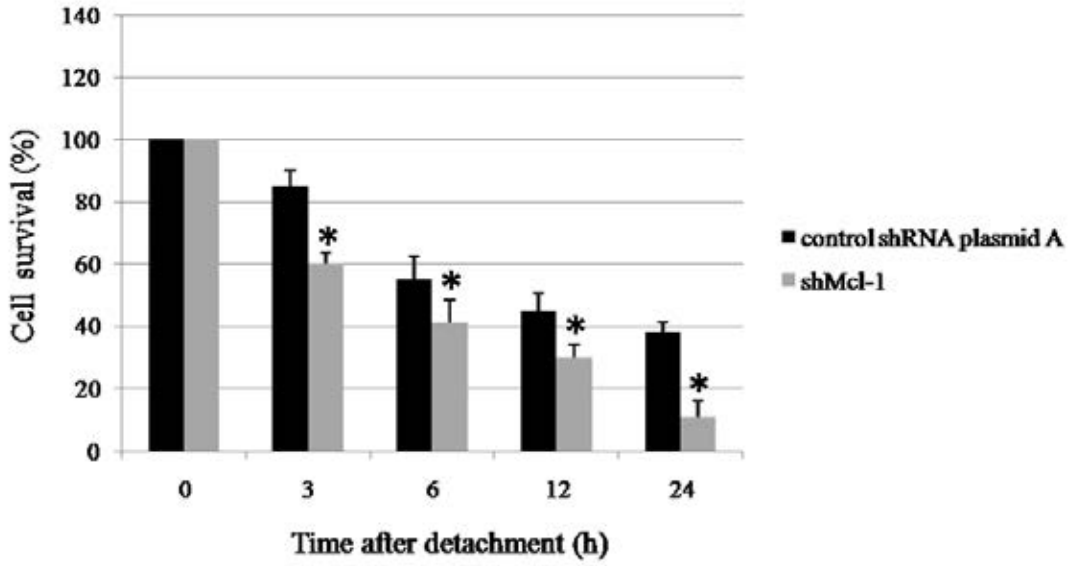

Figure 25 Downregulation of Mcl-1 decrease cell viability after detachment in H460. Subconfluent (90%) monolayer of control transfected and Mcl-1 knockdown H460 cells were detached and suspended in poly-HEMA coated plates for various times (0-24 h). At the indicated times after detachment, the cells were collected and the survival was determined by XTT assay. Viability of detached cells at time 0 h was considered as 100%. Columns are the mean ± S.D. (n = 3). *, $P < 0.05$ versus control transfected cells.

5.1.3 Mcl-1 alter the kinetic constant of cell viability after detachment in H460

By comparing the cell viability after detachment in each Mcl-1 variants, like Cav-1, HMcl-1 exhibits a substantial increase in anoikis resistance when compared to control transfected cells. Even though at 24 h after detachment, HMcl-1 cells still have more than 70% (72.31±2.82) cell viability whereas shMcl-1 shows approximately 10% (10.77±5.32) cell viability. This result suggested that Mcl-1 also has a critical role for anoikis resistance in H460 cells and it should be noted that, similar to Cav-1, the effects of Mcl-1 on anoikis of H460 was prominent at the first six hours after cell detachment.

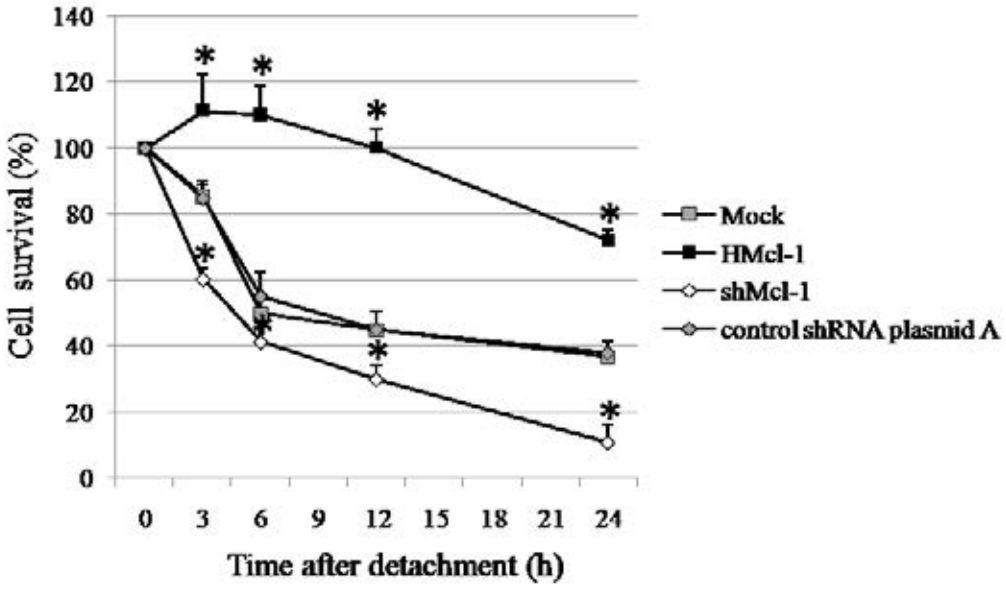

Figure 26 Plots between cell viability versus time after detachment in Mcl-1 variants H460 cells. Data point represents the mean ± S.D. (n = 3) *, $P < 0.05$ versus control transfected cells.

5.1.3.1 Mcl-1 alter the regression coefficient of cell viability after detachment

Table 4 and Figure 27 shows the change of regression coefficient (β) in regard to the Mcl-1 level, in the HMcl-1 which increased in Mcl-1, the regression coefficient changed from -8.36 to 1.44 suggesting the slow rate of cell death after cell detachment. As expected, the reducing level of Mcl-1 as in shMcl-1 transfectants had increased the magnitude of cell death after detachment for the first six hours. This result suggests the involvement of Mcl-1 in regulating cell death after the detachment in H460 cells.

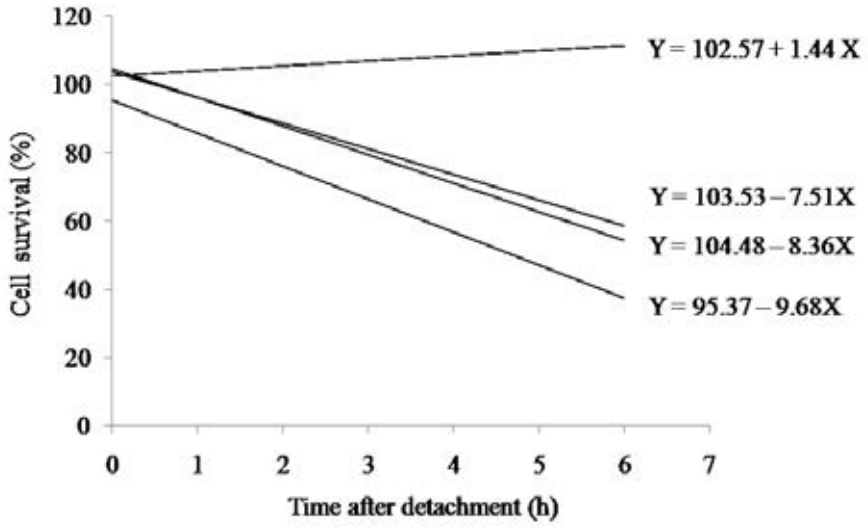

Figure 27 Regression plots of cell viability versus time after detachment in each different set of Mcl-1 variants H460 cells.

Transfectants	Equation	R^2	β	P value
Mock	Y = 104.48 – 8.36X (P-value < 0.0001)	0.959	-8.36	-
HMcl-1	Y = 102.57 + 1.44 X (P-value = 0.016)	0.719	1.44	< 0.0001
Control shRNA plasmid A	Y = 103.53 – 7.51X (P-value < 0.0001)	0.970	-7.51	-
shMcl-1	Y = 95.37– 9.68X (P-value < 0.0001)	0.965	-9.68	< 0.0001

Table 4 Regression analysis of cell viability in Mcl-1 variants H460 cells after detachment for 6 h.

5.2 Mcl-1 reduce apoptosis after detachment in H460 cells

5.2.1 Overexpression of Mcl-1 reduces apoptosis after detachment in H460

Analysis of cell apoptosis by Hoechst 33342 assay showed that Mcl-1 overexpressing cells were less apoptotic than control transfected cells at every time point detected which started from three hours until twenty four hours (Fig. 28).

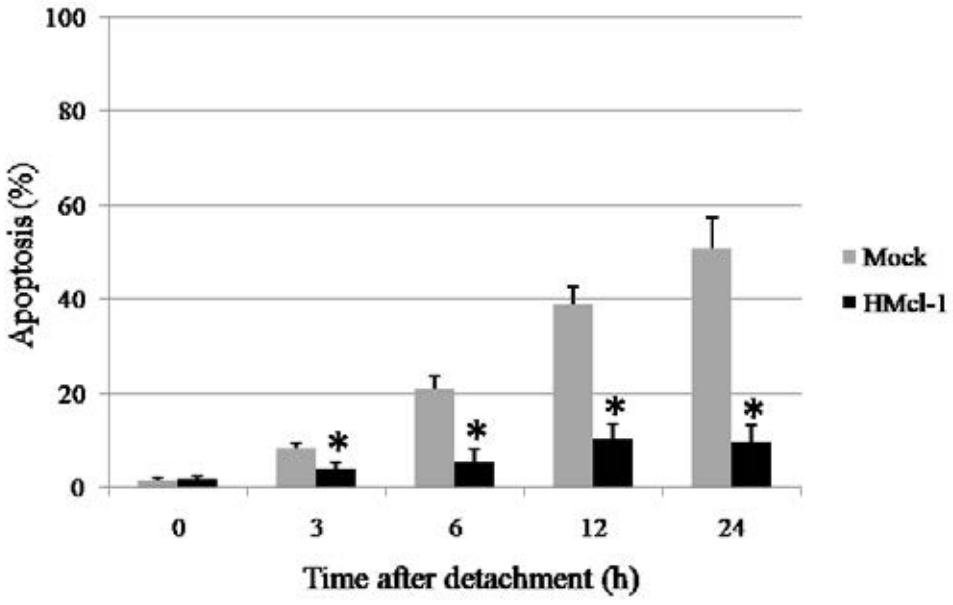

Figure 28 Overexpression of Mcl-1 reduces apoptosis after detachment in H460. Subconfluent (90%) monolayer of control transfected, Mcl-1 overexpressing H460 cells were detached and suspended in poly-HEMA coated plates for various times (0-24 h). At the indicated times after detachment, percentage of cell detachment-induced apoptosis was analyzed by Hoechst 33342 nuclear fluorescence. Columns are the mean ± S.D. (n = 3). *, $P < 0.05$ versus control transfected cells.

5.2.2 Downregulation of Mcl-1 increases apoptosis after detachment in H460

Analysis of cell apoptosis by Hoechst 33342 assay showed that downregulation of Mcl-1 protein level affects on higher apoptotic rate than control transfected cells (Fig. 29).

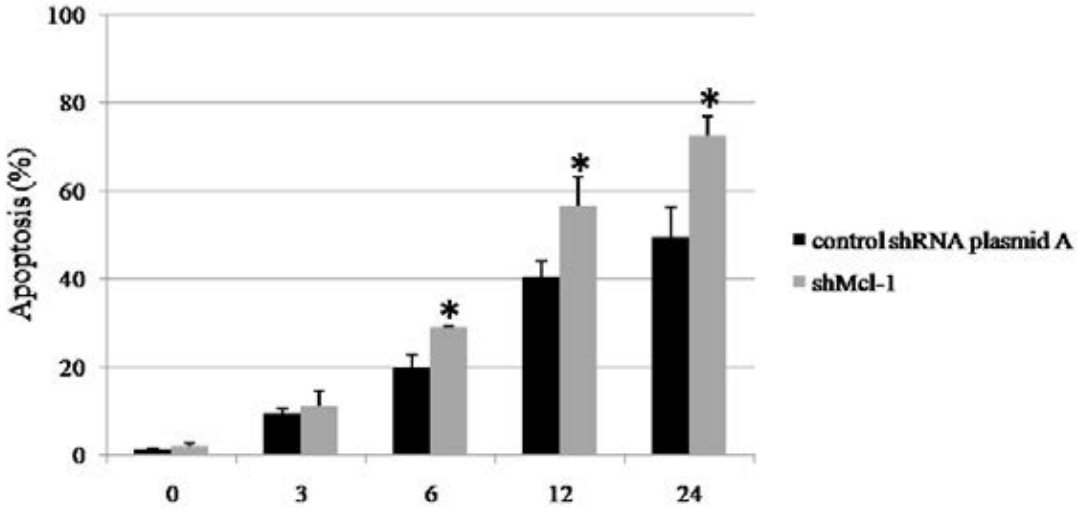

Figure 29 Downregulation of Mcl-1 increase apoptosis after detachment in H460. Subconfluent (90%) monolayer of control transfected, shMcl-1 cells were detached and suspended in poly-HEMA coated plates for various times (0-24 h). At the indicated times after detachment, percentage of cell detachment-induced apoptosis was analyzed by Hoechst 33342 nuclear fluorescence. Columns are the mean ± S.D. (n = 3). *, $P < 0.05$ versus control transfected cells.

5.2.3 Mcl-1 alters the kinetic of apoptosis after detachment in H460

Like Cav-1, by obtaining the data from apoptotic studies, the resulting graph demonstrated that, Mcl-1 has a profound effect on apoptosis after cell detachment at the first six hour while the remaining seems to be paralleled.

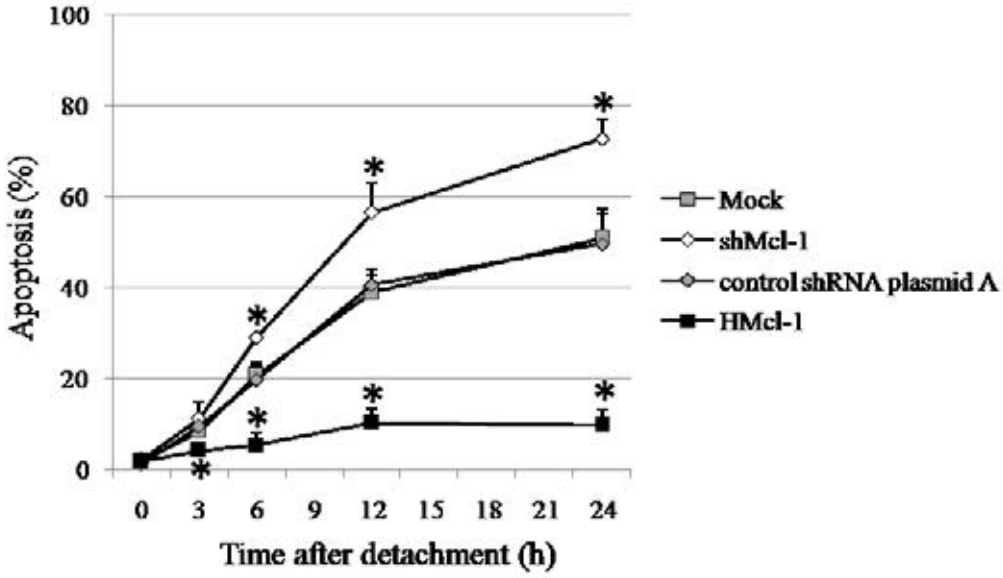

Figure 30 Plot between apoptosis versus time after detachment in Mcl-1 variants H460 cells. Data point represents the mean ± S.D. (n = 3) *, $P < 0.05$ versus control transfected cells.

5.2.3.1 Mcl-1 alter the regression coefficient of apoptosis after detachment

Table 5 and Fig. 31 shows the change of regression coefficient (β) in regard to the Mcl-1 level, in the HMcl-1 which increased in Mcl-1, the regression coefficient changed from 3.10 to 0.64 suggesting the slow rate of apoptotic cell death after cell detachment. As expected, the reducing level of Mcl-1 as in shMcl-1 had increased the magnitude of apoptotic cell death that the coefficient was shifted from 3.06 to 4.33 after detachment for the first six hours. Taken together, both cell viability studies and apoptosis studies highlighted the role of Mcl-1 in regulation of anoikis in H460 cells.

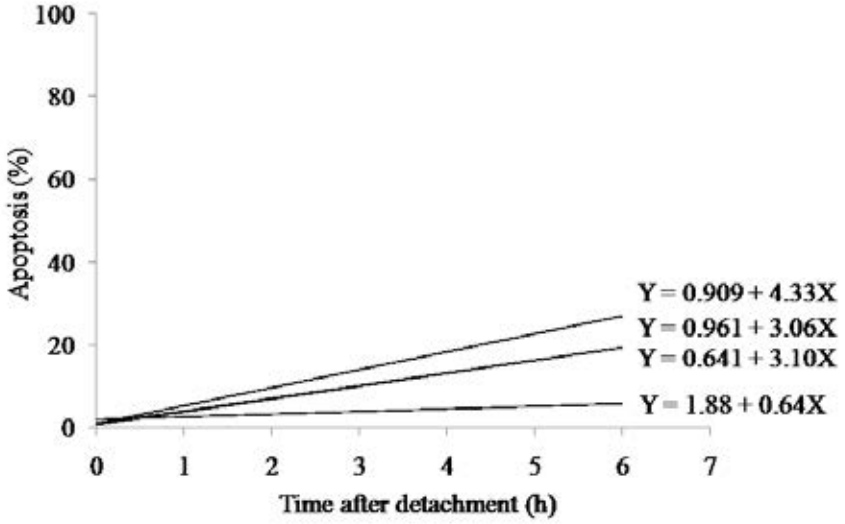

Figure 31 Regression plots of apoptosis versus time after detachment in each different set of Mcl-1 variants H460 cells

Transfectants	Equation	R^2	β	P value
Mock	Y = 0.641 + 3.10X (P-value < 0.0001)	0.986	3.10	-
HMcl-1	Y = 1.88 + 0.64X (P-value < 0.0001)	0.966	0.64	<0.0001
Control shRNA plasmid A	Y = 0.961 + 3.06X (P-value < 0.0001)	0.998	3.06	-
shMcl-1	Y = 0.909 + 4.33X (P-value < 0.0001)	0.946	4.33	<0.0001

Table 5 Regression analysis of apoptosis in Mcl-1 variants H460 cells after detachment for 6 h.

To visualize the primary mode of cell death after the detachment, morphological analyses of apoptotic and necrotic cell death by Hoechst 33342 and propidium iodide assays has been performed and the results showed that apoptosis was the primary mode of cell death induced by cell detachment in Mcl-1 variants H460 cells (Fig. 32).

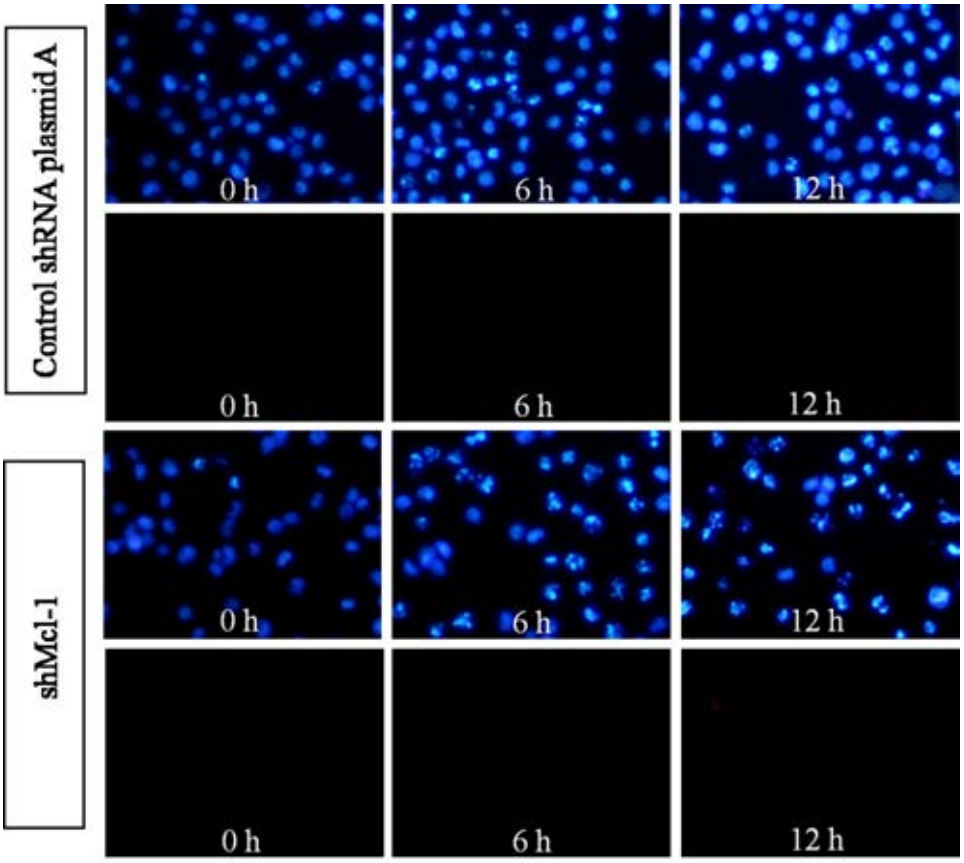

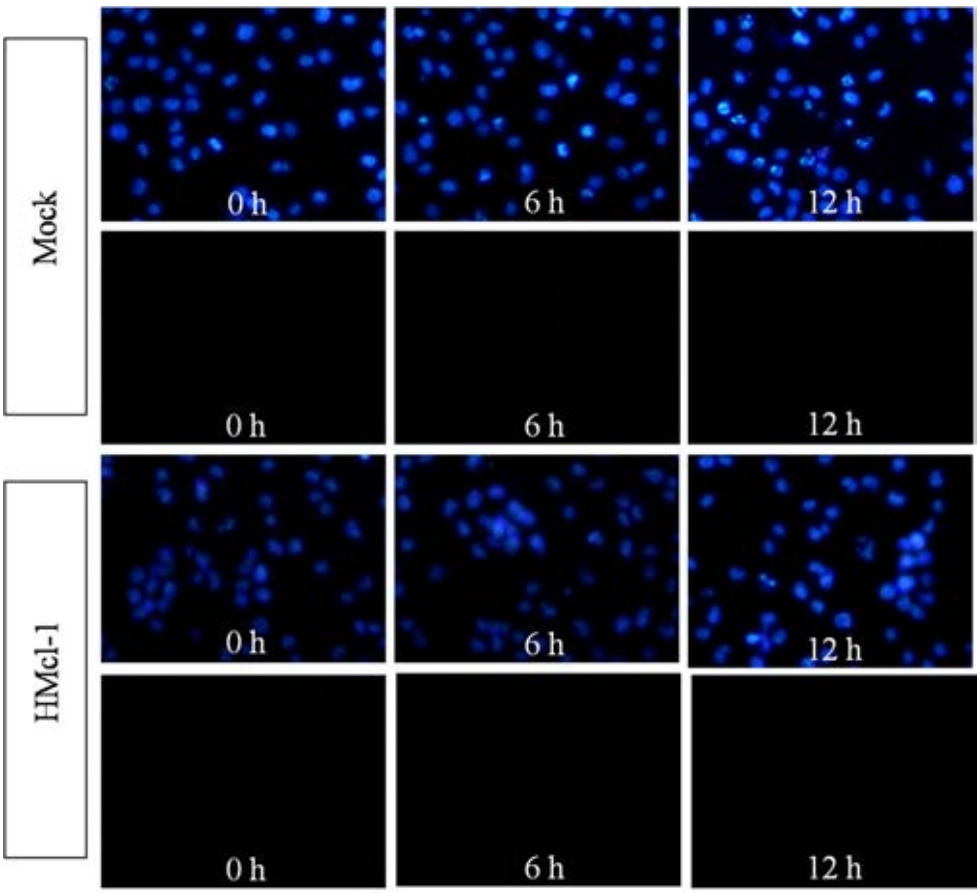

Figure 32 Morphology of detachment-induced apoptosis and necrosis in control transfected cells, Mcl-1 overexpressing (**A**) and Mcl-1 knockdown cells (**B**). Detached cells were suspended in poly-HEMA coated plates for 0-12 h and cell apoptosis and necrosis were determined by Hoechst 33342 and PI fluorescence measurements, respectively.

6. Mcl-1 promotes anchorage-independent growth of H460 cells

Like Cav-1 variants H460 cells, Mcl-1 variants were subjected to anchorage independent studies. Figure 33 shows that differential Mcl-1 expression could significantly affect the ability of H460 cells to grow under anchorage-independent conditions. In HMcl-1, large cell colonies have been observed whereas in basal Mcl-1 level H460 cells were found smaller size. Moreover, cav-1 shRNA H460 cells have the smallest colonies containing most dead cells as determined by trypan blue exclusion assay. These results indicated that Mcl-1 is a key determinant for anchorage-independent growth of H460 cells which exhibits similar characteristic as Cav-1 in this manner.

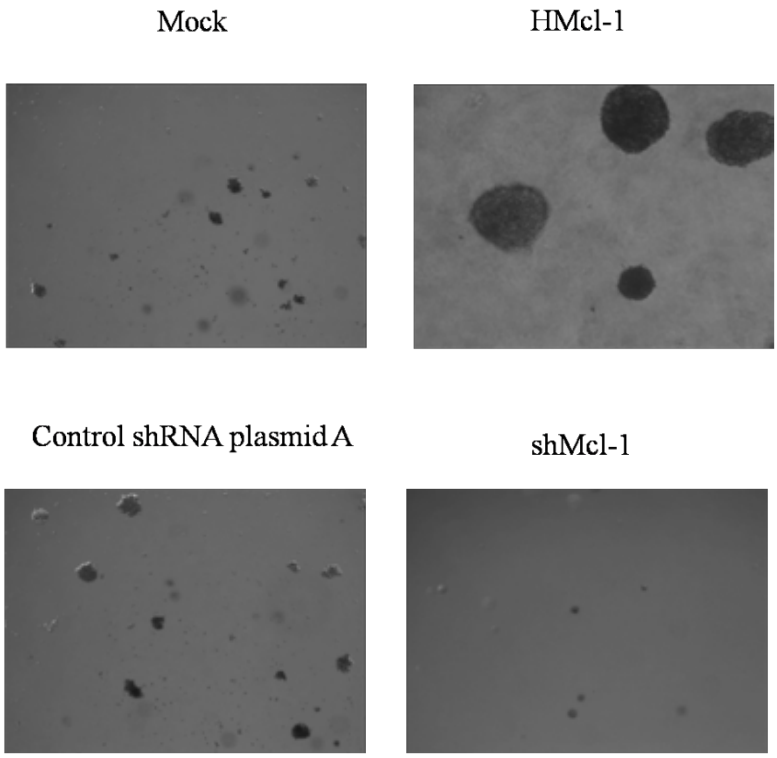

Figure 33 Effect of Mcl-1 expression on anchorage-independent growth of H460 cells in soft agar. A: Mock and HMcl-1 cells were detached and cultured under suspending conditions in soft agar containing growth medium (RPMI), 10% FBS, and 0.33% agarose as described in MATERIALS AND METHODS. B: Control shRNA plasmid A and shMcl-1 cells were detached and suspended in soft agar using the same conditions as in A. Cells were fed twice a week and photographed after 2 wk for their ability to proliferate and form colonies. The representative fields were photographed at ×10 magnification. The results are representative of three independent experiments.

7. Cell detachment induces Cav-1 and Mcl-1 downregulation

The role of Cav-1 and Mcl-1 in cancer cell anoikis is unclear. To provide evidence for the role of these proteins, the evaluation of the expression profiles of Cav-1 and Mcl-1 after cell detachment in lung cancer H460 cells were performed. The cells were detached, suspended in adhesion-resistant plates, and analyzed for Cav-1 and Mcl-1 protein expression by Western blotting.

7.1 Cell detachment induces Cav-1 downregulation

After cell detachment, Cav-1 expression gradually decreased over time in concomitant with cell viability and death, suggesting their potential relationship and role in anoikis regulation.

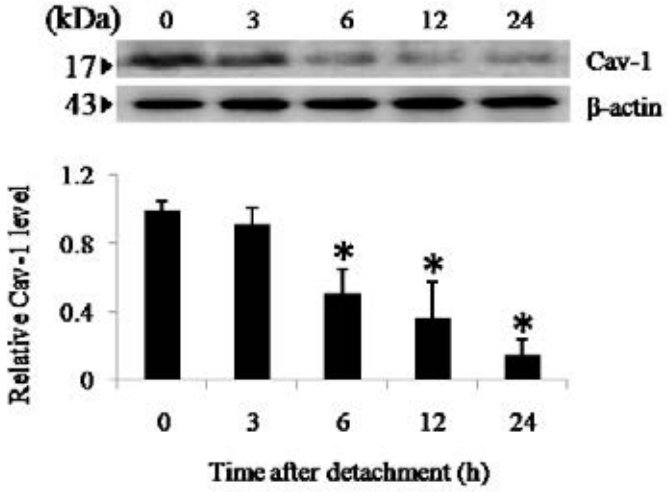

Figure 34 Cell detachment induces Cav-1 downregulation. H460 cells were detached and suspended in poly-HEMA coated plates for various times (0-24 h). Blots were probed with antibodies specific to Cav-1 and were reprobed with β-actin antibody. Columns are mean ± S.D. (n = 3)*, $P < 0.05$ versus control at time 0.

7.2 Cell detachment induces Mcl-1 downregulation

After cell detachment, Mcl-1 expression gradually decreased over time in concomitant with Cav-1 level. The reduction of Mcl-1 closely correlated with the Cav-1 reduction, suggesting these two proteins might have some degree of regulating with each other.

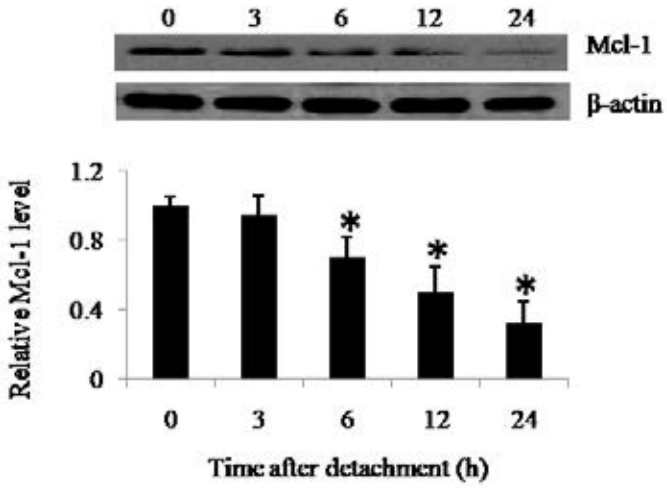

Figure 35 Cell detachment induces Mcl-1 downregulation. Cell detachment induces Mcl-1 downregulation. H460 cells were detached and suspended in poly-HEMA coated plates for various times (0-24 h). Blots were probed with antibodies specific to Mcl-1 and were reprobed with β-actin antibody. Columns are mean ± S.D. (n = 3)*, $P < 0.05$ versus control at time 0.

1.3 Correlation of Cav-1 and Mcl-1 reduction

The western blot results have shown that the level of Cav-1 and Mcl-1 were gradually reduced over time of detachment. The correlation analysis has been employed to confirm the reduction of these two proteins was directly correlated. SPSS analysis shows that the reduction of these two proteins has well correlated with Pearson correlation (*r)* = 0.986 (P value< 0.0001, N=3).

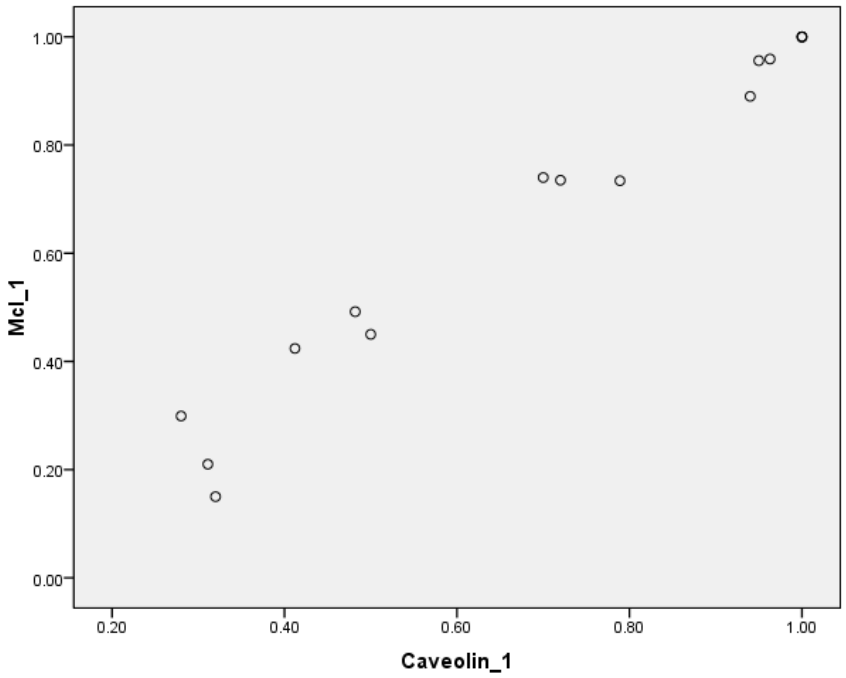

Figure 36 Correlation analysis of the expression of Cav-1 and Mcl-1 after detachment of H460 cells.

8. Interaction of Cav-1 and Mcl-1 protein

1.1 Immunoprecipitation study of Cav-1 and Mcl-1

According to the correlation analysis that indicates the closely correlation of this two proteins. Immunoprecipitation assay to assess the possibility of the direct interaction has been performed. Results clearly showed that Cav-1-Mcl-1 complex formation was most pronounced in HCav-1 cells, which express the highest level of Cav-1, and least expressed in Cav-1 knockdown (shCav-1) cells (Fig. 37). Moreover, consistent results were observed in the immunoprecipitation experiment using Mcl-1 antibody followed by Western blot analysis using Cav-1 antibody. These results suggest that Cav-1 plays a role in scaffolding Mcl-1 protein and that its interaction with Mcl-1 may play a role in regulating Mcl-1 level

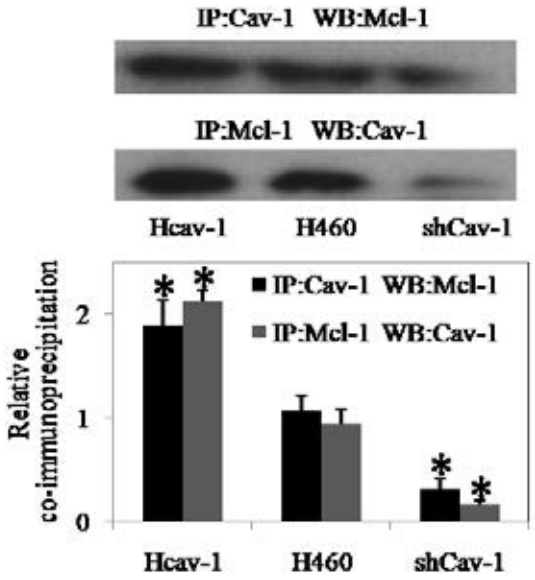

Figure 37 Immunoprecipitation study of Cav-1 and Mcl-1**.** Immunoprecipitation experiments were performed using specific anti-Cav-1 antibody, immunoblots were probed with anti-Mcl-1 antibody and vice versa. Equal amounts of protein (25 μg) were loaded in each lane. Columns are the mean ± S.D (n = 3) *, $P < 0.05$ versus H460 cells.

8.2 Localization of Cav-1 and Mcl-1 protein

In order to identify the localization of these two proteins, firstly, the immunofluorescence study was performed with the use of specific primary antibodies and the secondary antibodies linked to specific fluorescence probes. The results were demonstrated that, however, the localization of the Cav-1 protein seems to disperse throughout the cell cytoskeleton. Unfortunately, Mcl-1 protein which was known to localize mainly at the mitochondria, are also found to disperse throughout the cell structure (Fig. 38).

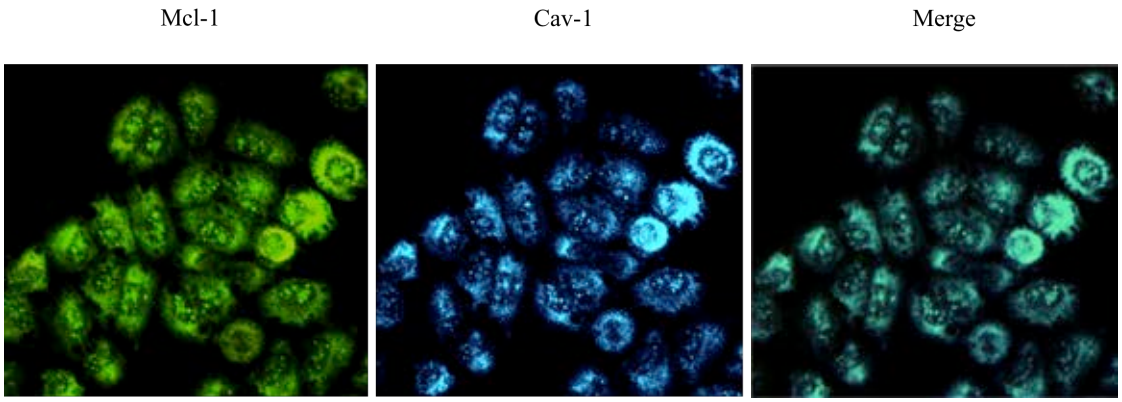

Figure 38 Localization of Cav-1 and Mcl-1 protein. H460 cells were analyzed for localization of Cav-1 and Mcl-1 by immunofluorescence microscopy. Immunofluorescence was performed using mouse anti-Cav-1 monoclonal antibody and rabbit anti-Mcl-1 polyclonal antibody, followed by appropriate secondary antibodies labeled with Alexa Fluor 350 and Alexa Fluor 488 to visualize Cav-1 and Mcl-1, respectively.

Mcl-1 and Cav-1 were found to be localized at the mitochondrial membrane [Chou et al., 2006; Liu et al., 2002], to investigate whether these interactions were occurred at the mitochondria, the Rhodamine-base probe, Mitotracker was employed to assess this specific localization. Adhered HCav-1, shCav-1, and H460 cells were stained with antibodies for Mcl-1, Cav-1, and MitoTracker, and their fluorescent signals were observed by microscopy. While the MitoTracker signals are relatively constant in these cells, the intensities of Cav-1 and Mcl-1 signals in these cells vary greatly (Fig. 39). Interestingly, cells that express a high level of Cav-1 (HCav-1) also exhibit a high level of Mcl-1, while those that express a low level of Cav-1 (shCav-1) also show a low level of Mcl-1, suggesting the stabilizing effect of Cav-1 on Mcl-1.

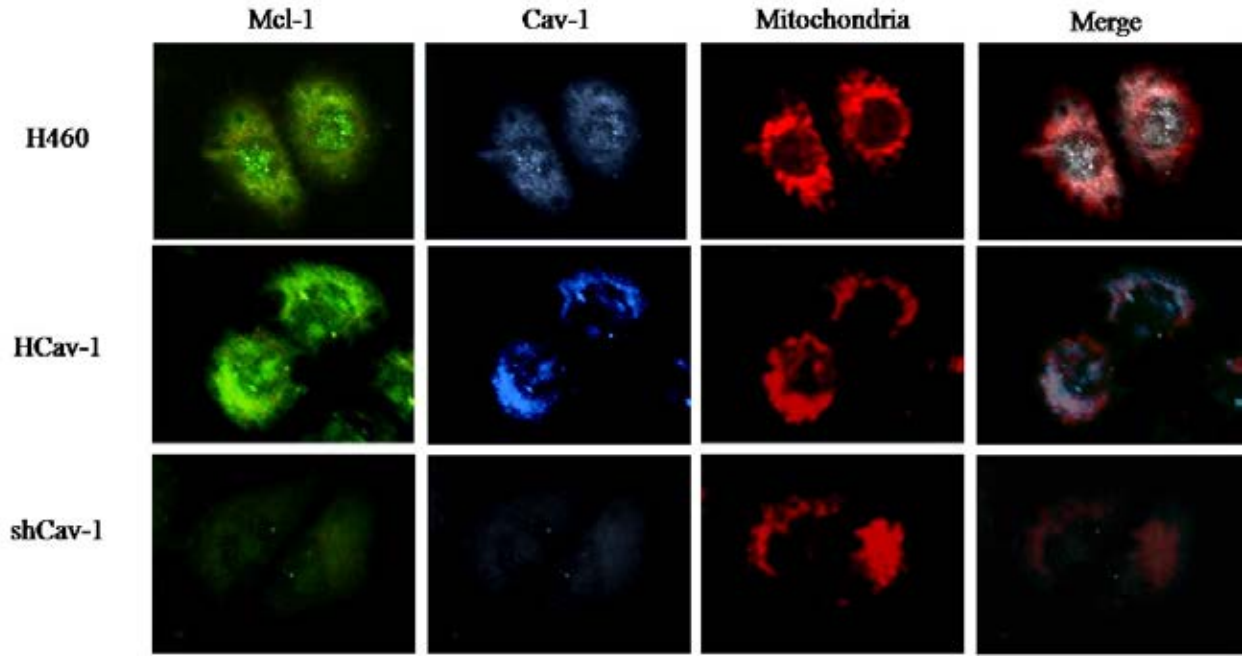

Figure 39 Differential expression of Cav-1 and Mcl-1 in HCav-1, shCav-1, and H460 cells. The cells were analyzed for localization of Cav-1 and Mcl-1 by immunofluorescence microscopy. Immunofluorescence was performed using mouse anti-Cav-1 monoclonal antibody and labeled with Alexa Fluor 350 (blue) and Alexa Fluor 488 (green) to visualize Cav-1 and Mcl-1, respectively. Cells were also stained with MitoTracker Red CMXRos (300 nM) to aid visualization of mitochondria.

9. Cav-1 stabilizes Mcl-1 in H460 cells

9.1 Mcl-1 basal level is dependent on Cav-1 level

Scaffolding function of Cav-1 leads to the hypothesis of Cav-1 that may regulates the expression of Mcl-1, to verify this, the cells with different Cav-1 level were firstly investigated for basal Mcl-1. Accordingly, the Mcl-1 levels were found directly proportional to the Cav-1 expression level in H460 cells.

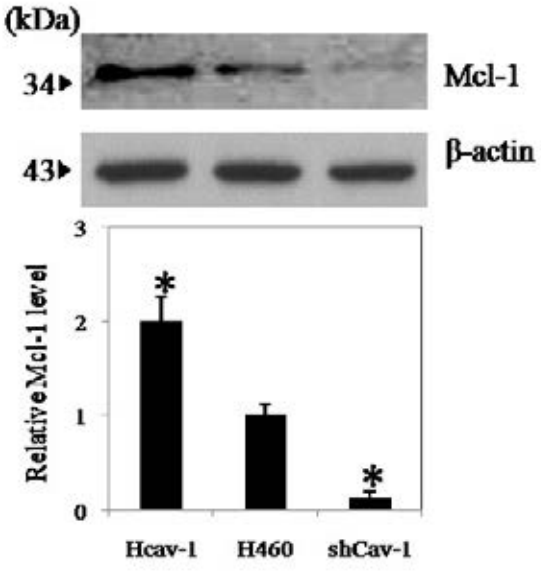

Figure 40 Relative basal Mcl-1 levels in Cav-1 variants H460 cells. Columns are the mean ± S.D (n = 3) *, $P < 0.05$ versus H460 cells.

9.2 Cav-1 stabilized Mcl-1 in detached state

To further study the effect of Cav-1 stabilization after cell detachment, HCav-1, shCav-1, and H460 cells were detached and incubated in adhesion-resistant plates for 0-12 h. Western blot analysis of Mcl-1 was then performed at 0, 6, and 12 h post-detachment. Figure 41 shows that at various times of the detachment, Mcl-1 levels in these cells varied depending on the expression levels of Cav-1 in each cell type. These findings strengthen the above finding that Cav-1 interacts with Mcl-1 and stabilizes the protein under different attachment conditions.

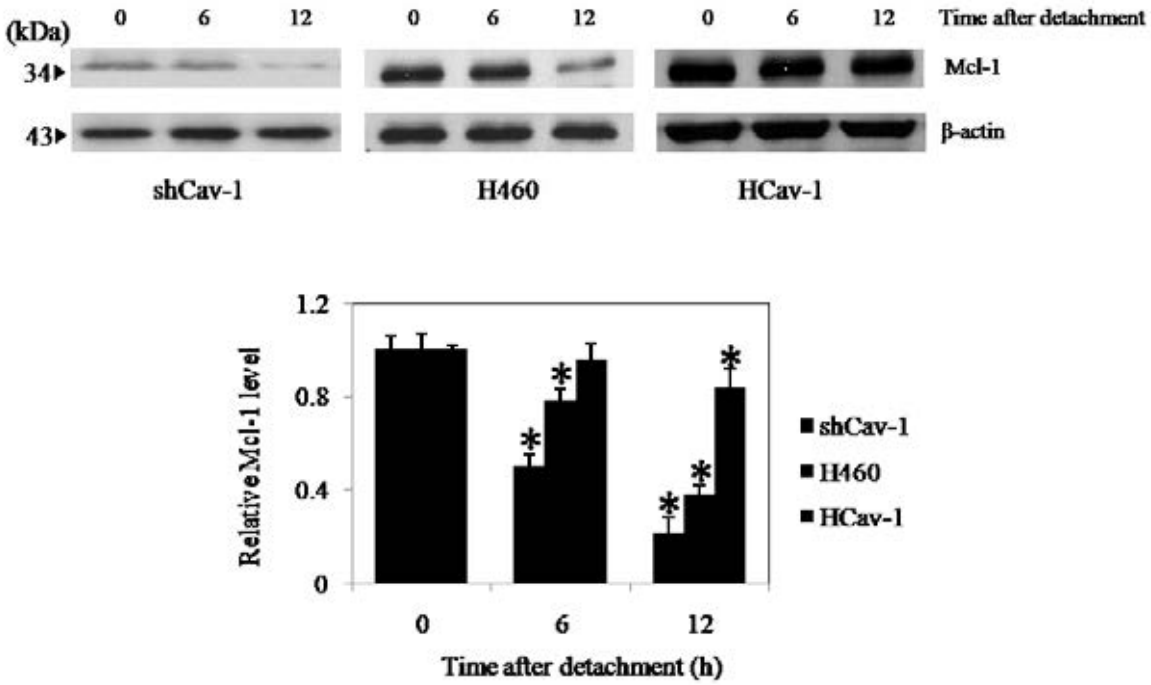

Figure 41 Relative Mcl-1 levels in shCav-1, HCav-1, and H460 cells after detachment for 0, 6 and 12 h. Columns are the mean ± S.D. (n = 3). *, $P < 0.05$ versus control at detachment time = 0 h.

10. Mcl-1 reduction after cell detachment is mediated through ubiquitin-proteasomal degradation

10.1 Mcl-1 mRNA level during detachment

Since Mcl-1 is the anti-apoptotic protein that plays a role in controlling anoikis in H460 as shown in this study. Moreover, the reduction of Mcl-1 protein also correlated well with the cell viability assay. To identify the mechanism(s) that is critical for the Mcl-1 protein reduction, firstly, the real-time PCR analysis for Mcl-1 mRNA was performed to indicate the role of transcription on the Mcl-1 protein level after detachment. As shown in Figure 42, the Mcl-1 mRNA rapidly decreased within 3 hour after detachment and remained unchanged up to 24 h after detachment.

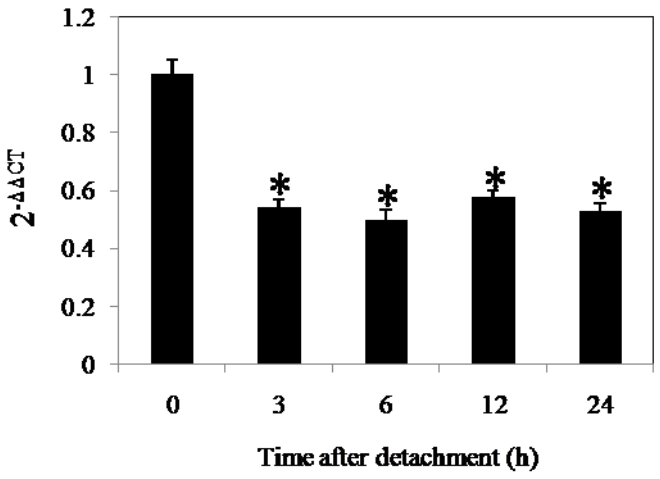

Figure 42 Real-time PCR analysis of Mcl-1 mRNA expression after cell detachment of H460 cells. The relative mRNA expression was determined by using the comparative C_T method as described under "*Materials and Methods*". Columns are the mean ± S.D. (n = 3). *, $P < 0.05$ versus control at detachment time = 0 h.

10.2 Mcl-1 down regulation after cell detachment is mediated by ubiquitin-proteasome system

Even though the real-time PCR results showed that the transcription of Mcl-1 protein is decreased after the cell detachment, however, the decreasing in transcription is not parallel with the Mcl-1 protein reduction as shown in Fig. 35. Another pathway of protein reduction especially protein degradation seems to play a critical role in this case. Then, to verify the involvement of ubiquitin-proteasomal system on Mcl-1 downregulation after cell detachment, the use of proteasome inhibitors has been employed. Figure 43 shows that cell detachment caused a substantial reduction in Mcl-1 protein level and that treatment of the cells with specific proteasomal inhibitors, lactacystin and MG132, completely inhibited the Mcl-1 reduction. These results indicate that Mcl-1 downregulation after cell detachment is mediated mainly by the proteasome degradation pathway.

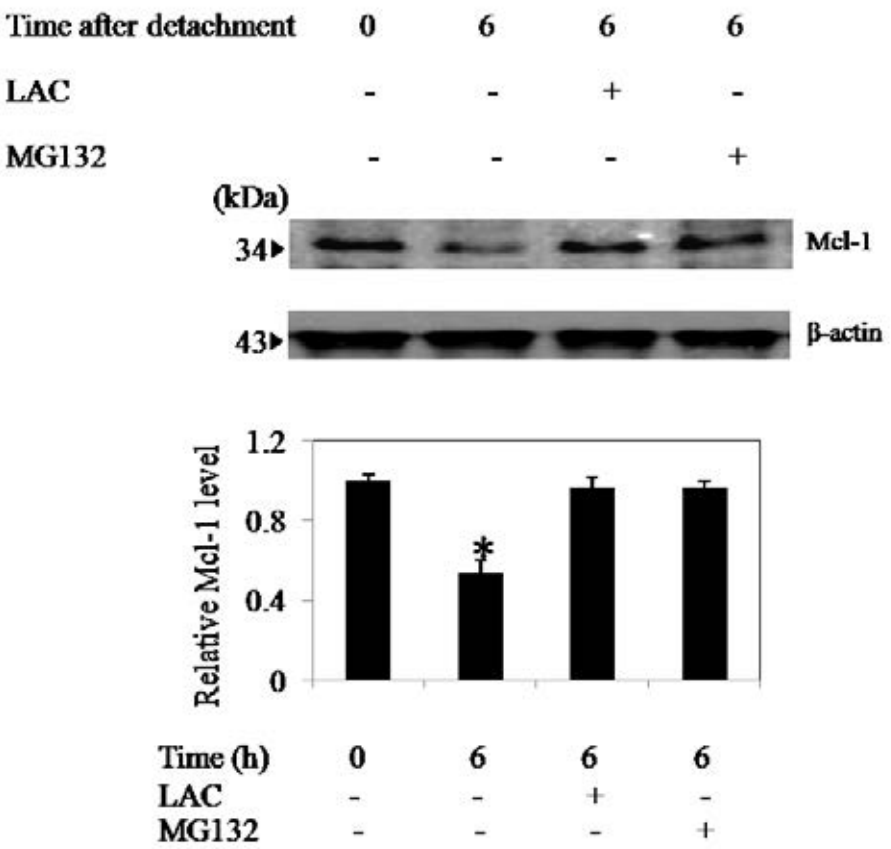

Figure 43 Relative Mcl-1 expression after detachment for 0-6 h in the presence or absence of lactacystin (LAC; 20 μM) or MG132 (10 μM) in H460 cells. Columns are the mean ± S.D. (n = 3). *, $P < 0.05$ versus control at detachment time = 0 h.

10.3 Mcl-1 ubiquitination after cell detachment

Proteasomal degradation of a protein is triggered by protein ubiquitination. In H460 cells, the formation of ubiquitin-Mcl-1 complexes (Ub-Mcl-1) gradually increased as early as 1 h after cell detachment and peaked at about 6 h. The increasing in ubiquitin-Mcl-1 complexes seem to parallel with the Mcl-1 protein reduction that is significantly reduced at 6h after detachment. These results also show that the level of ubiquitin-Mcl-1 complex formation at 6h after detachment reached the threshold to allow significant protein reduction at this time point.

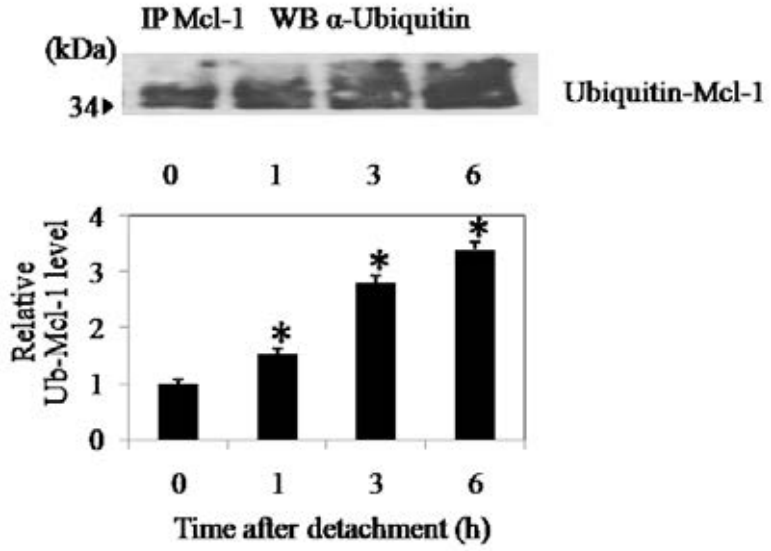

Figure 44 Mcl-1 ubiquitination after cell detachment. H460 cells were detached and suspended in poly-HEMA coated plates for various times. Cell lysates were prepared and immunoprecipitated (IP) with anti-Mcl-1 antibody. The resulting immune complexes were analyzed for ubiquitin by Western blotting (WB) using anti-ubiquitin antibody. Maximum Mcl-1 ubiquitination was observed at 6 h after cell detachment. The immunoblot signals were quantified by densitometry. Columns are the mean ± S.D. (n = 3). *, $P < 0.05$ versus control at detachment time = 0 h.

10.4 Cav-1 stabilizes Mcl-1 by attenuating Mcl-1 ubiquitination

To test the potential involvement of Cav-1 in regulating Mcl-1 ubiquitination, Mcl-1 immunoprecipitation and ubiquitination studies were performed in various Cav-1 expressing cells. The level of ubiquitin-Mcl-1 complex formation was minimal in Cav-1 overexpressing (HCav-1) cells and maximal in Cav-1 knockdown (shCav-1) cells as compared to normal H460 cells in both one and six hour after cell detachment (Fig. 45). These results indicate that Cav-1 attenuated the ubiquitination of Mcl-1 and stabilized the protein after cell detachment.

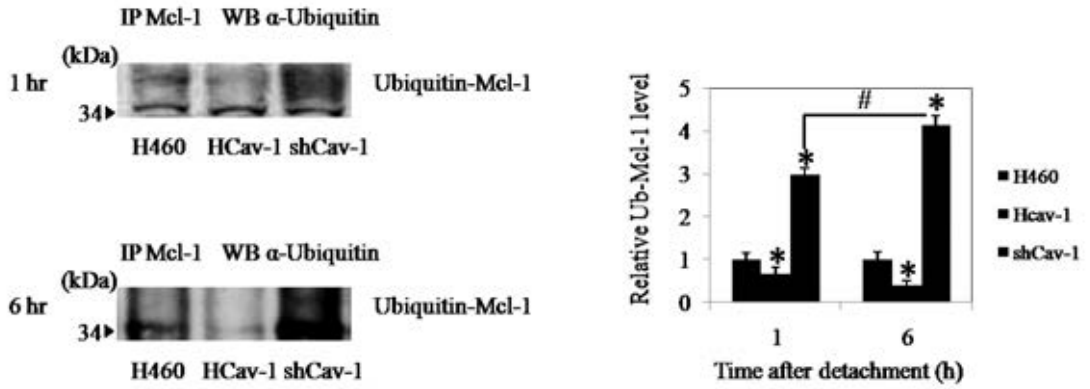

Figure 45 Cav-1 stabilizes Mcl-1 by attenuating Mcl-1 ubiquitination. HCav-1, shCav-1, and H460 cells were detached and suspended in poly-HEMA coated plates for 1 and 6 h. Cell lysates were immunoprecipitated (IP) with anti-Mcl-1 antibody and the resulting immune complexes were analyzed for ubiquitin by Western blotting (WB). Columns are the mean ± S.D. (n = 3). *, $P < 0.05$ versus H460 cells, #, $P < 0.05$ versus shCav-1 at time = 1h.

11. **Cav-1 regulates Mcl-1 expression and anoikis in human melanoma G361 cells**

11.1 Generation of Cav-1 overexpression and downregulation in G361 cells

An upregulation of Cav-1 and Mcl-1 has been found not only in non-small cell lung cancer but also in other forms of cancer such as human melanoma [Keuling et al., 2009; Nakashima et al., 2007]. To test whether Cav-1 might have a similar regulatory role on Mcl-1 and anoikis in other cancer cells, melanoma G361 cells were stably transfected with Cav-1, shCav-1, or control plasmids. After clonal selection, the cells were analyzed for Mcl-1, Cav-1, and anoikis. Figure 46 shows that the Cav-1 transfected cells (pEX_cav-1-YFP) expressed the highest level of Cav-1 protein, whereas the shCav-1 transfected cells (Cav-1 shRNA plasmid) exhibited the lowest level.

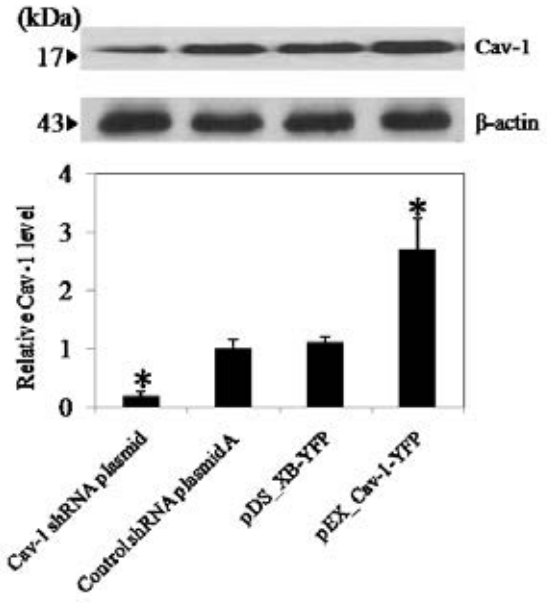

Figure 46 Generation of Cav-1 overexpression and downregulation in G361 cells. Control (pDS_XB-YFP; Control shRNA plasmid A), G361-Cav-1 (pEX_cav-1-YFP), and G361-shCav-1 (Cav-1 shRNA plasmid) transfected cells were grown and analyzed for Cav-1 expression by Western blotting. Blots were reprobed with β-actin antibody to confirm equal loading of samples. The immunoblot signals were quantified by densitometry and mean data from independent experiments were normalized to the results.

11.2 Caveolin-1 increase cell viability after detachment in H460 cells

11.2.1 Overexpression of Caveolin-1 increase cell viability after detachment in melanoma G361 cells

For investigation in the role of cav-1 on anoikis in human melanoma (G361) cells, cav-1 overexpressed and vector control cells were detached and incubated in adhesion-resistant poly-HEMA coated plates. Analysis of cell viability after detachment was determined by XTT assay. The detachment caused the cell gradually decrease in cell viability, after 6 h detachment, the cell viability were approximately 90% (91.76±1.18%), and 60% (60.32±7.9%) of the overexpressed and vector control cells respectively. Moreover, at 24 h after cell detachment, Cav-1 overexpressing cells (pEX_cav-1-YFP) exhibited approximately 60% (60.23±4.65%) viability, whereas control cells showed a survival rate of <40% (32.67±5.18%).

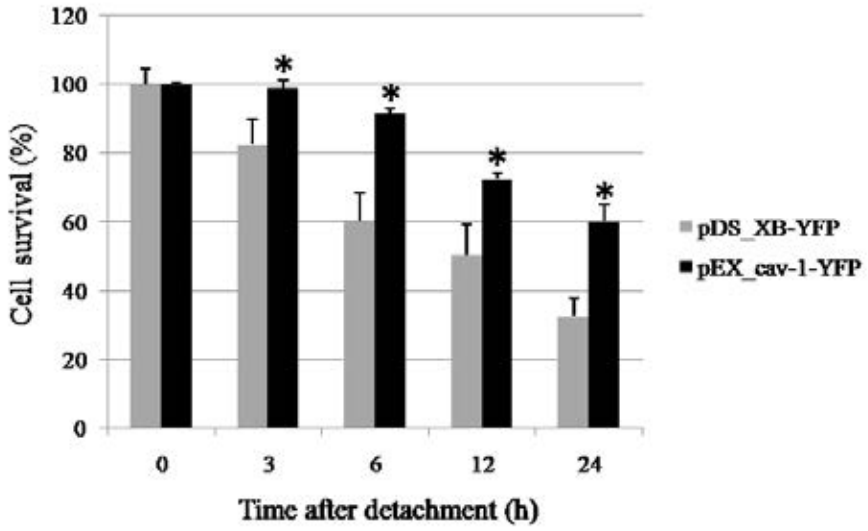

Figure 47 Overexpression of Caveolin-1 increase cell viability after detachment in melanoma G361 cells. Subconfluent (90%) monolayer of control transfected and cav-1 overexpressing G361 cells were detached and suspended in poly-HEMA coated plates for various times (0-24 h). At the indicated times after detachment, the cells were collected and the survival was determined by XTT assay. Viability of detached cells at time 0 h was considered as 100%.

11.2.2 Downregulation of Caveolin-1 decrease cell viability after detachment in melanoma G361 cells

To verify the role of knockdown Cav-1 on cell anoikis of G361, cav-1 shRNA transfected cells and vector control cells were detached and incubated in adhesion-resistant poly-HEMA coated plates. Analysis of cell viability after detachment was determined by XTT assay. The detachment caused the cell gradually decrease in cell viability, after 6 h detachment, the cell viability were approximately 60% (67.43±8.06%), and 40% (40.0±5.33%) of the vector control cells and cav-1 shRNA transfected cells respectively. Moreover, at 24 h after cell detachment, knockdown Cav-1 cells exhibited less than 20% (15.21±6.14%) viability, whereas control cells showed a survival rate around 30% (38.34±2.52%).

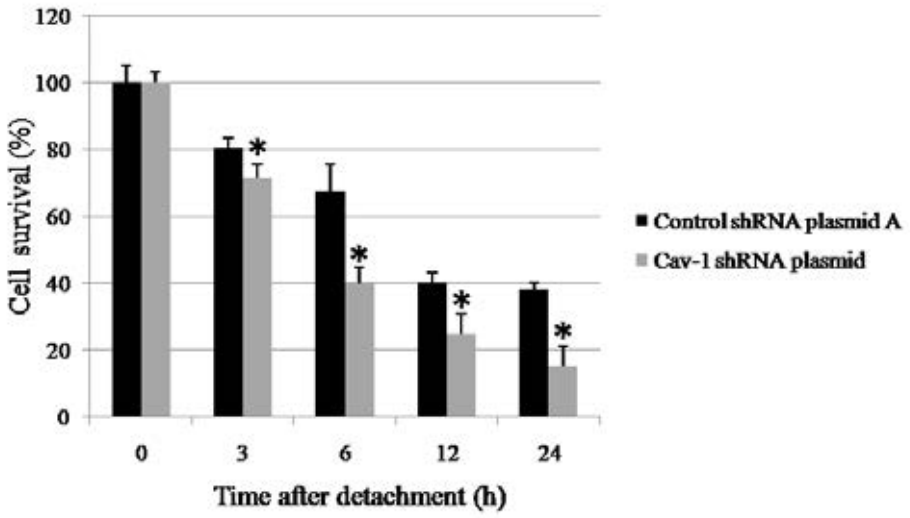

Figure 48 Downregulation of Caveolin-1 decrease cell viability after detachment in melanoma G361 cells. Subconfluent (90%) monolayer of control transfected and Cav-1 knockdown G361 cells were detached and suspended in poly-HEMA coated plates for various times (0-24 h). At the indicated times after detachment, the cells were collected and the survival was determined by XTT assay. Viability of detached cells at time 0 h was considered as 100%.

11.3 Cav-1 stabilizes Mcl-1 in G361 cells

To ensure the role of Cav-1 that may regulate the Mcl-1 in G361, to verify this, firstly, the Mcl-1 basal levels were investigated found directly proportional to the Cav-1 expression level in G361 cell (Fig. 49A). In order to test the interaction between Cav-1 and Mcl-1, cells were harvested at time 0 and at 6 h after detachment. Cell lysates were then prepared and analyzed for Mcl-1 expression by Western blotting. The results show that the levels of Mcl-1 in G361-Cav-1, G361-shCav-1, and G361 cells at 0 and 6 h post-detachment were highly dependent on the cellular level of Cav-1 in each cell (Fig. 49B).

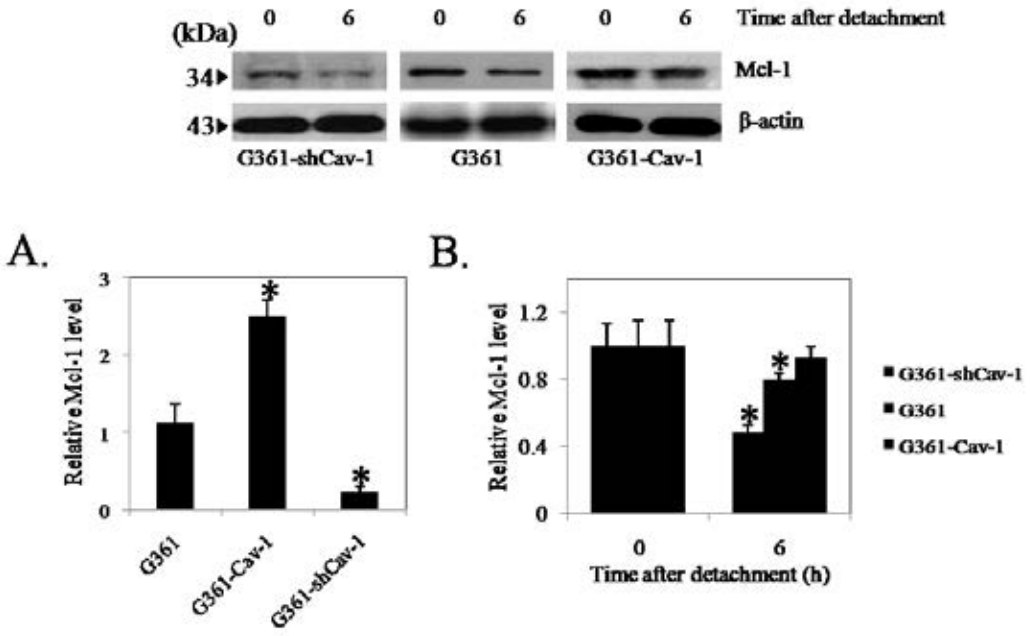

Figure 49 Cav-1 stabilizes Mcl-1 in G361 cells. **A.** Basal Mcl-1 level in differential Cav-1 expression G361 cells. **B.** Cav-1 stabilized Mcl-1 level in G361 cells. G361, G361-Cav-1 and G361-shCav-1 cells were detached and suspended in poly-HEMA coated plates for various times (0-6 h). Blots were probed with specific antibody to Mcl-1 and were reprobed with β-actin antibody. Columns are the mean ± S.D. (n = 3). *, $P < 0.05$ versus control G361 cells.

CHAPTER V

DISCUSSION AND CONCLUSION

When cells are detached from the extracellular matrix, the loss of anchorage-related signals results in an abrogation of certain cellular processes such as cell survival and growth [Hynes, 1999] and consequently initiate the process of anoikis [Frisch and Francis, 1994]. Since anoikis is an important cellular event controlling cancer metastasis, unraveling its underlying mechanisms is critical to the understanding of disease pathogenesis and its treatment. Among the many types of cancer, lung cancer has frequently been found to metastasize at the time of tumor detection. While the exact mechanisms of cancer metastasis have been extensively investigated, an upregulation of Mcl-1 [Song and Coppola, 2005] and Cav-1 [Rungtabnapa et al., 2011] has been implicated in lung cancer aggressiveness and progression. Mcl-1 was found to overexpress in NSCLC cells and regulate their survival and sensitivity to diverse apoptotic stimuli [Song and Coppola, 2005]. Apoptotic stimuli such as cell detachment induce Bim (activator of BH3-only protein) expression [Cheng et al., 2001]. Recently, Zhang has demonstrated that Mcl-1 can sequester Bim in NSCLC cells which supports the role of Mcl-1 in attenuating anoikis in this cancer cell type [Zhang et al., 2011]. Moreover, amplification or overexpression of Mcl-1 was shown to render cells resistant to detachment-induced apoptosis [Simpson et al., 2008] and the decrease in Mcl-1 level is required in the initiation of cell anoikis [Boisvert et al., 2009; Woods et al., 2007]. Previous studies showed that Cav-1 confers resistance to anoikis in cancer cells [Fiucci et al., 2002; Rungtabnapa et al., 2011]. Furthermore, the expression of Cav-1 has been used as a

biomarker for virulence of some cancers [Corn and Thompson, 2010]. The role of Cav-1 in cancer cell anoikis has been described in many ways such as the induction of survival pathways [Li, et al., 2003] and the reduction of Cav-1 and Mcl-1 [Rungtabnapa et al., 2011; Woods et al., 2007]. In this study, firstly, the role of Cav-1 and Mcl-1 were evaluated in parallel by using the transfections technique to generate the different Cav-1 and Mcl-1 transfectants. The regression analysis of the kinetic of cell viability and apoptosis studies clearly suggested the role of these two proteins in regulating anoikis in H460 cells. For further elucidates their role in H460 cell anoikis, by using endogenous level of Cav-1 and Mcl-1 in H460 cells, the results also shown the reduction of both Cav-1 and Mcl-1 level during cell anoikis. Correlation analysis of the protein reductions strengthen these finding with the Pearson correlation equal to 0.986. With tightly correlated, these results lead to the hypothesis that Cav-1 may directly interact with Mcl-1. The immunoprecipitation studies show that Cav-1 functioned as a scaffold protein for Mcl-1 binding (Fig. 37). In addition, the Cav-1-Mcl-1 complex significantly increased in the Cav-1 overexpressing (HCav-1) cells, but decreased in the Cav-1 knockdown (shCav-1) cells. Immunocytochemistry studies further confirmed the co-localization of Cav-1 and Mcl-1 in the cells which was largely associated with the mitochondria (Fig. 39).

In sought for the possible interaction site of Mcl-1, according to the sequence of cav-1 binding domain that had been suggested to match the following motifs: ΦXΦXXXXΦ, ΦXXXXΦXXΦ, ΦXΦXXXXΦXXΦ, where Φ is the aromatic amino acid (Phe (F), Tyr (Y) or Trp (W)) [Razani, 2002]. Interestingly, Mcl-1 sequence also contains the motif that resemble to that of cav-1 binding domain which contains ^{312}WDGFVEFF^{319} locating close to the transmembrane domain of Mcl-1.

This motif is of interesting for further elucidating the interaction with cav-1 and the interactions consequence in terms of Mcl-1 anti-apoptotic activity and also membrane localization.

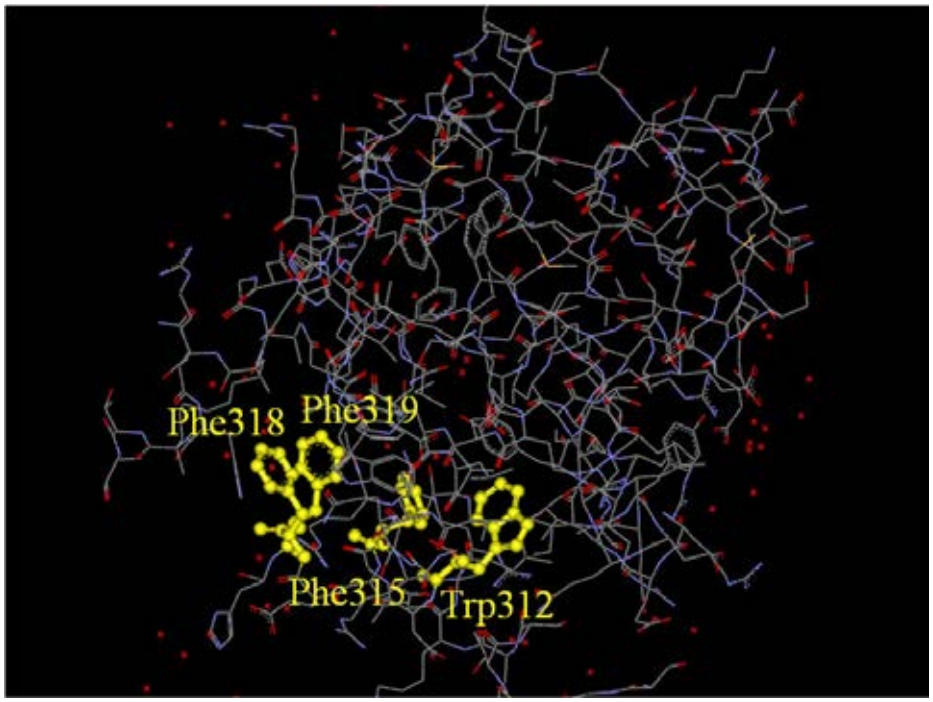

Figure 50 Structure of Mcl-1 residue 172-327 containing aromatic amino acid resemble to cav-1 binding domain (highlighted in yellow) that possible to interact with the scaffolding domain of Cav-1.

Since Mcl-1 is known to be a short half-life protein due to continuous proteasomal degradation [Woods et al., 2007], it is possible that its interaction with Cav-1 could affect its stability which was first demonstrated in this study. Although a rapid decline in Mcl-1 mRNA level was observed at 1 h post-detachment, the mRNA level remained relatively constant during the next 24-h period (Fig. 42). This observation resembled with the previous report of the slightly decrease in Mcl-1 transcription after cell detachment [Woods et al., 2007]. Because Mcl-1 protein level

was significantly decreased at 6 h post-detachment and continued to decline during the 24 h period, this finding ruled out transcriptional regulation as responsible for the Mcl-1 downregulation. Moreover, the observation that proteasome inhibitors completely inhibited detachment-induced Mcl-1 downregulation (Fig. 43) strongly supported protein degradation and stabilization of Mcl-1 by Cav-1 as a key control mechanism.

Proteasomal degradation of a protein is generally triggered by its ubiquitination [Glickman and Ciechanover, 2002]. The experiments found that Mcl-1 is ubiquitinated during cell detachment and that this process is inhibited by Cav-1. The mechanism by which Cav-1 inhibits Mcl-1 ubiquitination is unclear but likely involves steric hindrance of the ubiquitination sites by Cav-1. The interaction between Cav-1 and Mcl-1 may also affect Mcl-1 phosphorylation which has been linked to its ubiquitination. Since PI3K/Akt/GSK3β signaling is known to regulate Mcl-1 ubiquitination, and the phosphorylation of Mcl-1 at Ser159 by glycogen synthase kinase-3 was observed during cell anoikis [Woods et al., 2007] and was found to promote Mcl-1 ubiquitination and subsequent degradation [Maurer et al., 2006] these highlighted the role of PI3K/Akt/GSK3β signaling pathway in regulating Mcl-1 ubiquitination during anoikis. Moreover, some evidence suggests that cav-1 can modulate activity of this pathway [Shack et al., 2003], then, further studies to characterize the role of Cav-1 that reduce Mcl-1 ubiquitination via the PI3K/Akt/GSK3β signaling pathway is of interest.

Other molecular aspects of the relation between Cav-1 and Mcl-1 ubiquitination also require further investigation. At least three ubiquitin ligase

(MULE, β-TRPC and SCF/Fbw7) can also contribute to Mcl-1 ubiquitination, and the deubiquitinase USP9x has been implicated in its deubiquitination [Inuzuka et al., 2011; Thomas et al., 2010]. Whether cav-1 might inhibit one (or more) of the ubiquitin ligases or by affecting the deubiquitinase activity remains to be further characterized.

These studies extended the finding on the role of Cav-1 in Mcl-1 and anoikis regulation in lung carcinoma H460 cells to melanoma G361 cells due to their reported expression in human melanoma [Keuling et al., 2009; Nakashima et al., 2007]. We found that Cav-1-Mcl-1 interaction could be detected in G361 cells and that such interaction is dependent on the cellular level of Cav-1 which determines cellular susceptibility to anoikis (Fig. 49). These results support the general role of Cav-1 as anoikis regulator through Mcl-1 interaction.

In conclusion, this study reported a novel finding on the role of Cav-1 in anoikis regulation of human lung carcinoma and melanoma cells. While the role of Cav-1 and Mcl-1 in anoikis regulation has been reported, their association and the underlying mechanisms of regulation are unclear. This study found that Cav-1 interacts with Mcl-1 and stabilizes the protein by blocking its ubiquitination and subsequent degradation. Because an elevated expression of Cav-1 and Mcl-1 has been linked to the progression of cancer and metastasis, the findings of this study could be beneficial to the understanding on cancer etiology and metastasis mechanisms.

REFERENCES

Akgul, C., Moulding, D.A., White, M.R., Edwards, S.W. 2000. In vivo localisation and stability of human Mcl-1 using green fluorescent protein (GFP) fusion proteins. FEBS Letters 478(1–2): 72–76.

Akiyama, T., Dass C.R., and Choong, P.F.M. 2009. Bim-targeted cancer therapy: A link between drug action and underlying molecular changes. Molecular Cancer Therapeutics 8: 3173-3180.

Alberts B., Johnson A., Lewis J. 2008. Molecular biology of the cell 5th ed. Garland science. P. 393-95.

Boisvert, A. K., Longmate, W., Abel, E. V., and Aplin, A. E. 2009. Mcl-1 Is Required for Melanoma Cell Resistance to Anoikis. Molecular Cancer Research 7:549-556.

Borner, M. M., Brousset, P., Pfanner-Meyer, B., Bacchi, M., Vonlanthen, S., Hotz, M. A., *et al.* 1999. Expression of apoptosis regulatory proteins of the Bcl-2 family and p53 in primary resected non-small-cell lung cancer. British Journal of Cancer 79(5/6):952-958.

Burgermeister, E., Liscovitch, M., Röcken, C., Schmid, A.R.M., Ebert, M.P.A. 2008. Caveats of caveolin-1 in cancer progression. Cancer Letters 268: 187–201.

Chanvorachote, P., Nimmannit, U., Lu, Y., Talbott, S., Jiang, B. H., and Rojanasakul, Y. 2009. Nitric oxide regulates lung carcinoma cell anoikis through inhibition of ubiquitin-proteasomal degradation of caveolin-1. The Journal of Biological Chemistry 284(41):28476-28484.

Chen, L., Willis, S. N., Wei, A., Smith, B. J., Fletcher, J. I., Hinds, M. G., *et al*. 2005. Differential targeting of pro survival Bcl-2 proteins by their BH3-only ligands allows complementary apoptotic function. Molecular Cell 17:393-403.

Chen, L., Willis, S.N., Wei, A., Smith, B.J., Fletcher, J.I., *et al*. 2005. Differential targeting of prosurvival Bcl-2 proteins by their BH3-only ligands allows complementary apoptotic function. Molecular Cell 17(3): 393–403.

Cheng, E. H., Wei, M. C., Weiler, S., Flavell, R. A., Mak, T. W., Lindsten. T., *et al.* 2001. Bcl-2 and Bcl-xL sequester BH3 domain-only molecule preventing Bax and Bak-mediated mitochondrial apoptosis. Molecular Cell 8(3):705-711.

Chiarugi, P., and Giannoni, E. 2008. Anoikis: A necessary death program for anchorage-dependent cells. Biochemical Pharmacology 76:1352-1364.

Chou, C. H., Lee, R. S., and Yang Yen, H. F. 2006. An Internal EELD Domain Facilitates Mitochondrial Targeting of Mcl-1 via a Tom70-dependent Pathway. Molecular Biology of the Cell 17:3952-3963.

Clohessy, J. G., Zhuang, J., de Boer, J., Gil-Gmez, G. and Brady, H. J. 2006. Mcl-1 interacts with truncated Bid and inhibits its induction of cytochrome c release and its role in receptor-mediated apoptosis. The journal of biological chemistry 281:5750-5759.

Corn, P. G., and Thompson, T. C. 2010. Identification of a novel prostate cancer biomarker, caveolin-1: Implications and potential clinical benefit. Journal of Cancer Management and Research 2:111-122.

Couet, J., Li, S., Okamoto, T., Ikezu, T., and Lisanti, M. P. 1997a. Identification of peptide and protein ligands for the caveolin-scaffolding domain. Implications for the interaction of caveolin with caveolae-associated proteins. The Journal of Biological Chemistry 272:6525-6533.

Craig, D.S., Kika, A., and Aaron, D.S. 2008. Anoikis resistance and tumor metastasis. Cancer Letters 272: 177-185.

Day, C.L., Chen, L., Richardson, S.J., Harrison, P.J., Huang, D.C., *et al*. 2005. Solution structure of prosurvival Mcl-1 and characterization of its binding by proapoptotic BH3-only ligands. The Journal of Biological Chemistry 280(6): 4738–4744.

Day, C.L., Smits, C., Fan, F.C., Lee, E.F., Fairlie, W.D., *et al*. 2008. Structure of the BH3 domains from the p53-inducible BH3-only proteins Noxa and Puma in complex with Mcl-1. The Journal of Molecular Biology 380(5): 958–971.

Derenne, S., Monia,B., Dean, N. M., Taylor, J. K., Rapp, M.J., Harousseau,J.L., *et al*. 2002. Antisense strategy shows that Mcl-1 rather than Bcl-2 or Bcl-x(L) is an essential survival protein of human myeloma cells. Blood 100:194-199.

Ding, Q., He, X., Hsu, J. -M., Xia, W. Chen, C. T., Li, L. Y., *et al.* 2007. Degradation of Mcl-1 by β-TrCP Mediates Glycogen Synthase Kinase 3-Induced Tumor Suppression and Chemosensitization. Molecular and Cellular Biology 11:4006-4017.

Ding, Q., He,X., Xia,W., Hsu, J. -M., Chen, C. -T., Li, L. -Y., et. al. 2007. Myeloid Cell Leukemia-1 Inversely Correlates with Glycogen Synthase Kinase-3B Activity and Associates with Poor Prognosis in Human Breast Cancer. Cancer Research 67(10):4564-4571.

Engelman, J. A., Chu, C., Lin, A., Jo, H., Ikezu, T., Okamoto, T., *et al.* 1998. Caveolin-mediated regulation of signaling along the p42/44 MAP kinase cascade in vivo. A role for the caveolin-scaffolding domain. FEBS Letter 428:205-211.

Fiucci, G., Ravid, D., Reich, R., and Liscovitch, M. 2002. Caveolin-1 inhibits anchorage-independent growth, anoikis and invasiveness in MCF-7 human breast cancer cells. Oncogene 21:2365- 2375.

Fiucci, G., Ravid, D., Reich, R.,and Liscovitch, M. 2002. Caveolin-1 inhibits anchorage-independent growth, anoikis and invasiveness in MCF-7 human breast cancer cells. Oncogene 21: 2365- 2375.

Frisch, S. M., and Francis, H. 1994. Disruption of epithelial cell-matrix interactions induces apoptosis. Journal of Cell Biology 124(4):619-626.

Glickman, M. H., and Ciechanover, A. 2002. The Ubiquitin-Proteasome Proteolytic Pathway: Destruction for the Sake of Construction. Physiological Reviews 82:373-428.

Han, J., Goldstein, L. A., Hou, W. and Rabinowich, H. 2007. Functional linkage between NOXA and Bim in mitochondrial apoptotic events. The Journal of Biological Chemistry 282:16223-16231.

Hanahan, D. and Weinberg, R.A. 2000. The hallmark of cancer. Cell 100: 57-70.

Hayer, A., Stoeber, M., Ritz,D., Engel, S., Meyer, H. H., and Helenius, A. 2010. Caveolin-1 is ubiquitinated and targeted to intralumenal vesicles in endolysosomes for degradation. Journal of Cell Biology 191(3):615-629.

Ho, C. C., Huang, P. H., Huang H. Y., Chen, Y. H., Yang, P. C., and Hsu, S. M. 2002. Up-regulated caveolin-1 accentuates the metastasis capability of lung adenocarcinoma by inducing filopodia formation. The American Journal of Pathology 161:1647-1656.

Ho, C.C, Kuo, S.H., Huang, P.H., Huang, H.Y., Yang, C.H.,Yang, P.C. 2007. Caveolin-1 expression is significantly associated with drug resistance and poor prognosis in advanced non-small cell lung cancer patients treated with gemcitabine-based chemotherapy. Lung Cancer 59: 105-110.

Hurlstone, A. F., Reid, G., Reeves, J.R., Fraser, J., Strathdee, G., Rahilly, M., *et al.* 1999. Analysis of the CAVEOLIN-1 gene at human chromosome 7q31.1 in primary tumours and tumour-derived cell lines. Oncogene 18:1881-1890.

Hynes, R. O. 1999. Cell adhesion: old and new questions. Trends in Cell Biology 9(12):M33-37.

Inuzuka, H., Fukushima, H., Shaik, S., Liu, P., Lau, A. W., and Wei, W. 2011. Mcl-1 ubiquitination and destruction. Oncotarget 2:239-244.

Keuling, A. M., Felton, K. E., Parker, A. A., Akbari, M., Andrew, S. E., and Tron, V. A. 2009. RNA silencing of Mcl-1 enhances ABT-737-mediated apoptosis in melanoma: role for a caspase-8-dependent pathway. PLoS One 4(8):1-11.

Koleske, A.J., Baltimore, D., Lisanti, M.P. 1995. Reduction of caveolin and caveolae in oncogenically transformed cells. Proceeding of the National Academy of Sciences of the United States of America 92:1381–1385.

Kozopas, K.M. 1993. MCL1, a gene expressed in programmed myeloid cell differentiation, has sequence similarity to BCL2. Proceeding of the National Academy of Sciences of the United States of America 90(8): 3516–3520.

Lajoie, P., and Nabi, I. R. 2010. Lipid Rafts, Caveolae, and Their Endocytosis. International Review of Cell and Molecular Biology 282:135-136.

Lavie, Y., Fiucci, G., and Liscovitch, M. 1998. Up-regulation of caveolae and caveolar constituents in multidrug-resistant cancer cells. The journal of biological chemistry 273:32380-32383.

Li, G., Satyamoorthy, K., Meier, F., Berking, C., Bogenrieder, T. and Herlyn, M. 2003. Function and regulation of melanoma-stromal fibroblast interactions: when seeds meet soil. Oncogene 22:3162-3171.

Li, L., Ren, C. H., Tahir, S. A., Ren, C., and Thompson, T. C. 2003. Caveolin-1 Maintains Activated Akt in Prostate Cancer Cells through Scaffolding Domain Binding Site Interactions with and Inhibition of Serine/Threonine Protein Phosphatases PP1 and PP2A. Molecular and Cellular Biology 23(24):9389-9404.

Liu, P., Rudick, M., and Anderson, R. G. W. 2002. Multiple functions of caveolin-1. The journal of biological chemistry 277(44):41295-41298.

Livak, K.J., Schmittgen, T.D. 2001. Analysis of relative gene expression data using real-time quantitative PCR and the $2^{-\Delta\Delta CT}$ method. Methods 25: 402-408.

Lloyd, P. G., and Hardin, C. D. 2011.*Caveolae in cancer: two sides of the same coin?* Focus on "Hydrogen peroxide inhibits non-small cell lung cancer cell anoikis through the inhibition of caveolin-1 degradation." American Journal of Physiological-Cell Physiology 300:C232-C234.

Loza-Coll, M. A., Perera, S., Shi1, W., and Filmus, J. 2005. A transient increase in the activity of Src-family kinases induced by cell detachment delays anoikis of intestinal epithelial cells. Oncogene 24:1727-1737.

Luanpitpong, S., Talbott, S. J., Rojanasakul, Y., Nimmannit, U., Pongrakhananon, V., Wang, L., and Chanvorachote, P. 2010. Regulation of lung cancer cell migration and invasion by reactive oxygen species and caveolin-1. The Journal of Biological Chemistry 285(50):38832-38840.

Lutz, R.J. 2000. Role of the BH3 (Bcl-2 homology 3) domain in the regulation of apoptosis and Bcl-2-related proteins. Biochemical society 28(2): 51–56.

Maurer, U., Charvet, C., Wagman, A. S., Dejardin, E., and Green, D. R. 2006. Glycogen synthase kinase-3 regulates mitochondrial outer membrane permeabilization and apoptosis by destabilization of MCL-1. Molecular Cell 21(6):749-760.

Michels, J., O'Neill, J. W., Dallman, C. L., Mouzakiti, A., Habens, F., and Brimmell, M. 2004. Mcl-1 is required for Akata6 B-lymphoma cell survival and is converted to a cell death molecule by efficient caspase-mediated cleavage. Oncogene 23:4818-4827.

Michels, J., Johnson, P. W., and Packham, G. 2005. Mcl-1. The International Journal of Biochemistry & Cell Biology 37(2):267-271.

Mundy, D. I., Li, P. W., Luby-Phelps, K., and Anderson, R. G. W. 2012. Caveolin targeting to late endosome/lysosomal membranes is induced by perturbations of lysosomal pH and cholesterol content. Molecular Biology of Cell 23(5):864-880.

Nakashima, H., Hamamura, K., Houjou, T., Taguchi, R., Yamamoto, N., Mitsudo, K., *et al.* 2007. Overexpression of caveolin-1 in a human melanoma cell line results in dispersion of ganglioside GD3 from lipid rafts and alteration of leading edges, leading to attenuation of malignant properties. Cancer Science 98(4):512-520.

Nieman, M. T., Prudoff, R. S., Johnson, K. R., and Wheelock, M. J. 1999. N-cadherin promotes motility in human breast cancer cells regardless of their E-cadherin expression. The Journal of Cell Biology 147:631-644.

Opferman, J.T., Letai, A., Beard, C., Sorcinelli, M.D., Ong, C.C., Korsmeyer, S.J. 2003. Development and maintenance of B and T lymphocytes requires antiapoptotic MCL-1. Nature 426(6967): 671–676.

Parat, M.D. 2009.The Biology of Caveolae: Achievements and Perspectives. International Review of Cell and Molecular Biology 273: 117-162.

Parton, R.G., Simons, K. 2007. The multiple faces of caveolae. Nature Reviews Molecular Cell Biology 8: 185–194.

Prakash, S., Matouschek, A. 2004. Protein unfolding in the cell. Trends in Biochemical Sciences 29: 593-600.

Quest, A. F., Leyton, L., and Párraga, M. 2004. Caveolins, caveolae, and lipid rafts in cellular transport, signaling, and disease. Biochemistry and Cell Biology 82(1):129-144.

Racine, C., Belanger, M., Hirabayashi, H., Boucher, M., Chakir, J., and Couet, J. 1999. Reduction of caveolin 1 gene expression in lung carcinoma cell lines. Biochemical and Biophysical Research Communications 255:580-586.

Ravid, D., Maor, S., Werner, H., and Liscovitch, M. 2006. Caveolin-1 inhibits anoikis and promotes survival signaling in cancer cells. Advances in Enzyme Regulation 46:163-175.

Ravid, D., Maor, S., Werner, H., and Liscovitch, M. 2005. Caveolin-1 inhibits cell detachment-induced p53 activation and anoikis by upregulation of insulin-like growth factor-I receptors and signaling. Oncogene 24:1338-1347.

Razani, B. 2002. Caveolae: From Cell Biology to Animal Physiology. Pharmacological Reviews 54:431-467.

Ren, L.L., Tahir, C.H., Ren, S.A.,and Thompson,T.C. 2003. Caveolin-1 Maintains Activated Akt in Prostate Cancer Cells through Scaffolding Domain Binding Site Interactions with and Inhibition of Serine/Threonine Protein Phosphatases PP1 and PP2A. Molecular and Cellular Biology 23: 9389–9404.

Rosell, R., Felip, E., Garcia-Campelo, R., Balaña, C. 2004. The biology of non-small-cell lung cancer: identifying new targets for rational therapy. Lung Cancer 46: 135-148.

Rungtabnapa, P., Nimmannit, U., Halim, H., Rojanasakul, Y., and Chanvorachote, P. 2011. Hydrogen peroxide inhibits non-small cell lung cancer cell anoikis through the inhibition of caveolin-1 degradation. American Journal of Physiological-Cell Physiology 300:235-245.

Sanna, E., Miotti, S., Mazzi, M., Santis, G.D., Canevari, S.,Tomassetti, A. 2007. Binding of nuclear caveolin-1 to promoter elements of growth-associated genes in ovarian carcinoma cells. Experimental Cell Research 313: 1307–1317.

Shack, S., Wang, X. -T., Kokkonen, G. C., Gorospe, M., Longo, D. L., and Holbrook N. J. 2003. Caveolin-Induced Activation of the Phosphatidylinositol 3-Kinase/Akt Pathway Increases Arsenite Cytotoxicity. Molecular and Cellular Biology 23(7):2407-2414.

Shimazu, T., Degenhardt, K., Nur-E-Kamal, A., Zhang, J., Yoshida, T., Zhang, Y., *et al.* 2007. NBK/BIK antagonizes MCL-1 and BCL-XL and activates BAK-mediated apoptosis in response to protein synthesis inhibition. Genes & Development 21:929-941.

Simpson, C.D., Anyiwe, K., Schimmer, A.D. 2008. Anoikis resistance and tumor metastasis. Cancer Letters 272: 177–185.

Song, L., Coppola, D., Livingston, S., Cress, D., and Haura, E. B. 2005. Mcl-1 Regulates Survival and Sensitivity to Diverse Apoptotic Stimuli in Human Non-Small Cell Lung Cancer Cells. Cancer Biology and Therapy 4(3):267-276.

Stewart, D. P., Koss, B., Bathina, M., Perciavalle, R. M., Bisanz, K., and Opferman, J. T. 2010. Ubiquitin-Independent Degradation of Antiapoptotic MCL-1. Molecular and Cellular Biology 30(12):3099-3110.

Su, H., Yang, J. -R., Xu, T., Huang, J., Xu, L., Yuan, Y. *et al.* 2009. MicroRNA-101, Down-regulated in Hepatocellular Carcinoma, Promotes Apoptosis and Suppresses Tumorigenicity. Cancer Research 69(3):1135-1142.

Sunaga, N., Miyajima, K., Suzuki, M., Sato, M., White, M. A., and Ramirez, R. D. 2004. Different Roles for Caveolin-1 in the Development of Non-Small Cell Lung Cancer versus Small Cell Lung Cancer. Cancer Research 64:4277-4285.

Tahir, S. A., Yang, G., Ebara, S., Timme, T. L., Satoh, T., Li, L., *et al.* 2001. Secreted caveolin-1 stimulates cell survival/clonal growth and contributes to metastasis in androgen insensitive prostate cancer. Cancer Research 61:3882–3885.

Tang, Y., Zeng, X., He, F., Liao, Y., Qian, N., and Toi, M. 2011. Caveolin-1 is related to invasion, survival, and poor prognosis in hepatocellular cancer. Medical Oncology (Online Mar 17,2011)

Thomas, L.W., Lam, C. and Edwards, S.W. 2010. Mcl-1; the molecular regulation of protein function. FEBS letters 584(14): 2981-2989.

Thompson, T. C., Tahir, S. A., Li, L., Watanabe, M., Naruishi, K., Yang, G., *et al.* 2010. The Role of Caveolin-1 in Prostate Cancer: Clinical Implications. Prostate Cancer and Prostatic Diseases 13(1):6-11.

Tian, B., Lessan, K., Kahm, J., Kleidon, J., Henke, C. 2002. β_1-Integrin Regulates Fibroblast Viability during Collagen Matrix Contraction through a Phosphatidylinositol 3-Kinase/Akt/Protein Kinase B Signaling Pathway. The Journal of Biological Chemistry 277(27): 24667–24675.

Travis, W.D., Travis, L.B., Devesa, S.S. 1995. Lung cancer. Cancer **75** (Suppl. 1): 191–202.

Vaporciyan, A.A., Nesbitt, J.C., Lee, J.S., *et al*. 2000. Cancer Med. p.1227–1292.

Vaux, D.L., Cory, S., and Adams, J.M. 1988. Bcl-2 gene promotes haemopoietic cell survival and cooperates with c-myc to immortalize pre-B cells. Nature 335(6189): 440–442.

Wesarg, E., Hoffarth, S., Wiewrodt, R., Kroll, M., Biesterfeld, S., Huber, C., *et al.* 2007. Targeting BCL-2 family proteins to overcome drug resistance in non-small cell lung cancer. International Journal of Cancer 121:2387-2394.

Williams, T.M. and Lisanti, M.P. 2005. Caveolin-1 in oncogenic transformation, cancer, and metastasis. American Journal of Physiological-Cell Physiology 288: 494–506.

Willis, S. N., Chen, L., Dewson, G., Wei, A., Naik, E., Fletcher, J. I., *et al.* 2005. Proapoptotic Bak is sequestered by Mcl-1 and Bcl-xL, but not Bcl-2, until displaced by BH3-only proteins. Genes & Development 19:1294-1305.

Wilson**,** R.L., Brown, R.K.J. and Reisman, D. 2009. Surgical resection for metastatic non-small cell lung cancer to the pancreas. Lung Cancer 63(3):433-435.

Woods, N.T., Yamaguchi, H., Lee, F.Y., Bhalla, K.N., Wang, H.G. 2007. Anoikis, initiated by Mcl-1 degradation and Bim induction, is deregulated during oncogenesis. Cancer Research 67(22): 10744–10752.

Yang, G., Truong, L. D., Timme, T. L., Ren, C., Wheeler, T. M., Park, S. H., *et al.* 1998. Elevated expression of caveolin is associated with prostate and breast cancer. Clinical Cancer Research. 4:1873-1880.

Yeh, D., Chen, C., Sun, M. Z., Shao, S., Hao, L., Song, Y., *et al.* 2009. Caveolin-1 is an important factor for the metastasis and proliferation of human small cell lung cancer NCI-H446 cell. The Anatomical record 292(10):1584-1592.

Yoo, S. H., Park, Y. S., Kim H. R., Sung S. W., Kim, J. H., and Shim, Y. S. 2003. Expression of caveolin-1 is associated with poor prognosis of patients with squamous cell carcinoma of the lung. Lung Cancer 42:195-202.

Zhang, B., Gojo, I., and Fenton, R. G. 2002. Myeloid cell factor-1 is a critical survival factor for multiple myeloma. Blood 99:1885-1893.

Zhang, H., Guttikonda, S., Roberts, L., Uziel, T., Semizarov, D., Elmore, S. W., *et al.* 2011. Mcl-1 is critical for survival in a subgroup of non-small-cell lung cancer cell lines. Oncogene 30:1963-1968.

Zhang, S., Zhau, H. E., Osunkoya, A. O., Iqbal, S., Yang, X., Fan, S., *et al.* 2010. Vascular endothelial growth factor regulates myeloid cell leukemia-1 expression through neuropilin-1-dependent activation of c-MET signaling in human prostate cancer cells. Molecular Cancer 9:9.

Zhong, Q., Gao, W., Du, F., and Wang, X. 2005. Mule/ARF-BP1, a BH3-only E3 ubiquitin ligase, catalyzes the polyubiquitination of Mcl-1 and regulates apoptosis. Cell 121: 1085-1095.

Zhou, P., Levy, N. B., Xie, H., Qian, L., Lee, C. Y., Gascoyne, R. D., *et al.* 2001. MCL1 transgenic mice exhibit a high incidence of B-cell lymphoma manifested as a spectrum of histologic subtypes. Blood 97:3902-3909.

APPENDICES

APPENDIX A

PREPARATION OF REAGENTS

Acrylamide gel

Solution A	0.8% methylene bis acrylamide, 30% acrylamide
Solution B	4X Seperating buffer
Solution C	4X Stacking buffer

10% APS (ammonium persulfate) in DDW

TEMED (N, N, N', N'- tetramethylenediamine)

Solution A and APS	stored at 4 °C
Solution B, C and TEMED	stored at room temperature

1. Preparation of separating gel

To make two plates of 10% acrylamide gels (1.5 mm thick) were assembly, the ingredients of separating gel are

Solution A	3.75 ml
Solution B	3.75 ml
10% APS	75 µl
TEMED	15 µl
DDW	7.50 ml

All of the ingredients were thoroughly mixed. The mixture was then immediately poured to the glass, avoid air bubbles. Then 100-200 µl of isobutanal was added to the top of the gel to cover the gel and get rid of the air bubbles. Gel was leaved to polymerization about 20-30 min.

2. **Preparation of staking gel**

Once the separating gel has completely polymerized, isobutanol was removed from the top of the gel, and rinsed with DDW. To make stacking gel, the ingredients are

Solution A	0.75 ml
Solution C	1.875 ml
10% APS	37.5 µl
TEMED	7.5 µl
DDW	4.875 ml

All of the ingredients were thoroughly mixed. The mixture was then immediately poured the gel between the glass plates, avoided air bubbles. The combs were inserted between the two glass plates of two sets of gel apparatus. The gels were leaved for approximately 30-40 min to polymerize. The whole gel can be keep in 1X running buffer in 4°C for a week.

3. Application of samples

Once the stacking gel has completely solidated, the combs were gently removed. The wells were rinsed out thoroughly with running buffer using syringe. The samples were applied by long sample loading tip. The chamber was connected to power supply which set up at 120 V for 1.5 h.

4X Separating buffer

To make 200 ml of separating buffer, the ingredients are

Tris	36.34 g
DDW	180 ml

Tris was dissolved in DDW with continuously stirring. The solution was adjusted the pH to 8.8 with 1M HCl, then add 0.8 g of SDS and water to 200 ml.

4X Stacking buffer

To make 100 ml of 4X separating buffer, the ingredients are

Tris	6.056 g
DDW	94 ml

Tris was dissolved in DDW with continuously stirring. The solution was adjusted the pH to 6.8 with 1M HCl, then add 0.4 g of SDS and water to 100 ml.

Running buffer

To make 1 liter of 5X running buffer (250 mM Tris, 1.92 M glycine, and 0.5 % SDS) for stock solution, the ingredients are

Tris	30.2 g
Glycine	144.13 g
SDS	5g

All ingredients were dissolved in DDW with continuously stirring. The solution was adjusted volume to 1000 ml. Before use, the solution was diluted to 1X running buffer (50 mM Tris, 0.384 M glycine, and 0. 1 % SDS) with DDW, 5X running buffer : DDW= 4 : 1.

Transfer buffer

To make 1 liter of 10 X transfer buffer (1 M Tris, and 1.92 M glycine) for stock solution, the ingredients are

Tris	121.14 g
Glycine	144.13 g

All ingredients were dissolved in DDW with continuously stilling. The solution was adjusted volume to 1000 ml. Before use, the solution was diluted to 1000 ml of 1X running buffer (0.1 M Tris, 0.192 M glycine) supplemented with 5% methanol, 10X transfer buffer : methanol : DDW = 100 ml: 50ml : 850 ml.

Tris-buffered saline, 0.1 % Tween 20 (TBST)

To make 1 liter of 10 X TBST (100 mM Tris, 1 M NaCl, and 0.1 % Tween20) for stock solution, the ingredients are

Tris	12.11 g
NaCl	58.44 g
Tween 20	10 ml

All ingredients were dissolved in DDW with continuously stirring. The solution was adjusted volume to 1000 ml. Before use, the solution was diluted to 1 X

TBST (10 mM Tris, 100 mM NaCl, and 0.01 % Tween 20) with DDW, 10X TBST : DDW = 1 : 9.

6X Sample buffer

To make 10 ml of 6X sample buffer for stock solution, the ingredients are

Solution C	7 ml
SDS	1 g
Glycerol	3 ml
2-Mercaptoethanol	0.42 ml
Bromphenol blue	1.2 mg

All ingredients were dissolved in DDW with continuously stirring. The solution was adjusted volume to 10 ml. 6X sample buffer was aliquot into 1 ml/tube and stored at -20 °C.

Lysis buffer

To make 1 ml of lysis buffer, the ingredients are

10X Lysis buffer (Cell signaling, Inc)	100 µl
DDW	850 µl
100 mM PMSF	10 µl
25X Complete protease inhibitor	40 µl

All ingredients were dissolved in DDW 1 ml. It should be freshly prepared before use every times.

Stripping buffer

To make stripping buffer 100 ml, the ingredient are

150 mM Glycine pH 10.8	33.3 ml
1M KCl	10 ml
Guanidine hydrochloride	66.9 g
0.5 M EDTA	10 µl
2-Mercaptol ethanol	140 µl

All ingredients were dissolved in glycine 33.3 ml with continuously stirring. The solution was adjusted volume to 100 ml and stored at room temperature.

APPENDIX B

TABLES OF EXPERIMENTAL RESULTS

Table 6 Different levels of Cav-1 expression in transfectants of H460 cells.

Transfectants	Relative Cav-1 level
Cav-1 shRNA plasmid	0.50±0.05*
Control shRNA plasmid A	1.00±0.09
pDS_XB-YFP	1.00±0.13
pEX_cav-1-YFP	2.56±0.32†

Each value represents the mean ± S.D. of three independent experiments. Asterisks refer significant difference from the control shRNA plasmid A: *, $p < 0.05$, Daggers refer significant difference from the pDS_XB-YFP: †, $p < 0.05$ determined by student's *t*-test.

Table 7 Percentage of cell survival in pDS_XB-YFP and pEX_cav-1-YFP after detachment was evaluated by XTT assay at the end of each time point (time dependency).

Time after detachment (h)	**Cell viability (%)**	
	pDS_XB-YFP	**pEX_cav-1-YFP**
0	100.00±1.47	100.00±0.80
3	90.30±4.76	100.01±1.33
6	47.10±2.62	85.36±3.35*
12	40.20±3.37	78.98±6.32*
24	32.04±2.87	62.27±5.23*

Each value represents the mean ± S.D. of three independent experiments. Asterisks refer significant difference from the control group (control transfected, pDS_XB-YFP) at specific time points: *, $p < 0.05$ determined by student's *t*-test.

Table 8 Percentage of cell survival in control shRNA plasmid A and cav-1 shRNA plasmid after detachment was evaluated by XTT assay at the end of each time point (time dependency).

Time after detachment (h)	**Cell viability (%)**	
	Control shRNA plasmid A	**Cav-1 shRNA plasmid**
0	100.00±6.1	100.00±1.39
3	86.45±4.76	78.89±5.32
6	51.34±7.43	32.67±7.21*
12	39.4±5.43	20.83±2.03*
24	30.22±3.5	17.85±4.53*

Each value represents the mean ± S.D. of three independent experiments. Asterisks refer significant difference from the control group (control transfected, control shRNA plasmid A) at specific time points: *, $p < 0.05$ determined by student's *t*-test.

Table 9 Percentage of cell survival in Cav-1 transfectants after detachment from time 0 to 6h was evaluated by XTT assay at the end of each time point (time dependency).

Time after detachment (h)	**Cell viability (%)**			
	pDS_XB-YFP	pEX_Cav-1-YFP	Control shRNA plasmid A	Cav-1 shRNA plasmid
0	100.00±1.52	100.00±2.55	100.00±4.26	100.00±5.71
1	99.88±5.32	99.99±3.91	99.23±3.11	97.34±3.73
2	95.32±4.32	100.12±4.58	96.76±4.27	90.32±3.37
3	91.21±5.71	100.18±2.45	85.66±3.20	77.21±4.86
4	78.43±6.43	95.32±5.82	80.54±4.54	60.77±2.63
5	60.55±5.11	90.87±3.83	60.19±2.94	46.11±6.20
6	46.41±2.71	84.33±3.15	51.59±6.04	32.51±3.29

Each value represents the mean ± S.D. of five independent experiments. The data were used for regression analysis of cell viability.

Table 10 Percentage of apoptosis in pDS_XB-YFP and pEX_cav-1-YFP after detachment was evaluated by Hoechst 33342 assay at the end of each time point (time dependency).

Time after detachment (h)	**Apoptosis (%)**	
	pDS_XB-YFP	**pEX_cav-1-YFP**
0	0.27±0.25	0.33±0.13
3	8.74±3.38	0.44±0.21
6	19.35±4.32	6.34±5.21*
12	39.62±8.11	8.88±2.03*
24	55.39±6.50	11.99±3.04*

Each value represents the mean ± S.D. of three independent experiments. Asterisks refer significant difference from the control group (control transfected, pDS_XB-YFP) at specific time points: *, $p < 0.05$ determined by student's *t*-test.

Table 11 Percentage of apoptosis in control shRNA plasmid A and cav-1 shRNA plasmid after detachment was evaluated by XTT assay at the end of each time point (time dependency).

Time after detachment (h)	**Apoptosis (%)**	
	Control shRNA plasmid A	**Cav-1 shRNA plasmid**
0	0.53±0.25	0.17±0.09
3	10.11±3.38	12.09±7.32
6	17.32±5.98	39.98±10.54*
12	33.23±8.88	53.61±4.32*
24	52.55±6.50	77.85±3.21*

Each value represents the mean ± S.D. of three independent experiments. Asterisks refer significant difference from the control group (control transfected, control shRNA plasmid A) at specific time points: *, $p < 0.05$ determined by student's *t*-test.

Table 12 Percentage of apoptosis in Cav-1 transfectants after detachment from time 0 to 6h was evaluated by Hoechst 33342 assay at the end of each time point (time dependency).

Time after detachment (h)	**Apoptosis (%)**			
	pDS_XB-YFP	pEX_Cav-1-YFP	Control shRNA plasmid A	Cav-1 shRNA plasmid
0	0.31±0.14	0.48±0.24	0.67±0.34	0.15±0.10
1	3.21±0.43	0.39±0.31	3.72±0.56	4.15±0.16
2	6.43±1.21	0.42±0.37	7.22±0.72	8.05±0.09
3	8.02±3.19	0.45±0.18	10.42±2.99	11.98±6.79
4	12.18±4.16	2.41±0.19	12.47±3.49	21.36±5.73
5	15.66±5.65	4.41±0.25	14.87±4.63	30.88±4.29
6	19.19±6.3	6.52±4.81	18.88±5.82	40.59±11.04

Each value represents the mean ± S.D. of four independent experiments. The data were used for regression analysis of apoptosis after detachment.

Table 13 Different levels of Mcl-1 expression in transfectants of H460 cells.

Transfectants	**Relative Mcl-1 level**
shMcl-1	0.25±0.12*
Control shRNA plasmid A	1.00±0.08
Mock	1.00±0.11
HMcl-1	2.01±0.21†

Each value represents the mean ± S.D. of three independent experiments. Asterisk refers significant difference from the control shRNA plasmid A: *, $p < 0.05$, Dagger refers significant difference from Mock: †, $p < 0.05$ determined by student's *t*-test.

Table 14 Percentage of cell survival in Mock and HMcl-1 after detachment was evaluated by XTT assay at the end of each time point (time dependency).

Time after detachment (h)	**Cell viability (%)**	
	Mock	**HMcl-1**
0	100.00±0.25	100.00±0.34
3	85.51±3.18	111.17±11.03*
6	50.01±3.89	110.01±9.05*
12	45.12±0.96	100.17±5.67*
24	36.82±1.24	72.31±2.82*

Each value represents the mean ± S.D. of three independent experiments. Asterisks refer significant difference from the control group (control transfected, Mock) at specific time points: *, $p < 0.05$ determined by student's *t*-test.

Table 15 Percentage of cell survival in control shRNA plasmid A and shMcl-1 after detachment was evaluated by XTT assay at the end of each time point (time dependency).

Time after detachment (h)	**Cell viability (%)**	
	Control shRNA plasmid A	**shMcl-1**
0	100.00±0.55	100.00±0.91
3	84.98±4.98	60.34±3.18*
6	55.09±7.32	41.26±7.43*
12	44.99±5.33	29.89±4.32*
24	37.98±3.32	10.77±5.32*

Each value represents the mean ± S.D. of three independent experiments. Asterisks refer significant difference from the control group (control transfected, control shRNA plasmid A) at specific time points: *, $p < 0.05$ determined by student's *t*-test.

Table 16 Percentage of cell survival in Mcl-1 transfectants after detachment from time 0 to 6h was evaluated by XTT assay at the end of each time point (time dependency).

Time after detachment (h)	**Cell viability (%)**			
	Mock	HMcl-1	Control shRNA plasmid A	shMcl-1
0	100.00±0.55	100.00±0.59	100.00±0.44	100.00±0.92
1	95.30±1.53	103.70±0.33	95.55±2.83	86.57±2.22
2	90.50±1.39	107.7±1.98	90.65±4.39	73.56±2.15
3	84.67±3.14	108.58±10.72	85.03±4.72	60.75±3.11
4	73.52±2.63	110.01±5.21	75.04±3.54	53.6±5.48
5	62.04±5.12	109.39±3.82	65.7±4.01	47.34±3.74
6	49.82±4.23	108.92±6.72	54.98±6.99	42.43±2.83

Each value represents the mean ± S.D. of five independent experiments. The data were used for regression analysis of cell viability.

Table 17 Percentage of apoptosis in Mock and HMcl-1 after detachment was evaluated by Hoechst 33342 assay at the end of each time point (time dependency).

Time after detachment (h)	**Apoptosis (%)**	
	Mock	**HMcl-1**
0	1.64±0.53	1.78±0.58
3	8.32±1.14	4.04±1.25*
6	20.76±2.82	5.38±2.54*
12	38.92±3.67	10.24±3.13*
24	50.86±6.43	9.66±3.5*

Each value represents the mean ± S.D. of three independent experiments. Asterisks refer significant difference from the control group (control transfected, Mock) at specific time points: *, $p < 0.05$ determined by student's *t*-test.

Table 18 Percentage of apoptosis in control shRNA plasmid A and shMcl-1 after detachment was evaluated by Hoechst 33342 assay at the end of each time point (time dependency).

Time after detachment (h)	**Apoptosis (%)**	
	Control shRNA plasmid A	**shMcl-1**
0	1.24±0.47	2.07±0.71
3	9.43±1.12	11.15±3.52
6	19.72±3.22	28.97±0.38*
12	40.64±3.32	56.54±6.43*
24	49.55±6.72	72.67±4.42*

Each value represents the mean ± S.D. of three independent experiments. Asterisks refer significant difference from the control group (control transfected, control shRNA plasmid A) at specific time points: *, $p < 0.05$ determined by student's *t*-test.

Table 19 Percentage of apoptosis in Mcl-1 transfectants after detachment from time 0 to 6h was evaluated by Hoechst 33342 at the end of each time point (time dependency).

Time after detachment (h)	**Apoptosis (%)**			
	Mock	HMcl-1	Control shRNA plasmid A	shMcl-1
0	1.69±0.82	1.52±0.72	1.21±0.53	3.91±1.56
1	3.87±1.11	2.54±0.23	4.02±1.15	5.09±1.12
2	6.04±0.74	3.37±0.76	6.73±2.65	8.18±2.16
3	8.92±2.49	4.17±1.11	10.37±2.10	10.43±4.21
4	12.50±2.73	4.49±2.4	12.81±2.5	17.1±3.42
5	16.61±3.17	5.01±2.92	16.34±4.26	23.5±2.36
6	19.99±1.03	5.44±2.19	19.55±2.56	29.07±1.16

Each value represents the mean ± S.D. of four independent experiments. The data were used for regression analysis of apoptosis after detachment.

Table 20 Reduction of Cav-1 expression in response to the detachment of H460 cells.

Time after detachment	Relative Cav-1 level
0	1.00±0.05
3	0.91±0.10
6	0.51±0.14*
12	0.37±0.21*
24	0.15±0.09*

Each value represents the mean ± S.D. of three independent experiments. Asterisks refer significant difference from the control at time=0: *, $p < 0.05$ determined by One-way ANOVA.

Table 21 Reduction of Mcl-1 expression in response to the detachment of H460 cells.

Time after detachment	Relative Mcl-1 level
0	1.00±0.04
3	0.95±0.11
6	0.70±0.12*
12	0.50±0.15*
24	0.32±0.13*

Each value represents the mean ± S.D. of three independent experiments. Asterisks refer significant difference from the control at time=0: *, $p < 0.05$ determined by One-way ANOVA.

Table 22 Reduction of Cav-1 and Mcl-1 expression in response to the detachment of H460 cells.

Time after detachment	Relative Cav-1 level	Relative Mcl-1 level
0	1.00±0.08	1.00±0.06
3	0.95±0.02	0.94±0.04
6	0.74±0.05	0.74±0.01
12	0.46±0.05	0.45±0.03
24	0.30±0.02	0.22±0.07

Each value represents the mean ± S.D. of three independent experiments Levels of Cav-1 and Mcl-1 obtained from the same nitrocellulose membranes. The data were used for the correlation of Cav-1 and Mcl-1 reduction after detachment of H460 cells

Table 23 Relative co-immunoprecipitation of Cav-1-Mcl-1 complex in H460 cells.

Transfectants	**IP:Cav-1, WB:Mcl-1**	**IP:Mcl-1, WB:Cav-1**
HCav-1	1.9±0.23*	2.12±0.12*
H460	1.00±0.15	0.95±0.14
shCav-1	0.32±0.10*	0.17±0.03*

Each value represents the mean ± S.D. of three independent experiments. Asterisks refer significant difference from the control H460 cells *, $p < 0.05$ determined by One-way ANOVA.

Table 24 Mcl-1 basal level is dependent on Cav-1 level in H460 cells.

Transfectants	Relative Mcl-1 level
HCav-1	2.05±0.25*
H460	1.00±0.12
shCav-1	0.12±0.07*

Each value represents the mean ± S.D. of three independent experiments. Asterisks refer significant difference from the control H460 cells: *, $p < 0.05$ determined by One-way ANOVA.

Table 25 Cav-1 stabilize Mcl-1 in detached H460 cells.

Time after detachment	Relative Mcl-1 level		
	shCav-1	**H460**	**HCav-1**
0	1.00±0.06	1.00±0.07	1.00±0.02
6	0.50±0.05*	0.78±0.05*	0.96±0.07
12	0.21±0.07*	0.38±0.04*	0.84±0.08*

Each value represents the mean ± S.D. of three independent experiments. Asterisks refer significant difference from the control at time=0: *, $p < 0.05$ determined by One-way ANOVA.

Table 26 Mcl-1 transcription level in response to the detachment of H460 cells.

Time after detachment	$\mathbf{2^{-\Delta\Delta CT}}$
0	1.00±0.05
3	0.54±0.03*
6	0.50±0.03*
12	0.57±0.02*
24	0.53±0.03*

Each value represents the mean ± S.D. of three independent experiments. Asterisks refer significant difference from the control at time=0: *, $p < 0.05$ determined by One-way ANOVA.

Table 27 Effects of Proteasome inhibitors on Mcl-1 level after detachment of H460 cells.

Time after detachment	Relative Mcl-1 level
0	1.00±0.03
6	0.54±0.06*
6+LAC	0.97±0.05
6+MG132	0.96±0.03

Each value represents the mean ± S.D. of three independent experiments. Asterisks refer significant difference from the control at time=0: *, $p < 0.05$ determined by One-way ANOVA.

Table 28 Mcl-1 ubiquitination after cell detachment of H460 cells.

Time after detachment (h)	Relative Ub-Mcl-1 level
0	1.00±0.07
1	1.53±0.10*
3	2.80±0.14*
6	3.40±0.15*

Each value represents the mean ± S.D. of three independent experiments. Asterisks refer significant difference from the control at time=0: *, $p < 0.05$ determined by One-way ANOVA.

Table 29 Cav-1 stabilize Mcl-1 by attenuating Mcl-1 ubiquitination.

Time after detachment	Relative Ub-Mcl-1 level		
	shCav-1	**H460**	**HCav-1**
1	2.98±0.15*	1.00±0.15	0.67±0.15*
6	4.14±0.22*,†	1.00±0.17	0.39±0.12*

Each value represents the mean ± S.D. of three independent experiments. Asterisks refer significant difference from the control H460 cells: *, $p < 0.05$ determined by One-way ANOVA. Dagger refers significant difference from the control shCav-1 at time = 1h: †, $p < 0.05$ determined by One-way ANOVA.

Table 30 Different levels of Cav-1 expression in transfectants of G361 cells.

Transfectants	**Relative Cav-1 level**
Cav-1 shRNA plasmid	0.18±0.09*
Control shRNA plasmid A	1±0.15
pDS_XB-YFP	1±0.12
pEX_cav-1-YFP	2.70±0.52†

Each value represents the mean ± S.D. of three independent experiments. Asterisks refer significant difference from the control shRNA plasmid A: *, $p < 0.05$, Daggers refer significant difference from the pDS_XB-YFP: †, $p < 0.05$ determined by student's *t*-test.

Table 31 Percentage of cell survival in pDS_XB-YFP and pEX_cav-1-YFP transfectants G361 cells after detachment was evaluated by XTT assay at the end of each time point (time dependency).

Time after detachment (h)	**Cell viability (%)**	
	pDS_XB-YFP	**pEX_cav-1-YFP**
0	100.00±4.5	100.00±0.67
3	82.55±7.31	99.08±2.33*
6	60.32±7.9	91.76±1.18*
12	50.43±9.05	72.55±1.8*
24	32.67±5.18	60.23±4.65*

Each value represents the mean ± S.D. of three independent experiments. Asterisks refer significant difference from the control group (control transfected, pDS_XB-YFP) at specific time points: *, $p < 0.05$ determined by student's *t*-test.

Table 32 Percentage of cell survival in Control shRNA plasmid A and Cav-1 shRNA plasmid transfectants G361 cells after detachment was evaluated by XTT assay at the end of each time point (time dependency).

Time after detachment (h)	**Cell viability (%)**	
	Control shRNA plasmid A	**Cav-1 shRNA plasmid**
0	100.00±5.21	100.00±3.19
3	80.44±3.27	71.34±4.62*
6	67.43±8.06	40.01±5.33*
12	40.34±3.81	25.26±6.08*
24	38.34±2.52	15.21±6.14*

Each value represents the mean ± S.D. of three independent experiments. Asterisks refer significant difference from the control group (control shRNA plasmid A) at specific time points: *, $p < 0.05$ determined by student's *t*-test.

Table 33 Mcl-1 basal level is dependent on Cav-1 level in G361 cells.

Transfectants	Relative Mcl-1 level
G361	1.00±0.25
G361-Cav-1	2.53±0.21*
G361-shCav-1	0.23±0.07*

Each value represents the mean ± S.D. of three independent experiments. Asterisks refer significant difference from the control G361 cells: *, $p < 0.05$ determined by One-way ANOVA.

Table 34 Cav-1 stabilize Mcl-1 in detached G361 cells.

Time after detachment	Relative Mcl-1 level		
	G361-shCav-1	**G361**	**G361-Cav-1**
0	1.00±0.13	1.00±0.15	1.00±0.15
6	0.48±0.05*	0.80±0.03*	0.93±0.07

Each value represents the mean ± S.D. of three independent experiments. Asterisks refer significant difference from the control at time=0: *, $p < 0.05$ determined by One-way ANOVA.

VITA

Mr. Preedakorn Chunhacha was born on Sep 26, 1978 in Bangkok. He received his B.Sc. in Pharmacy with honored (GPA3.54) from the Faculty of Pharmaceutical Sciences, Chulalongkorn University in 2002.